PhD-FSTM-2023-101
The Faculty of Science, Technology and Medicine

DISSERTATION

Defence held on 19/09/2023 in Esch-sur-Alzette

to obtain the degree of

DOCTEUR DE L'UNIVERSITÉ DU LUXEMBOURG

EN SCIENCES DE L'INGENIEUR

by

Emmanuella Onyinyechi OSUEBI-IYKE
Born on 06 September 1992 in Awo Omamma, (Nigeria)

EXPERIMENTAL ANALYSIS OF THE COST AND BENEFITS OF CARBON ALLOCATION TO SHOOTS AND ROOTS

Dissertation defence committee

Dr. Stanislaus Schymanski, dissertation supervisor
Luxembourg Institute of Science and Technology

Prof. Willy Werner
University of Trier, Germany

Prof. Stéphane Bordas, Chairman
University of Luxembourg

Dr. Jack Hale
University of Luxembourg

Dr Robert Koller, Vice Chairman
Forschungszentrum Jülich GmbH, Germany

Acknowledgments

I would like to extend my deepest gratitude to everyone who have supported and encouraged me throughout this remarkable journey.

First and foremost, I want to express my special gratitude to my late dad, whose constant inspiration and words of encouragement from the beginning of my PhD until his passing kept me motivated and determined to reach this point.

I also wish to acknowledge my late best friend, Chiamaka Okeoma Egbuna (my Twinnie), whose unwavering support during her lifetime spurred me on. Her belief in my future as a doctor made it nearly impossible for me to quit along the way. Though she is no longer with us, I am certain she would be proud of my accomplishments from the heavens.

I am incredibly thankful to my supervisor, Dr. Stanislaus Schymanski, without whom this project would not have come into existence. He has been the best supervisor any PhD student could hope for. Stan, thank you for always being there when I needed help or had questions. Your unwavering belief in me, even when I doubted myself, and your continuous support pushed me through to the finish line. Your mentorship has been invaluable, especially during the difficult time when I lost my dad. You were not just my supervisor; you were a true mentor, and I am deeply grateful for that.

Special thanks to my CET members, Dr. Jack Hale and Prof. Willy

Werner, for their unwavering support throughout these years. I appreciate all your efforts in framing and guiding my research. Prof. Werner, you have been a part of my academic journey since I arrived in Europe, from my first day in the vegetation ecology class at the University of Trier until now. Thank you so very much. Jack, I fondly remember our engineering math discussions, and your dedication to explaining things to me in the simplest way possible was truly commendable. You are an incredible teacher, and I am thankful for your guidance.

To the engineers who worked on this project with me, Oliver O'Nagy, Frank Minette, and Adriano Gama, my heartfelt thanks. There would be no growth chamber or penetrometer without your invaluable help and support. Thank you for assisting with the set-up, managing logistics, and patiently answering my numerous questions. Most importantly, thank you for making difficult tasks seem easy. I learned so much from each of you. Oli, you truly are the best, and your gestures like buying me ice cream and indulging my love for food will forever be cherished. Your unwavering support and presence, even at the shortest notice, have meant the world to me. To Dr. Thomas Schleeh, thank you so much for your idea on using chemicals to test my growth chamber.

To François Barnich, Dennis Pittois, and Loic Leonard, I am grateful for all the help with analyzing my samples.

To Drs. Dagmar van Dusschoten, Daniel Pflugfelder, and Robert Koller, thank you immensely for allowing me to use your facility for my dynamic root imaging. Your support made my stays at Jülich highly productive and enjoyable. Robert, thanks also for accepting to be part of my defense jury.

To Professor Stéphane Bordas, thank you for accepting to be my jury chair at short notice. I really appreciate.

To my dearest friends, Dr. Youri Nouchokgwe, Dr. Mike Mousley, Elmer Kanjo Ekinzog, thank you for always being there to answer all my math and code-related questions. Elmer, you are my personal stack overflow, and

your willingness to help me troubleshoot code errors and provide solutions has been invaluable. Mike, your unwavering support, whether it's discussing ideas, equations, or problem-solving, has meant so much to me. I also appreciate how you enlisted your twin, Phil, to help with statistics questions when needed. Youri, you have been with me since day one, and your continuous support has been a source of strength. Thank you for always being there and supporting me, especially during the difficult time when I lost my dad. To my girl, Nwachinaemereogo Okwuobasi, Nwachi nwanne m, thanks for always calling Otunne. It reminds me of my dad and keeps me going. Thanks for filing the vacuum that Twinnie left in my life. you are absolute wonderful. To Ogechukwu Nwaokolobia, my ride or die, thanks for always asking "when will you finish this your PhD sef ?" To Somtochukwu Ezike-Nadialine, my forever big sis. You always show up for me in ways I cannot fully describe with words. Thank you for your consistent support and encouragement. Your love and care in Luxembourg kept me going even in my lowest moments.

To Chiazo Anomi and Esther Chukwu, thank you both for your invaluable help with childcare. Your love and care for ChiChi made it possible for me to continue working on my project.

To all CATs and my office mates, I want to express my gratitude for creating a fantastic working environment during my research. I cherish all the lunches, coffee breaks, and corridor discussions we had together.

To my girls, Poorani, Melody, Nathasia who stood by me during my lowest moments, I extend my heartfelt appreciation. Your encouragement and support have been instrumental, and I am truly grateful.

To my sister, Ndidiamaka Iyke Iroh. I love how you love and celebrate me. After daddy, you are my biggest hype woman! Thank you for always encouraging me and being there for me. You are the best sister I could ever ask for!

To my mother-in-law, Bamijoko Gege, I love you dearly. Thank you for

taking over childcare, especially during the last three months of my thesis writing. Your support in numerous ways has been invaluable.

Chiamaka, my daughter, your presence has transformed my life and given it new meaning. You are my greatest inspiration, and my goal to be your role model has been a driving force throughout this journey. Thank you for being my motivation, even without knowing it.

And to my dearest husband, Dr. Olatunji Gege; my rock, my cheerleader, my confidant, my protector, my favorite proofreader, and my other eye, I am grateful for everything you have done and sacrificed to ensure that I had all the support I needed to pursue this degree. You are my rock, and no one does it better. I love you! Your unwavering love and encouragement have been a constant source of strength, and I am forever grateful to have you by my side.

Table of contents

General Abstract

Over five decades since Mooney's (Mooney, 1972) submission about the pivotal role of quantitative data in predicting plant success in different environments, the understanding of the regulation of carbon (C) allocation and its trade-off remains deficient, hindered by measurement complexities in crucial components such as respiration and root exudation. This PhD capitalizes on technological advancements on plant gas exchange measurements to experimentally explore the C costs and benefits of plant roots and shoots across different soil penetration resistances, aiming to contribute empirical data to improve the robustness of predictive models and accuracy in long-term plant responses.

This study organizes it's findings into three chapters focusing on the development and testing of a growth chamber to monitor plant gas fluxes and presenting the results on studies on C assimilation, transpiration and above and below-ground respiration and the associated cost-benefit relationships in terms of water and N acquisition.

In the first chapter, a novel plant growth chamber is introduced, enabling concurrent monitoring of above and below-ground gas exchange. Testing the growth chamber with chemicals and plants highlights its potential for advancing research involving the measurement of plants' fluxes. Challenges in accurately quantifying root C allocation are addressed and minimized

using a custom-developed potting substrate.

Utilizing the growth chamber developed in Chapter 1, the second study investigates the cost and benefit ratios of C allocation in response to different soil penetration resistance in maize plants. The findings highlight elevated root respiration costs under high soil penetration resistance. However, increased below-ground respiration costs were not associated with a decrease in water and nutrient uptake per root length under high bulk density conditions. Due to higher root respiratory cost incurred by the plants grown under the high soil bulk density, the cost/benefit ratio was higher for this group.

The third chapter extends the investigation to a comparative analysis between maize and barley plants, emphasizing species-specific traits and bulk density effects on the studied cost-benefit relationships. Maize demonstrated a higher water use efficiency (WUE) compared to barley, while the root respiration cost per water uptake for maize was twice that of barley. However, N uptake per root length in maize was higher than those of barley, providing evidence of increased N demand and heightened respiration cost in maize. Comparing the respiratory cost of N uptake between the two species revealed similarities in this relationship for both species. This finding highlights that while different species vary in their different uptake strategies, the environment imposes the cost for resources acquisition. The similarity in the cost/benefit ratio of N acquisition in maize and barley highlights the fundamental costs associated with resource uptake, and suggests that they are species-independent.

Furthermore, both species exhibited similar respiration to assimilation suggesting that the energy investment in below-ground respiration is proportionate to C assimilated above-ground across both species. Similar to the second chapter, high bulk densities were associated with higher root respiration per root length across both species, while high bulk density treatments in barley corresponded to increased water uptake rates. Connecting this

finding with those of Chapter 2 where higher soil penetration resistance did not diminish benefits in terms of water and N acquisition, the findings in this study correspond with the well-documented adaptive responses of root systems to optimize resource acquisition under constrained conditions and highlights the complexity of cost-benefit relationships under adverse below-ground conditions.

While this research provided valuable insights into C allocation patterns and their cost/benefit ratios, unanswered questions involve isolating the cost of root penetration and investigating the cost/benefit ratios associated with rhizosphere interactions in field conditions. Scaling these findings to larger plants necessitate longer-term experiments, to measure these ratios under various plant developmental stages.

Recommendations for future studies include adopting an integrated approach that combines dynamic root imaging with continuous respiration measurements for a detailed understanding of C costs and benefits across different plant physiological processes and a wide range of environmental conditions.

General introduction

Motivation

Plants play a vital role in maintaining a balanced climate, managing water resources, and sustaining our food supply. Through photosynthesis, they absorb carbon dioxide (CO_2) and release oxygen (O_2), helping to stabilize atmospheric composition and regulate global temperatures. Additionally, their root systems enhance soil structure, preventing erosion and improving water retention, which is crucial for sustainable agriculture and mitigating drought effects. As we rely on plants for nourishment, their resilience to changing conditions becomes paramount. Plants are continually adapting to shifts in temperature, precipitation, and other environmental factors, ensuring their survival and productivity. Understanding and supporting these adjustments are essential for maintaining the delicate balance of ecosystems that underpin our well-being.

One way of understanding these dynamic changes is through ecosystem modelling. However, current ecosystem prediction models are significantly limited when it comes to predicting long term environmental changes. This limitation primarily stems from their reliance on parameter calibrations extracted from historical observations and the assumption that environmental

conditions remain stationary over time (Teuling et al., 2010; Chiew and Vaze, 2015; Robinson et al., 2019; Harper et al., 2021). Furthermore, to simplify model complexity, some of these models use plant functional types (PFTs) for parameterization. While functional types are useful for simplifying vegetation classification based on ecological traits, they may oversimplify the diversity and flexibility of actual plant responses to environmental conditions, leading to inaccurate predictions under new conditions (Wullschleger et al., 2014).

In contrast to models with empirically prescribed traits and behaviour, optimality-based models optimize resource allocation for plant fitness under diverse environmental constraints, considering trade-offs in growth, reproduction, and defense (Schymanski et al., 2008). These models play a vital role in predicting plant-environment interactions, like stomatal regulation, leaf area, and rooting depths. However, it is essential to recognize and accurately account for physical constraints that influence these interactions. Precise delineation of these constraints is critical for setting appropriate boundary conditions for biological control and accurately translating biological control variables into energy and matter exchange rates with the environment. Furthermore, it is crucial to acknowledge that most plant responses to environmental factors come with energetic costs. Energetic costs in plants refer to the expenditure of energy for both regular metabolic functions, such as growth, maintenance and reproduction, and adaptive responses to environmental stressors, including the activation of defense mechanisms and adaptations to abiotic factors. For plants to successfully maintain positive carbon and energy balances, these costs need to be factored into the equation. Neglecting these costs could result in incomplete or inaccurate assessments of plant behavior and ecosystem dynamics. Therefore, a comprehensive understanding of both optimality principles and the energetic costs associated with plant responses is imperative to formulating more robust and reliable vegetation models. By bridging these knowledge gaps, we can enhance our

ability to predict and manage the complex interactions between plants and their environment more effectively.

Plant resource allocation is often thought to be guided by a cost-benefit relationship. These ratios represent the trade-offs that plants face in allocating resources and the potential advantages they can attain from these allocations (Givnish, 1986). Photosynthetic water-use efficiency (WUE) and nitrogen-use efficiency (NUE) has been extensively studied and widely used as a key metric to express the above-ground cost and benefit of plant growth. The allocation of resources, particularly carbon (C) and nitrogen (N), to above-ground structures is plays a pivotal role in water (H_2O) and nitrogen utilization for photosynthesis and overall plant productivity. The interplay between shoot photosynthetic capacity, C and N investment in photosynthetic apparatus and H_2O loss as highlighted in previous studies (Field and Mooney, 1986; Mooney, 1972), are significant cost parameters that are often weighed against the the photosynthetic benefits of plant shoots. However, in contrast, the exploration of below-ground cost and benefit has not received adequate attention, even though root systems, as vital conduits for water and nutrient uptake, play an integral role in plant functioning and survival, significantly influencing overall ecosystem dynamics. This could be because studying below-ground processes especially gas exchange poses technical difficulties and measurement complexities.

Existing ecosystem prediction models often neglect the energetic costs associated with the mechanical exploration of the soil volume by plant roots, potentially impacting the overall C balance of plants. For example, foliage maintenance costs in the model proposed by (Schymanski et al., 2009) were parameterized based on empirical observations across a wide range of species. However, due to the lack of targeted below-ground observations, fine root maintenance costs were only parameterized using observations from a single species, (Schymanski et al., 2008). It's worth noting that this approach was based on the hypothesis that the relationship between fine root water uptake

capacity and the rates of fine root respiration would exhibit a certain degree of similarity across a diverse range of species. This methodology, while informative, overlooks the energetic costs related to the mechanical exploration of the soil volume by plant roots, which could conceivably be a substantial component of the overall C balance (Ruiz et al., 2015), limiting the generalization of the findings. For instance, a study highlighted increasing energy costs of root penetration with increasing soil penetration resistance within the same species (Colombi et al., 2017). This highlights the need for further investigation into the energetic costs related to root functioning and their implications for plant carbon allocation. Species-independent cost-benefit ratios in ecosystem modeling offer substantial advantages. Such ratios could enhance model generalization, allowing seamless application across diverse plant species and environmental conditions. The transferability of models could potentially become more efficient, particularly in predicting ecosystem responses to changing environmental factors.

To address these knowledge gaps and contribute to improving the accuracy of predictions, this PhD thesis aims to comprehensively explore the cost and benefits of plant roots, alongside the shoots. By experimentally quantifying these costs, I seek to establish more consistent physical underpinnings for existing models to make more reliable predictions and enhance the accuracy of mid to long-term plant responses to environmental changes. In order to overcome the technical difficulty associated with measuring below-ground C investments, I present the development and testing of a custom growth that allows precise control of environmental conditions, enabling more accurate measurements of below-ground gas exchange processes in plants. Using this growth chamber, plant growth experiments will be carried out to provide new insights into below-ground plant physiological processes and enhancing the overall scientific rigor of the study. Furthermore, using this growth chamber, I carry out experiments under different bulk densities using two species with different photosynthetic pathways.

The overall goal of this research is to contribute to a deeper understanding of the cost and benefits of plant roots in response to environmental changes as well as to understand the role of species-specific traits on the general trade-off patterns. By shedding light on these energetic trade-offs through my experiments, I hope to contribute to improving the reliability of plant response models and provide valuable insights for sustainable management of ecosystems facing environmental challenges in the long run.

Outline of the thesis

The thesis is composed of three main chapters:

1. Chapter 1: **A novel plant growth chamber for continuous monitoring of above-ground and below-ground gas exchange**.

2. Chapter 2: **Experimental assessment of the relation between above-ground and below-ground carbon investments in maize plants and their cost-benefit ratios**. All data and computations for Chapter 1 and 2 are found here:

   https://doi.org/10.5281/zenodo.10384366 .

3. Chapter 3: **Evaluating cost-benefit ratios of carbon allocation across species and environmental conditions**. All data and computations presented in this Chapter are found here:

   https://doi.org/10.5281/zenodo.10386962 .

In Chapter 1, a growth chamber with separation of the above and below-ground compartment using a wax layer is presented. This chamber allows for continuous monitoring of CO_2 and H_2O fluxes in both compartments using a LI-6800 infrared gas analyzers. To minimize heterotrophic soil respiration, a C depleted potting substrate is used for growing the experimental plants.

In Chapter 2, the influence of soil penetration resistance on the cost-benefit ratios of maize plants is discussed.

In Chapter 3, cost-benefit ratios are evaluated across two species (maize and barley) and two bulk densities. This analysis aims to determine whether the ratios exhibit more variability across distinct plant species or diverse environmental conditions.

Chapter 1

A novel plant growth chamber for continuous monitoring of above-ground and below-ground gas exchange

This chapter will be submitted as a methods paper to AoB Plants.

1.1 Abstract

Plants absorb carbon (C) from the atmosphere during the day through photosynthesis and release water vapor. C assimilated above-ground is either respired, utilized for growth and maintenance, stored or translocated to the roots. The exact amount of root C allocation does not equal root biomass due to significant C loss through root respiration and exudation. This makes it challenging to accurately assess the C costs and benefits of plant root systems in terms of water and nutrient uptake. To better quantify the costs and benefits of plant roots, a novel plant growth chamber that enables continuous and separate monitoring of above and below-ground gas exchange is developed and tested. The two compartments were separated by a gas impermeable

layer of fat, and a custom-developed C-depleted potting mixture was used to reduce CO_2 release due to microbial decomposition of pre-existing soil C. Each compartment of the growth chamber was connected to an infrared gas analyzer, enabling simultaneous monitoring of above-ground (CO_2 assimilation, nocturnal respiration and H_2O transpiration) and below-ground fluxes (H_2O evaporation and CO_2 respiration). As a first test of the system's performance in accurately quantifying the fluxes under study, chemical agents, calcium carbonate ($CaCO_3$) and hydrochloric acid (HCl) were used to cause a known amount of CO_2 release below ground, while soda lime was used to cause CO_2 uptake above ground. Fluxes were measured over several days and the cumulative exchange of CO_2 above and below-ground was then compared to the total amount of CO_2 released or taken up by the chemical agents, determined by chemical analysis before and after the experiment. Finally, the system was tested with real plants to demonstrate its ability to measure the dynamics of above and below-ground fluxes simultaneously. C content of the plant biomass and potting substrate were determined before and after the experiment in order to assess whether the measured fluxes were consistent with the change in total C storage in the system. The tests with reference chemicals revealed a rapid response in the measured fluxes below-ground to a change in CO_2 evolution (within tens of minutes) and deviations of less than 10 nmol s^{-1} between the measured mean CO_2 flux and the chemically determined CO_2 evolution. For the CO_2 absorption above ground, the error was 1%. Tests with real plants revealed that the difference between cumulative fluxes and increase in plant biomass was between 14 to 17%, i.e. the plants seemed to have taken up 17% more C than was found in the plant biomass at the end of the experiment. The missing C in the below-ground carbon pool (excluding root biomass) could not be accounted for. Comparison of cumulative evapo-transpiration rates (including below-ground evaporation) with the cumulative weight loss between watering events revealed a close correspondence between these independent estimates of water loss (within

11%). The experimental system described here has the potential to greatly advance research on shoot-root interplay and C allocation in small plants.

1.2 Introduction

Plant shoots use solar energy to produce sugars out of atmospheric carbon-dioxide (CO_2) through photosynthesis. These sugars are then converted to a variety of organic compounds, translocated to other plant parts or stored away for later use. Roots, on the other hand, play essential roles in anchorage and the uptake of water and nutrients from the soil. Additionally, they engage in biological and chemical interactions with the soil. Root interactions with the soil occur primarily within the rhizosphere, a narrow region of soil directly influenced by the presence of plant roots. The rhizosphere provides a diverse range of habitats conducive to the thriving of a myriad of microorganisms, encompassing bacteria, actinomycetes, protozoa, nematodes, microalgae, and fungi. In the rhizosphere, chemical and biological processes are intensified due to the release of root exudates, which attract microorganisms and impact nutrient cycling (Eshel and Beeckman, 2013).

Shoot gas exchange (assimilation and transpiration) has been studied extensively at various scales from leaf (Kennedy and Johnson, 1981; Schlüter et al., 2003; Kopczewski et al., 2020) to whole canopies (Kölling et al., 2015; Salvatori et al., 2021) in a bid to understand the functioning and response of plants and ecosystems to their environment. Commercially available gas exchange measurement systems for single leaves have been developed to precisely control and measure the environmental conditions surrounding the photosynthetic tissue. These systems have been improved over time to be versatile enough to be carried out alongside deductions of other photosynthetic parameters like leaf conductance and intercellular CO_2 mole fraction (Long and Bernacchi, 2003; Kölling et al., 2015). This advancement makes the study of leaf gas-exchange, predominantly photosynthesis, more acces-

sible and enables more detailed investigations compared to canopy gas exchange (Iersel and Bugbee, 2000).

Single leaf gas exchange measurements provide valuable insights about the immediate physiological responses of individual leaves. However, such measurements often exhibit weak correlations with net primary production (NPP) (Gent, 1998). NPP represents the comprehensive accumulation of biomass and energy over time at the whole plant level. Thus, the correlation may be weakened by factors such as variations in leaf age, canopy position, and distribution of resources within the plant, all of which can influence NPP but may not be fully captured in isolated leaf-level measurements (Iersel and Bugbee, 2000; Kölling et al., 2015). Conversely, studies conducted at the level of the entire shoot and canopy offer a closer approximation of natural growth environments, leading to improved precision when quantifying shoot gas exchange rates and their relationship with NPP dynamics (Donahue et al., 1997).

Plant growth chamber systems that allow for the monitoring of whole shoot gas exchange have been developed and applied to a wide variety of plants (Donahue et al., 1997; Burkart et al., 2007; Kölling et al., 2015). These systems allow gas exchange measurements of plant shoots while isolating the root zone to avoid any interference from the roots and soil respiration. Developments documented in recent studies of whole shoot gas exchange measurements include flexible systems that enable simultaneous multi-plant measurements while incorporating different lid sizes to allow the measurement of different-sized herbaceous species (Kölling et al., 2015), small trees (Kläring and Körner, 2020; Birami et al., 2020), enabling the simulation of dynamic environmental conditions such as light (Salvatori et al., 2021) as well as measuring small plant and whole canopy gas exchange at different airspeeds (Poulet et al., 2020).

Approximately 50% of the total above-ground photoassimilates are translocated below-ground (Lambers, 1987). Consequently, roots play a substantial

role in the C budget of plants through autotrophic root respiration, accounting for a C loss of 30% to 60% below-ground (Lambers, 1987). Additionally, roots constitute at least 50% of the total soil respiration (Hanson et al., 2000). Despite its smaller contribution, root exudation represents a notable fraction of C loss from plants. Up to 20% of assimilated C is lost through root exudation (Sasse et al., 2018). However, quantifying these costs, especially root respiration's impact on the overall plant carbon balance, is challenging due to various technical difficulties and inherent variability.

Experimental and technical difficulties in the isolation of root gas exchange (respiration) from other soil respiration components especially in intact plants have resulted in less progress in quantifying root respiration and is manifested in the reduced number of studies that focus on studying root respiration as compared to shoot gas exchange (Kuzyakov and Larionova, 2005).

In the early stages, assessing root respiration relied primarily on invasive techniques that disrupted the natural state of roots. These methods involved uprooting the plants from their native environments and subjecting them to short-term incubation, followed by measuring their respiration over a period ranging from two to forty-eight hours. These processes included integrating various components (component integration) and, in some cases, excising roots from the plant for analysis. Displacing roots from their natural environment to measure respiration produce generally unreliable data, that do not reflect reality and differs significantly from one experiment to the next (Kuzyakov and Larionova, 2005).

In a semi-destructive approach known as the root exclusion method, roots were intentionally excluded from the soil, allowing for a comparison of respiration values with those obtained from rooted soil. This method aimed to assess the contribution of roots to overall respiration in the soil ecosystem. This method, despite its use as an alternative approach, has its limitations. Merely comparing respiration values between rooted and root-free soil is not

a reliable measure for root respiration. This is due to the fact that excluding roots does not completely isolate the rhizosphere microbes, which persist in degrading exudates even when separated from the soil matrix. Additionally, the presence of rhizodeposits from living roots can induce rhizosphere priming effects, further complicating the accurate estimation of autotrophic root respiration (Kuzyakov and Larionova, 2005). These considerations underscore the challenges in precisely quantifying root respiration using the root exclusion method and highlight the need for more refined techniques in studying this aspect of plant physiology.

Diverging from the destructive methods of root respiration analysis, alternative experimental approaches were employed that involved carrying out root respiration measurements in intact plants by either growing roots in nutrient solutions (Bloom et al., 1992), inorganic media like gravel (White and Childers, 1944) or using tree girdling and shading techniques.

Tree girdling rely on limiting the flow of photosynthate to the roots and comparing heterotrophic respiration to whole soil respiration at a latter time. This method assume the constancy of the former without taking into account decomposition of newly dead roots (Kuzyakov and Larionova, 2005). Tree shading on the other hand has a disadvantage in that it relies on the assumption that the shaded area beneath the tree canopy is representative of the root system's respiration rate. This assumption may not always hold true as root respiration can vary spatially within the root system thereby underestimating or overlooking localized hotspots or areas of higher root respiration, leading to potential inaccuracies in the overall estimation of root respiration. Additionally, the presence of the tree canopy itself can influence environmental conditions, such as light availability and temperature, which can further affect root respiration rates (Kuzyakov and Larionova, 2005). Therefore, while the tree shading method is a convenient and non-destructive approach, it may not provide a precise assessment of root respiration. Root respiration measurements in nutrient solutions do not account for energy expenditure

and concomitant respiratory fluxes that may arise due to soil penetration by plant roots and can only be done with plants that thrive in hydroponic media. Concerns persist about potential inaccuracies in estimating respiratory fluxes due to the artificial nature of these methods (Kuzyakov and Larionova, 2005).

Efforts to design root respiration measurements similar to natural conditions have led to observations of root respiration in soil substrates. Minchin et al. (1977) carried out continuous and in-situ monitoring of below-ground respiration on intact cowpea plants rooted in a soil medium by using infrared gas analysis to measure CO_2 produced by the roots within 15 to 35 days. Similarly, Bouma et al. (1997) designed an automated and open gas exchange system that allowed continuous measurements on multi plant chambers with intact roots in soil. Their innovative system enabled the measurement of below-ground respiration across a range of soil CO_2 concentrations and temperature conditions.

It is important to note that both studies measured total below-ground respiration and did not distinguish between the heterotrophic and autotrophic fractions. However, the latter study utilized an autoclaved fine sandy soil and referred to their findings as root respiration, assuming a minimal contribution from microbial respiration in the sterilized sandy soil, as proposed by Palta and Nobel (1989).

While the individual gas exchange of shoots and roots and whole plant gas exchange has been extensively studied and documented in the literature, the simultaneous monitoring of these fluxes, with spatial separation, has only recently gained attention from a limited number of researchers. The significance of such systems cannot be overstated, as both shoot and root processes occur in parallel with each other in nature. Ideally, studying these processes simultaneously allows for a more comprehensive understanding of plant physiology and the interplay between shoots and roots. Furthermore, it offers the opportunity to explore the costs and trade-offs associated with plant root

resource acquisition processes and understand the underlying mechanisms that drive these trade-offs, shedding light on the strategies plants employ to optimize their growth and survival in varying environmental conditions.

Kläring et al. (2014) described an approach for simultaneously monitoring root and shoot gas exchange in a single cucumber plant cultivated in a hydroponic solution within a plant cuvette. This study provided valuable insights into the coordination of these processes in a controlled environment. In a more recent publication, Kläring and Körner (2020) expanded upon this concept by presenting a scaled-up approach that allows for the simultaneous monitoring of at least eight plants in a greenhouse setting. This offers the advantage of separately monitoring the gas exchange of shoots and the hydroponic root environment while maintaining precise control over environmental conditions. This expanded experimental setup provides a more comprehensive understanding of plant gas exchange dynamics at a larger scale albeit in a hydroponic medium. It also offers climate control, root environment manipulation, and the introduction of air pollutants and plant-relevant gases into the chambers.

Additionally, a similar multi-plant experiment involving soil-grown plants have been conducted, coupled with C isotope discrimination analysis (Barthel et al., 2011). This study, while providing great insights into the diel variations in gas exchange and C assimilation processes, shedding light on the temporal dynamics of root and shoot interactions in Beech (Fagus sylvatica) saplings, did not explicitly differentiate between root respiration and soil respiration. In a comparable study, experiments were conducted using Miller (Pinus halepensis) seeds. The plants were subjected to different conditions, including well-watered and drought-treated. Continuous measurements of gas exchange were taken at the whole-tree level and supplemented by primary metabolite analysis to shed light on the effects of elevated CO_2 on tree water use efficiency and carbon metabolism under drought and well-watered conditions (Birami et al., 2020).

Although a few studies have documented the simultaneous monitoring of root and shoot gas exchange, they are not without limitations. Research conducted in hydroponic environments presents particular drawbacks, such as limited mechanical resistance for roots, the absence of dynamic rhizosphere interactions, and potential alterations in root architecture due to hydroponic growing conditions, which may reduce stress response adaptations and impact the practical relevance of the findings. On the other hand, the studies performed using soil substrates initiated their research at a later stage such as with tree saplings or established plants, rather than starting from the germination or seed stage. This approach may not fully capture the gas exchange dynamics during the early developmental stages of plants.

Hence, there is need for additional research that encompasses a wider variety of plant species and includes the monitoring of gas exchanges from the initial stages of plant growth. This broader approach is essential for achieving a more comprehensive understanding of root-shoot interactions.

Addressing these gaps, the main objective of this study was to develop and evaluate a plant growth chamber that allows for semi-continuous, separate, and simultaneous monitoring of above-ground (shoot) and below-ground (root) gas exchange throughout the entire life cycle of a plant. The study was carried out on a C depleted substrate. Additionally, soil respiration measurements were taken using a custom potting mixture to establish baseline levels of respiration. This comprehensive approach aimed to enhance our understanding of plant gas exchange dynamics and its interaction with the soil environment.

To accomplish these objectives, two distinct yet interconnected experiments were conducted, each serving a specific purpose:

1. Testing the accuracy of the growth chamber setup in quantifying the target fluxes in each compartment.

2. Assessing the system's effectiveness in capturing shoot and root fluxes and respiration from the seedling stage up to the point where they

develop into small plants.

These experiments collectively aimed to provide valuable insights into the design and performance of the growth chamber setup, allowing for a comprehensive understanding of shoot and root gas exchange processes over the course of a plant's life cycle.

1.3 Materials and Methods

1.3.1 Description for a Single Growth Chamber

The growth chamber (GC) consists of two distinct compartments, and a connecting cylinder which connects them (Figure 1.2). The materials and dimensions of the growth chamber were selected and designed to ensure compatibility with the plant magnetic resonance imaging (MRI) facility at the Institute of Bio- and Geosciences, IBG-2: Plant Sciences, Forschungszentrum Jülich GmbH.

The below-ground compartment consists of a plexiglas cylinder with a length of 300 mm and an inner diameter of 80 mm while the above-ground compartment consists of a larger plexiglas cylinder with a length of 300 mm and an inner diameter of 140 mm, each cylinders with a separate lid (Figure 1.1).

The connecting cylinder was constructed by vacuum casting using polyurethane (PX 5213). The design is such that it consists of four cylindrical sections to enable a transition between the narrow below-ground and the wide above-ground part, while leaving a separated air space above the soil in the below-ground compartment for soil gas exchange, and a sealed connection for the plant to grow its roots in the soil while keeping its shoot in the above-ground control volume.

The first cylindrical section of the connecting cylinder allows for a perfect alignment of the above-ground plexiglas cylinder. The second section consists

of six holes equipped with teflon-tape sealed quick release tube connectors CPC PMC4204 (Colder Products Company, Minnesota, USA). Three of the holes in this section are paired with three corresponding holes in the third section equally equipped with teflon-tape sealed quick release tube connectors Masterflex^{TM} 30621-32 (Antylia Scientific, Illinois, USA) all working together as air/water inlet/outlets to the two growth chamber compartments). The third section also houses the seed chamber and allows a perfect alignment of the below-ground plexiglas cylinder. The seed chamber is the fourth cylinder of the connecting plate. It serves to hold the seed in place and creates a sealed connection between the two growth chamber compartments. The above-ground compartment was separated from the below-ground compartment via a fat layer, as modified from Koebernick et al. (2015).

All dimensions of the component parts of the growth chamber are presented in Figure 1.1 while the 2D schematic and the actual live growth chamber are shown in Figure 1.2.

1.3.2 Growth Chamber Light Supply

Each growth chamber was supplied with an individual light source mounted on PVC columns to shield each growth chamber from its neighbours and to prevent light supply interference between chambers. Each column consisted of a single LED lamp (Cree XLamp CXA2520, Durham, USA), covered with a reflector (Carclo 12684-R2 54mm Medium Spot Mirror Reflector, Vossloh Schwabe Deutschland GmbH, Schorndorf, Germany) and mounted on an aluminum bar (180 mm X 25 mm) and screwed to a 3D-printed ring with outer diameter of 150 mm.

The entire light unit was then attached to a non-transparent white PVC tube of 630 mm length and inner diameter of 150 mm. The base of the tube was slightly expanded to accommodate the connecting cylinder. These light columns were calibrated to deliver light of 600 μmols m^{-2} s^{-1} photosynthetic photon flux density (PPFD)) at the top of the above-ground cylinder,

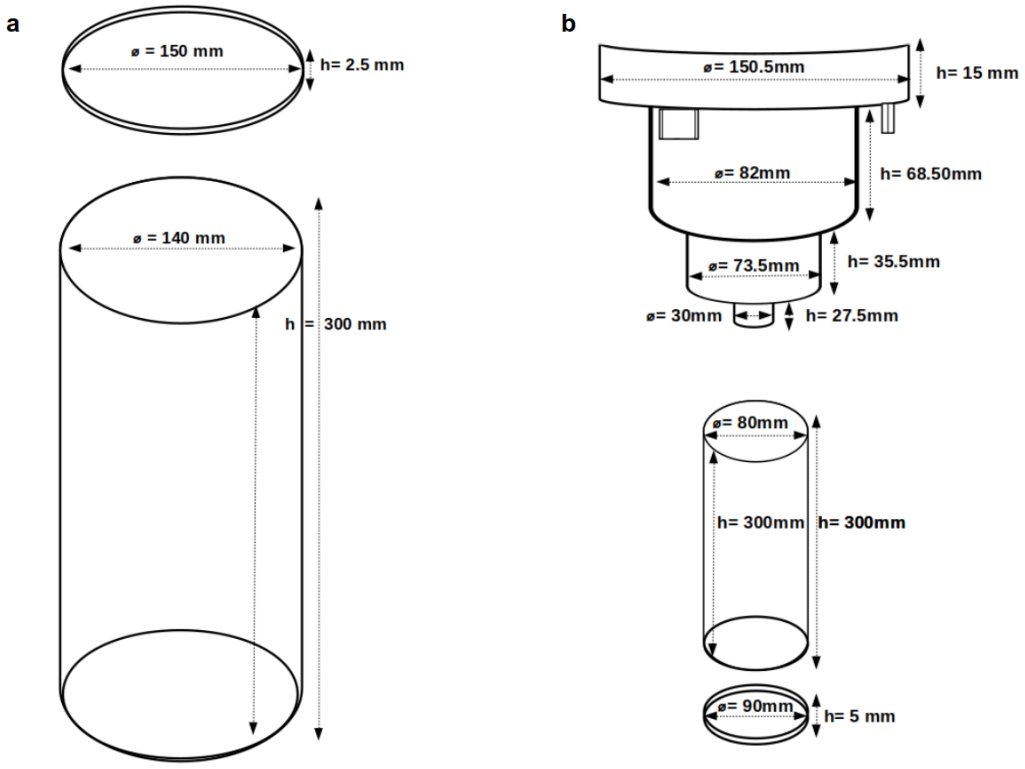

Figure 1.1: **(a)** Above-ground and lid compartment with relevant dimensions; **(b)** Upper: Connecting cylinder with relevant dimensions; Lower: Below-ground compartment and lid with relevant dimensions.

corresponding to the height that the plants reached after 3 weeks during experimental test runs.

1.3.3 Complete Growth Chamber Setup and Gas Exchange System

To enable continuous and simultaneous measurements of CO_2 and H_2O exchange in each growth chamber compartment, two portable photosynthesis systems (LI-6800, LI-COR, Lincoln, NE, USA), one for each compartment, were used. These were connected to a multiplexing system in order to enable

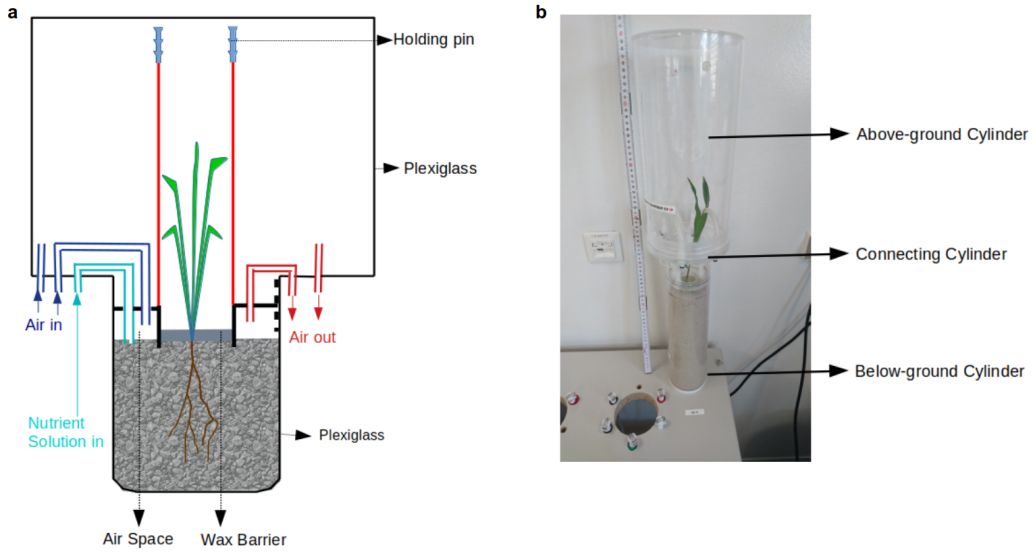

Figure 1.2: **(a)** 2D Schematic of a single whole plant growth chamber showing the above and below ground compartments; **(b)** A live whole plant growth chamber showing the three compartments.

repetitive measurements on 15 growth chambers in short succession.

Ambient air was drawn from the outside about three meters above the ground to avoid large fluctuations in CO_2 concentrations using a polyamide hose of 17 mm (1.510.1601.14 Polyamid Hose, DN17, HUMMEL AG, Denzlingen, Germany). The incoming air was then split into two channels, one for the above-ground compartments and the other for the below-ground. Each channel was passed through a 50 l mixing container to introduce an additional buffer and avoid spikes in CO_2 concentrations. To reduce soil evaporation, water was added to the mixing container connected to the below-ground air supply. From each mixing container, air was supplied to the LI-6800.

Gas exchange in both compartments was measured using the LI-6800, one chamber at a time using eight 8-way multiplexers (Vici 8-Port Multiposition Selector Valves, Vici AG International, Schenkon, Switzerland). This was necessary so that during a measurement, both the air entering and exiting the chamber was passing through the LI-6800. For 15 chambers, 2 multiplex-

ers were needed for each flow path, i.e. 8 multiplexers for two (above-ground and below-ground) times two (incoming and outgoing air) flow paths. When transitioning between growth chambers, the switching time of the multiplexers is logged using a custom control program developed in LabVIEW (National Instruments, Munich, Germany). The LI-6800 pumps were set up to pump air at a flow rate of 300 μmols s^{-1} for below-ground and 1000 μmols s^{-1} for above-ground measurements. The airflow to the two chamber compartments was regulated by thirty gas pumps (19K Gas Diaphragm Pump 24 V BLDC, Boxer GmbH, Ottobeuren, Germany), fifteen for each compartment of the growth chambers. This allowed independent control of air flow to each chamber. The temperature of the outgoing air from the growth chamber compartments were measured using thermocouples and the values read using the digital multimeter (DMM) (Keithley DAQ6510, Tektronics, Beaverton, Oregon, USA).

The flow rate of air through the pumps to the growth chambers was calibrated using a flow meter (Honeywell AWM5102VN Flow Sensor, Honeywell International Inc, Charlotte, NC, USA) and set at the same flow rate as the two LI-6800 gas analyzers to minimize changes in steady-state conditions when switching between air supplies through the pumps and the LI-6800. Air flow rate was checked every two days to control for any changes. All tubings were sealed tightly using either parrafilm or vinyl polysiloxane impression material to avoid fluctuations in CO_2 concentrations due to e.g. breathing near the experimental setup.

The full set-up of the growth chamber gas exchange system is presented in Appendix Figure1.8 and the full set-up of the growth chamber is presented in Figure 1.3. A table of all component parts of the full set-up is presented in Appendix Table 1.2. Detailed information about the growth chamber and complete gas-exchange set-up is found in the url below:

https://doi.org/10.5281/zenodo.10275809 .

To enable semi-continuous measurement of fluxes, the LI-6800 gas ana-

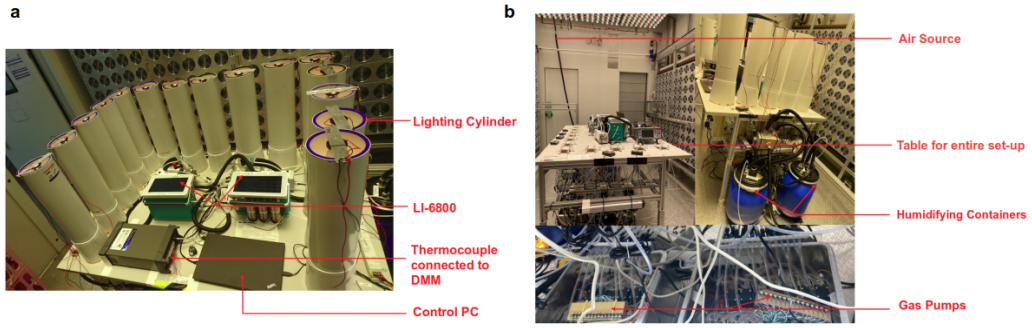

Figure 1.3: Full set-up of the growth chamber and gas exchange system featuring **(a)** 15 growth chambers (covered by their individual light columns), two LI-6800, thermocouple connected to a digital multimeter (DMM) and the control PC and **(b)** Full set-up table without growth chambers, air source, humidyifying containers and gas pumps. Multiplexers and air tubes are under the table and not very visible.

lyzers were switched between the growth chambers every ten minutes such that every growth chamber is measured about 10 times in a 24-hour period. Gas concentrations were calculated based on differences in CO_2 and H_2O flowing into the reference cell and out of the growth chamber compartments using the formulae as described by the LI-6800 handbook below:

$$\mathrm{A} = \frac{\mu_o(C_a w_o - C_a - C_o(w_a - 1))}{C_a - w_a + 1} \tag{1.1}$$

$$\mathrm{E} = \frac{\mu_o(C_a w_a + w_a - w_o(C_a + 1))}{C_a - w_a + 1} \tag{1.2}$$

Where A (mol s^{-1}) refers to CO_2 concentration of the air coming out from sample cell. A is positive for the removal and negative for the addition of CO_2. E (mol s^{-1}) refers to H_2O gain (evapotranspiration) in air coming out from sample cell. μ_o (mol s^{-1}) refers to the molar flow rate of air entering the chamber, C_a (mol mol^{-1}) and C_o (mol mol^{-1}) refer to the mole fraction of CO_2 in the incoming air and in the chamber respectively while w_a (mol mol^{-1}) and w_o (mol mol^{-1}) refer to the mole fraction of water in the incoming

air and in the chamber respectively.

When retrieving data from the LI-6800, CO_2 fluxes are expressed as positive for CO_2 uptake and negative for CO_2 release. To classify assimilation or respiration fluxes during the experiments, I employ a light on and off regime. For below-ground measurements, all negative fluxes are categorized as respiration. In the above-ground context, when the light is off, negative values are attributed to respiration, while positive values represent above-ground net shoot assimilation. During data analysis, respiration is depicted as positive CO_2 release, whereas assimilation is denoted as positive CO_2 uptake. The addition of H_2O to the airstream is registered as a positive value by the LI-6800, and this convention is maintained both during data analysis and in the figures. Data was continuously logged directly on the LI-6800 at five-second intervals throughout the experiment's duration. To prevent system crashes and data loss, a new file was automatically initiated every twenty-four hours.

Leaks in the gas tubing systems could be detected by spikes in CO_2 concentrations measured by the LI-6800 when exhaling near a leak. Furthermore, to ensure that the separation between the above-ground and below-ground part was leak proof, CO_2 rich air (exhaled air) was introduced in either the above or below ground compartment, followed by verification if the CO_2 concentration in the other compartment was affected. Experiments commenced after all leaks were found and resolved.

During test runs, it was observed that air from the previous chamber was still left in the gas tubes and would erroneously be recorded for the preceding chamber. Also, slight changes in the flow rates between the LI-6800 and the pumps led to unsteady flux signals during switches from one chamber to the next. This was also the case after the matching procedure of the infrared gas analyzers (IRGA) (an in-built procedure of the LI-6800 to ensure that CO_2 and H_2O concentration in the sample and reference cell are equal when receiving identical air streams); a procedure performed every thirty minutes.

To mitigate against this, data was continuously recorded between chambers in order to determine the average time it takes to stabilize the fluxes after switching from one chamber to the next and after matching the IRGAs. It was observed that it took about a minute to stabilize the fluxes and so during data analysis, the first one minute of data after switches or matches was discarded by excluding the data logged during this time frame before subsequent data analysis was carried out.

1.3.4 Test of Measurement Accuracy

The first set of experiments were carried out to verify the capability of the set-up to capture and accurately quantify gas fluxes within the growth chamber compartments using chemicals to either absorb or evolve CO_2. Another objective was to quantify the delays in fluxes due to lack of mixing. These tests were performed with one growth chamber, with each compartment hooked up to a separate LI-6800.

Chemically Simulated Above-ground Assimilation

To simulate CO_2 assimilation, a similar method as Salvatori et al. (2021) was adopted. 20 g of soda lime ($CaHNaO_2$) was homogenized in an air-tight ziploc bag, 10 sub-samples were taken from this and the initial C concentration per mass of sample was measured with an elemental analyzer (Vario MacroCube, Elementar, Hesse, Germany). The remaining 18.73 g was placed on a flat aluminum plate and placed in the above-ground compartment of the growth chamber. This compartment was sealed and isolated from the below-ground compartment and CO_2 concentrations of the incoming and outgoing air were measured for four days. At the end of the experiment, the soda lime was removed, weighed again and another 10 sub-samples were taken to determine post-exposure C-content per mass of sample. At the end of the experiment, the amount of C accumulated by the soda lime in grams was

calculated by taking the difference between total C in used and unused soda lime samples as obtained by elemental analysis. The time integral of the CO_2 assimilation rate over the experimental period (equation 1.3) was compared to the difference between initial and final amount of C in the soda lime as a means to validate the fluxes measured by the LI-6800.

$$\Delta F_{soda\ lime} = \int_{t1}^{tn} F_{ass} dt \tag{1.3}$$

where $\Delta F_{soda\ lime}$ (mol) is total C fixed absorbed by the soda lime and F_{ass} (mol s^{-1}) is the rate of assimilatory fluxes in the chamber.

Chemically Simulated Below-ground Respiration

We used calcium carbonate ($CaCO_3$) and hydrochloric acid (HCl) to simulate below-ground CO_2 evolution (analogous to soil respiration). The reaction between calcium carbonate ($CaCO_3$)and hydrochloric acid (HCl) evolves CO_2. CO_2 evolution from this reaction was then quantified by the LI-6800 to determine its concentration in the out-going air stream from that compartment. The equation is given below:

$$2HCl + CaCO_3 \rightarrow CaCl_2 + CO_2 + H_2O \tag{1.4}$$

In order to evaluate that subtle changes in the below ground compartment could be measured instantaneously during experiments involving plants, it was pertinent to determine the amount of time it will take for the set-up to detect fluxes during measurements; and if the expected flux release rates will be properly quantified by the LI-6800. To do this, we adopted the method of Iersel and Bugbee (2000).

Three CO_2 evolution rates (20, 40 and 80 nmol s^{-1}) were simulated by dripping 10 ml 0.1 M HCl at 0.024, 0.046 and 0.096 ml min^{-1} flow rates respectively into a 50 ml plastic container containing 50 g $CaCO_3$ positioned at the bottom of the below-ground compartment of the growth chamber and iso-

lated from the above-ground compartment using parafilm. The syringe delivering the HCl was connected to a syringe pump (LEGATO 110, KD Scientific Inc, Holliston, MA, USA). To account for gas diffusion times through the different chamber contents, we used an empty cylinder, and two below-ground cylinders, each packed with dry and wet potting medium; quartz:bentonite (80:20) respectively. The below-ground cylinders were packed to a bulk density of 1.4 gcm^{-3} by filling the cylinder with the appropriate mass of potting substrate and shaking until it filled the volume of the below-ground cylinder. The wet substrate contained 20 % water by volume. The resulting CO_2 release rates were measured and compared to the expected results.

1.3.5 Utilitization of Custom Potting Mixture and Growth Chamber to Capture Above and Below-Ground Fluxes

The next set of experiments were designed to test the utility of the custom potting substrate to support plant growth and test the capability of the set up to capture above and below-ground fluxes in living plants over a specified experimental period. Maize (Zea mays L. var. Badische gelbe) was used to carry out the preliminary tests.

Potting Substrate

The substrate used to grow the experimental plants was a custom-made C-depleted potting mixture. Preliminary plant growth experiments with different potting substrates consisting of burnt (at 600 °C) and unburnt samples of a standard soil Lufa Speyer 2.1 (LUFA Speyer, Germany), bentonite, vermiculite and quartz in different proportions (Appendix Table 1.3) showed that plant growth in the mixture of 80 % quartz and 20 % bentonite (QB) was the most similar to the control soil (unburnt Lufa Speyer 2.1). The substrate has a maximum water holding capacity (WHC) (field capacity) of 32.0 ± 2.2

g/100 g as measured following the method of (Blažka and Fischer, 2014) and was fertilized using 5 g/l of Peter's allrounder fertilizer (20+20+20+TE, ICL Growing Solutions, Tel Aviv, Israel). The % C content of the components of the potting mixture are 6.94 ± 1.31, 0.0020 ± 0.0008 and 0.06 ± 0.02 for Peter's allrounder, fertilizer, quartz and bentonite respectively. 3 bulk densities were used in the experiments (1.40, 1.45, 1.55 gcm^{-3}), with 5 chambers for each bulk density. All growth chambers had a volumetric "soil" water content of 20%.

Plant Material

The CO_2 and H_2O fluxes (assimilation, nocturnal respiration, and transpiration above-ground) and (respiration and evapotranspiration below-ground) were monitored over a nineteen day period for fifteen maize plants. Seeds of maize (Zea mays L. var. Badische gelbe) were weighed and sterilized in 70 % ethanol for a minute, germinated on wet filter paper in sealed petri dishes and placed in a dark cabinet at room temperature for 72 hours. After germination, the seedlings were transferred to the soil substrate, buried 3 cm deep in the middle of the seed chamber.

Separation of Growth Chamber Compartments

The separation of the above-ground and below-ground compartments was achieved by pouring melted palm fat at a temperature of 28 °C (semi-solid consistency) in the seed chamber, creating a 0.7 cm thick separation layer between the below and above-ground compartment, adapting the method of Koebernick et al. (2015). In experimental test runs, different proportions of different wax mixtures (parrafin (melting point: 52°C), beeswax (melting point: 62°C) vaseline (melting point: 46°C) were also tested but could not be used in the experiments because the test seedlings incurred heat damage and failed to thrive.

Despite the similarity in temperature between coconut fat (melting point:

33°C) and palm fat (melting point: 32°C), the former was excluded from the experiment due to its inherent brittleness and proneness to cracking. This characteristic had the potential to compromise the integrity of the established separation layer.

Growth Conditions

Plants were grown in a climate chamber in a 14/10 hours light/dark regime, and a temperature of 20 °C during light and 16 °C during the dark. Between the fifth and ninth day of the experiment, the lights were permanently switched on due to a malfunction of the timer. Lighting was provided using the light columns described in Section Growth Chamber Light Supply. Fertilizer was supplied once at the beginning of the experiment and the plants were rewatered to a constant weight every other day from the top of the below-ground cylinder using the water supply tubes in the growth chamber.

Gas Fluxes Measurement

The above and below-ground gas exchange of the fifteen maize plants were studied for nineteen days using the set-up described in Complete Growth Chamber Setup and Gas Exchange System.

Pre-experimental Total and Dissolved C Analysis

The pre-experimental total C content of the maize seeds was determined by randomly selecting 10 seeds, oven-drying them at 65 °C for 24 hours to eliminate any extra moisture that may have been absorbed while in storage, weighed, homogenized and analyzed for total C using an elemental analyzer (Vario MacroCube, Elementar, Hesse, Germany). The mass percentage of C in the seeds was subsequently calculated.

For the potting medium's total C content, each component (quartz, bentonite, and fertilizer) was individually analyzed for total C, and the mass

percentage of C was calculated. This process involved using 3-6 homogenized sub-samples for each component. The resulting C values were then aggregated to establish the pre-experimental C content in the potting medium for each cylinder. These total C assessments were conducted four times for quartz and twice for bentonite and the fertilizer to determine the range. The mean values from these distinct experiments were employed to estimate the total C content of the entire below-ground cylinder.

The dissolved organic carbon (DOC) content of all the components of the potting substrate were analyzed by dissolving and mixing 5 - 6 sub-samples of each thoroughly in 250 ml of water. The samples used here were sampled separately from those used for the the total C experiments described above. The decanted solvent was filtered through a 0.4 μm syringe filter and analyzed for DOC using a Torch TOC Combustion Analyzer (Teledyne Tekmar, Mason, OH, USA). The resulting concentration in mg/l was multiplied by the volume of wash water to obtain the DOC concentration in mg. The pre-experimental DOC then was then calculated for each chamber as described above. DOC experiments were performed twice for the fertilizer and once for quartz and bentonite. The mean value of the two DOC experiments for the fertilizer was used for whole below-ground cylinder DOC estimates.

Harvest and Post-Experimental Total C and DOC Analysis

At the end of the gas-exchange experiments, plant shoots were harvested and the fresh mass measured on a weighing balance. Subsequently, the bottom of the below-ground cylinder was removed and the substrate gently pushed out using a piston. The potting substrate was carefully washed with up to 8 l in a large bowl to disengage the roots, while leaving them as intact as possible. This was done by placing a 2 mm mesh size sieve on top of a fine sieve (0.5 mm mesh-size) in a large container. Roots escaping from the 2 mm sieve settled on the finer sieve to prevent loss of roots. Roots were patted dry with paper towels to remove adhering water and root fresh mass measured. Any

roots stuck to the paper towels were carefully removed using plastic tweezers. Root and shoots were dried in a drying oven at 65 °C for 48 hours, the dry mass measured and sub samples (about 50 mg) analyzed for total C using an elemental analyzer (Vario MacroCube, Elementar, Hesse, Germany).

Water and soil mixture washed out from the roots were mixed thoroughly by hand and the water decanted from the soil. The wash water was hand-mixed again and using a 40 ml syringe, a sub-sample was drawn and filtered through a 0.4 μm syringe filter and analyzed for DOC using a Torch TOC Combustion Analyzer (Teledyne Tekmar, Mason, OH, USA). The soil was sub-sampled (about 500 mg) and dried at 105 °C for 48 hours and analyzed for total C using an elemental analyzer (Vario MacroCube, Elementar, Hesse, Germany).

Data Analysis

At the end of the experiments, data logged on the LI-6800 was stored in an ASCII-file. This file contains data on date and time of the measurement, flow rates, CO_2 and H_2O concentration in the reference and sample cells, LI-6800 calculated CO_2 (A) and H_2O (E) fluxes and so on. The data was downloaded and the fluxes were assigned to the appropriate growth chambers using the switch time recorded in the labview program of the multiplexers. The formula described in Section Complete Growth Chamber Setup and Gas Exchange System was applied to obtain E and A for both compartments. As quality control, the calculations were confirmed with those calculated by the LI-6800. Median values of the fluxes were calculated every 10 minutes to eliminate extreme outliers which may arise due to fluctuations in CO_2 and H_2O concentration in the reference cell. The daily means of the calculated medians fluxes were then calculated for assimilation, nocturnal respiration and transpiration rates above-ground and respiration and evapotranspiration rates below-ground for all chambers.

Ignoring exudation, it is expected that net primary production (NPP)

can be obtained by taking the time integral of net C fluxes above ground and subtracting it from the integral of C fluxes below ground thus:

$$\Delta F_{C,\ chamber} = \int_{t1}^{tn} F_{c,\ above} dt + \int_{t1}^{tn} -F_{c,\ below} dt \tag{1.5}$$

where $\Delta F_{C,\ chamber}$ (mol) is integrated Li-6800 fluxes and represents total C fixed in the plant biomass (NPP), i.e. the total C assimilated minus the total C respired above and below-ground, $F_{c,\ above}$ and $F_{c,\ below}$ (mol s^{-1}) refer to the integral of net above-ground assimilatory and below-ground respiratory fluxes respectively.

Total H_2O fluxes from the chamber are calculated by adding the time integral of above ground transpiration fluxes to evaporation fluxes below ground thus:

$$\Delta F_{W,\ chamber} = \int_{t1}^{tn} F_{w,\ above} dt + \int_{t1}^{tn} F_{w,\ below} dt \tag{1.6}$$

where $\Delta F_{W,\ chamber}$ (mol) is total H_2O loss from the growth chamber, $F_{w,\ above}$ and $F_{w,\ below}$ (mol s^{-1}) refer to the mean rate of above-ground transpiration and below-ground evaporation fluxes respectively.

Since it is possible to account for all the pools and fluxes in the system, it is expected that $\Delta F_{C,\ chamber}$ will be equal to the sum of the change in state of the plant, potting substrate and wash water C pools.

The change in the C pools are calculated thus:

$$\Delta C_{plant} = C_{plantDM} - C_{seed} \tag{1.7a}$$

$$\Delta C_{substrate} = C_{substrate,\ f} - C_{substrate,\ i} \tag{1.7b}$$

$$\Delta C_{washwater} = C_{washwater,\ f} - C_{washwater,\ i} \tag{1.7c}$$

where C_{plant}, $C_{substrate}$, $C_{washwater}$ are the total C in the plant biomass, potting substrate and wash water as determined by elemental analysis. $C_{plantDM}$ is the C in the plant dry mass at the end of the experiment, C_{seed} is the

estimated C content of the planted seed at the start of the experiment. Subscripts i and f denote initial and final C in the respective C pools. In equation 1.7b, $C_{substrate,\ i}$ refers to the pre-experimental insoluble C in the substrate. This was obtained by subtracting the estimated inital DOC content of the wash water from the estimated initial total C for each below-ground cylinder. In equations 1.7a to 1.7c, units of all variables were either expressed in grams as measured or converted to moles of C. The C concentration per dry mass of plant samples in grams, obtained through elemental analysis, was converted to moles by dividing by 12 g/mol. Biomass in grams was converted to moles by dividing by 30 g/mol, assuming that biomass was represented by CH_2O. This conversion was performed in cases where elemental analysis of the plant material was not feasible.

It is expected that the sum of LI-6800 measured H_2O fluxes above and below-ground ($\Delta F_{W,\ chamber}$ (mol)) should be equal to the gravimetric water loss ($W_{chamber}$ (mol)) from the chambers at the end of the experimental period.

1.3.6 CO_2 Respiration in Custom Potting Mixture

In order to determine base soil respiration in the custom potting substrate, three growth chambers with distinct characteristics from a prior plant growth experiment were selected. The first growth chamber was filled with the potting mixture at a bulk density of 1.5 gcm^{-3}. It served as a seedless control. The second chamber contained a seed which failed to have any apparent germination while the third chamber failed to germinate until the sixth day of the experiment. The last two chambers were packed at a bulk density of 1.4 and 1.5 gcm^{-3} respectively. Following similar conditions as described in Utilitization of Custom Potting Mixture and Growth Chamber to Capture Above and Below-Ground Fluxes, soil respiration was monitored in all three chambers for 10 days and time integral of soil respiration fluxes (-$F_{c,\ below}$, mol s^{-1}) was calculated at the end of the experiment to get the total respiration

in moles.

1.4 Data Availability

All data and computations presented in this Chapter are found here:
https://doi.org/10.5281/zenodo.10384366 .

1.5 Results

1.5.1 Measurement Accuracy

Chemically Simulated Above-ground Assimilation

During the CO_2 absorption experiment using soda lime, the rate of absorption remained consistent (Appendix Figure 1.10), demonstrating an average absorption rate of 37.25 nmol s^{-1} from the beginning until the end of the experiment. There was a 2.1 % increase in the initial weight of the soda lime from 18.73 g to 19.13 g at the end of the experiment. The results of the elemental analysis yielded mean %C by mass values of 0.25 ± 0.03 and 1.23 ± 0.20 for the 10 samples of soda lime before and after the experiment respectively. The difference between pre and post experimental C content of the soda lime sub-samples was 0.19 g (0.0157 moles of C). Time integral of assimilation rate over the experimental period was 0.0156 moles of CO_2, indicating a measurement accuracy within 1% margin of error.

Chemically Simulated Below-ground Respiration

The time series results (Figure 1.9) showed a fast response of the measured CO_2 evolution signal upon injection of 0.1 M HCl into $CaCO_3$ with a steady state usually established within a few minutes. The expected CO_2 evolution signal across the three injection rates and below-ground cylinder contents was

successfully quantified. It was observed that fluxes were mostly overestimated with a mean overall relative uncertainty of about 8 %. In one chamber, the flux was grossly overestimated by 28.5 % (Table 1.1). In general, an absolute error of ± 10 nmol s^{-1} was observed regardless of the intensity of the flux. There was no systematic difference in the flux signals across the different chamber contents (Appendix Figure 1.4).

Table 1.1: Expected and measured CO_2 evolution rate across different HCl injection rates and below-ground (BG) cylinder contents. An absolute error of ± 10 nmol s^{-1} applies regardless of the intensity of the flux. The mean relative error is 8%.

Below-ground (BG) Column Content	**Expected CO_2 Evolution Rate (nmol s^{-1})**	**Measured Mean CO_2 Evolution Rate (nmol s^{-1})**	**Absolute Error (nmol s^{-1})**	**Relative Error (%)**
HCl Injection at 0.024 ml min^{-1}				
Empty BG Column	20	22.6	2.6	13
Dry Substrate Filled	20	18.9	-1.1	-6
Wet Substrate Filled	20	25.7	5.7	29
HCl Injection at 0.048 ml min^{-1}				
Empty BG Column	40	43.2	3.2	8
Dry Substrate Filled	40	42.3	2.3	6
Wet Substrate Filled	40	38.9	-1.1	-3
HCl Injection at 0.096 ml min^{-1}				
Empty BG Column	80	89.3	9.3	12
Dry Substrate Filled	80	83	3	4

1.5.2 Above and Below-Ground Fluxes in Maize Plants

The whole time series of above-ground CO_2 fluxes for all 15 growth chambers (Appendix Figure 1.11, left) show a complete snapshot of the typical output of fluxes measured using the set-up, together with the accompanying fluctuations and outliers. Only the time series of CO_2 fluxes is presented, highlighting the diurnal variations. These diurnal variations are shown in greater detail for one chamber (Appendix Figure 1.11, right). Appendix Figures 1.12 and 1.13 illustrates the progression of the data as it is cleaned up as described in (Section Data Analysis) to arrive at the mean daily flux values.

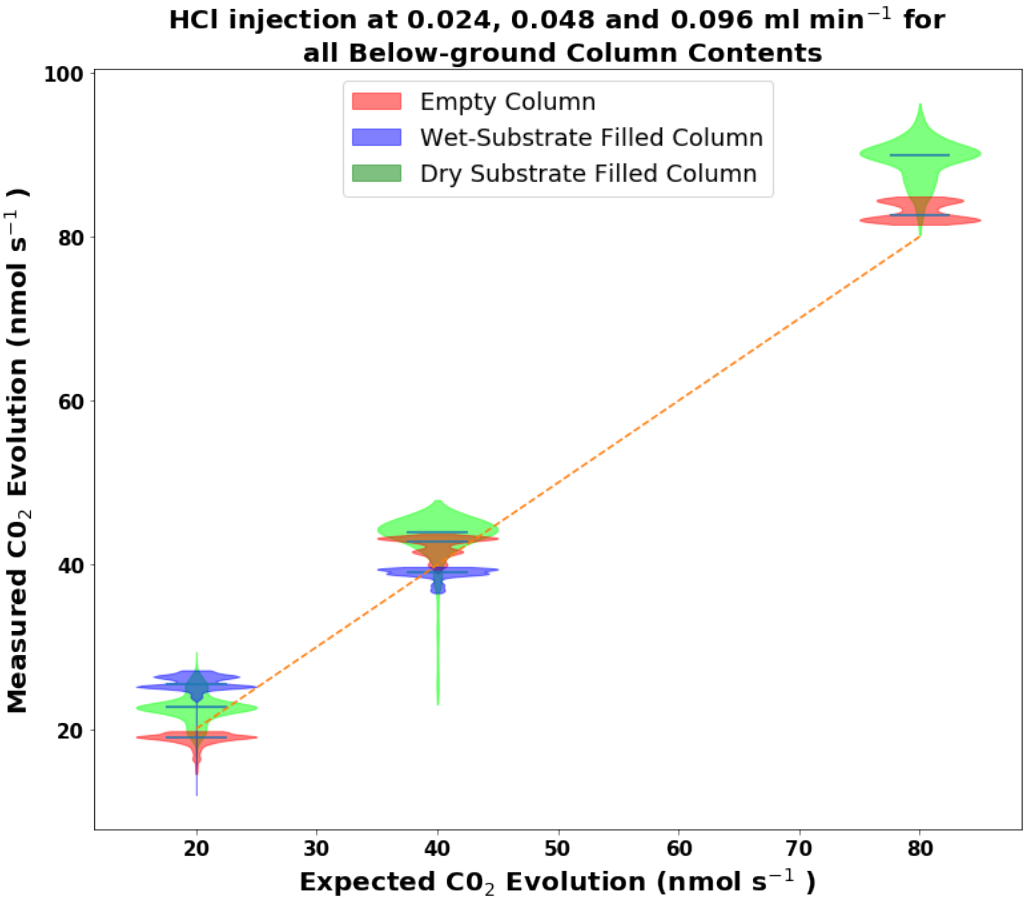

Figure 1.4: Violin plot of expected vs. measured chemically simulated below ground CO_2 evolution rates across different chamber contents. The total spread is consistent regardless of the intensity of flux, with an absolute error of ± 10 nmol s^{-1}. The dashed red line represents the 1:1 line, i.e. perfect correspondence between expected and observed values.

For a comprehensive understanding of the daily trajectory of the fluxes, their daily means were analyzed in greater detail. The results show that the system was able to capture daily changes in the measured fluxes. Mean daily above-ground assimilation and nocturnal respiration across the studied plants showed a close correspondence throughout the experiment. Above-ground assimilation exceeded nocturnal respiration and was an order of magnitude

higher at the end of the experimental period (Appendix Figure 1.12).

Below-ground respiration also increased throughout the course of the experiment (Appendix Figure 1.12) and is of a similar order of magnitude as above-ground nocturnal respiration.

The total C in the plant biomass (mol) at the end of the experiment was correlated with the integrated LI-6800 net C fluxes ($R^2 = 0.94$). In order to further highlight this correlation between the two parameters in question, the results of two separate experiments are displayed on the same chart. Results from experiment 2 show a similar correlation for both parameters in question ($R^2 = 0.98$) (Figure 1.5). The results of these two analyses show that the difference between cumulative fluxes and increase in plant biomass was between 14% to 17% i.e. the plants seemed to have taken up 14% to 17% more C than was found in the plant biomass at the end of the experiment.

To account for C in the system not incorporated into the plant biomass, a mass balance approach was utilized. The difference between the change in the C content of the plants and the net C fluxes determined by the LI-6800 was calculated. Subsequently, this difference was plotted against the sum of the change in C content of the potting substrate and wash water. However, no significant correlation between these variables was revealed in the analysis (Appendix Figure 1.14).

The above-ground day and night time transpiration increased daily as the plants increased in size. Day time transpiration was four times higher than night time transpiration. On the other hand, below ground evapotranspiration decreased with time (Appendix Figure 1.13).

The total evapotranspiration (sum of above and below ground H2O fluxes) measured by the LI-6800 was similar to total gravimetrically measured evapotranspiration at the end of the experimental period with a mean relative error of -11% (Figure 1.6).

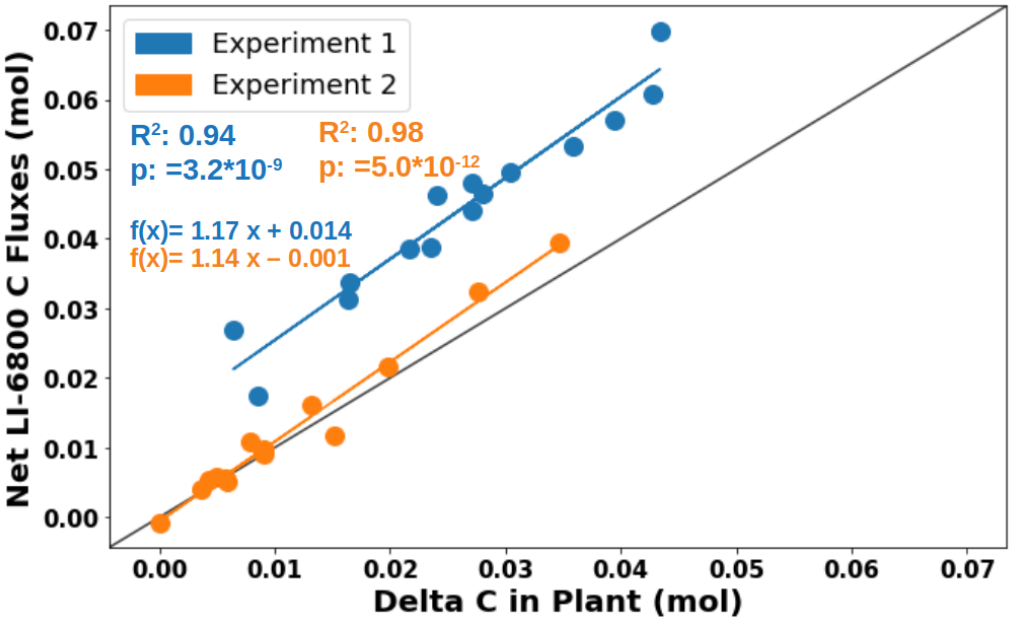

Figure 1.5: Correlation analysis between the sum of delta C pools and integrated net fluxes from the LI-6800. Data is pooled from two different experiments. The linear regression p value for each independent variable tests the null hypothesis that the variable has no correlation with the dependent variable.

1.5.3 CO_2 Respiration in Custom Potting Medium

The results of the analysis performed to determine the basal respiration of the custom potting substrate (Figure 1.7) indicated minimal respiration across all chambers. The mean daily basal respiration of the potting substrate in the growth chamber without seed germination (GC A) was about 1 nmols s^{-1}, throughout the course of the experiment. The growth chamber containing the plant with stalled seed germination (GC B) maintained mean daily respiration values of around 2 nmols s^{-1} and slowly increased as germination occurred. The seedless control chamber (GC C) had respiration values of about 1 nmols s^{-1} in the first few days, increased to up to 3 nmols s^{-1} on the third day, and slowly decreased ending up at about 2 nmols s^{-1} at the

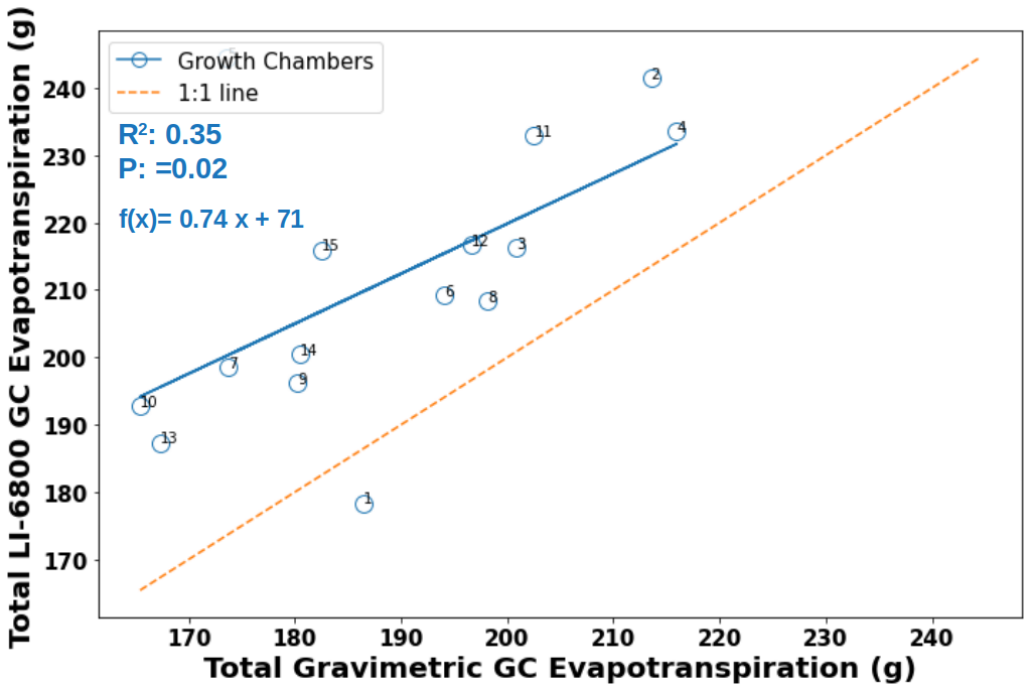

Figure 1.6: Total LI-6800 measured vs gravimetrically derived evapotranspiration.

end of the experimental period.

1.6 Discussion

1.6.1 Measurement Accuracy

Gas exchange measurements in whole plants have been extensively studied, with recent advancements in simultaneous monitoring of roots and shoots. However, only a limited number of studies have focused on tests and system calibration (Iersel and Bugbee, 2000; Salvatori et al., 2021). Adopting similar methods like these authors, both compartments of the growth chamber were tested using chemical agents, calcium carbonate ($CaCO_3$) and hydrochloric acid (HCl) to cause a known amount of CO_2 release below ground, and soda

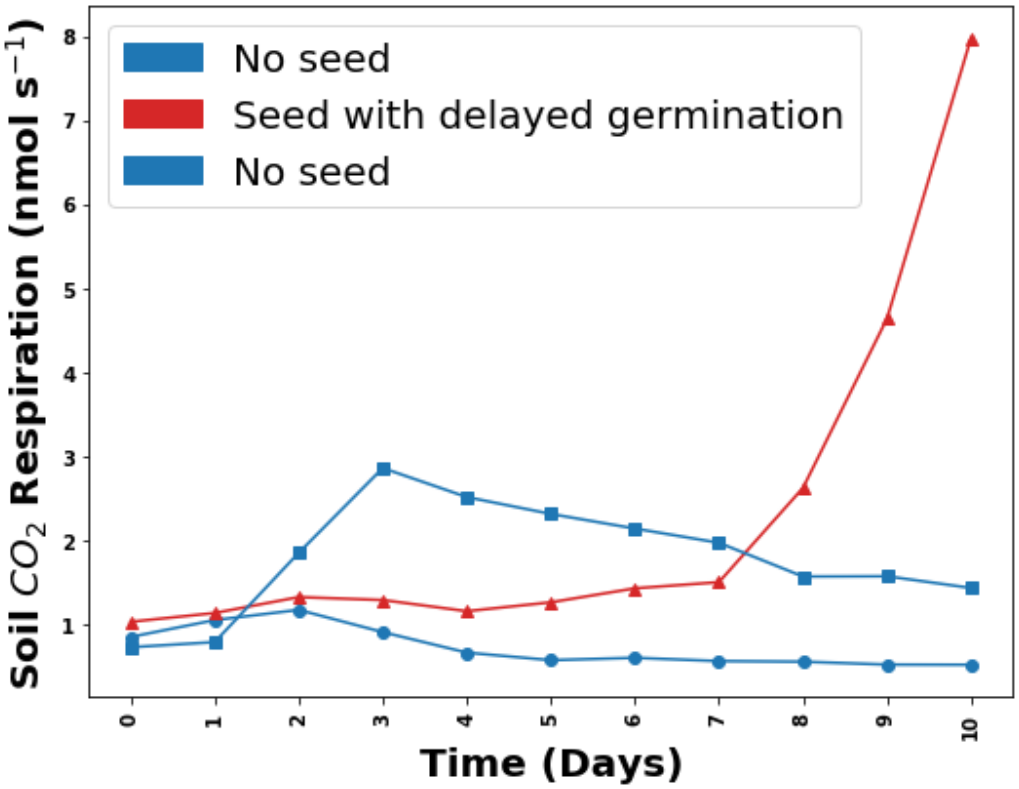

Figure 1.7: Time series of CO2 evolution in the custom potting substrate over a 10-day period. (GC A = growth chamber without seed germination; GC B = growth chamber containing the plant with stalled seed germination and GC C = seedless control).

lime to cause CO_2 uptake above ground. The aim of the tests was to assess the system's performance in accurately quantifying the fluxes under study. The calibration outcomes for the above-ground compartment displayed a reduced error margin (1%) in contrast to the earlier investigation conducted by (Salvatori et al., 2021) (7%) and validates the effectiveness of the experimental setup in measuring CO_2 assimilation with minimal error. On the other hand, the time series results of the below-ground calibration experiment demonstrated a rapid response of the CO_2 evolution signal upon HCl injection into $CaCO_3$, reaching a steady state within a short time. This indicates

the effectiveness of the experimental setup in capturing the CO_2 evolution process in real time. Despite this prompt signal behavior, assessments conducted for the below-ground section yielded a mean relative uncertainty of 8%, (Table 1.1) exceeding the uncertainties observed in a calibration experiment involving similar chemicals within a comprehensive plant gas exchange system (Iersel and Bugbee, 2000), where an impressive precision of 100% was achieved.

The relative uncertainty, varying between -6% to 29% (8% on average), alongside the relatively confined absolute uncertainty fluctuating between -1 and 9 nmol s^{-1}, highlight potential sources of error. Possible contributors to this uncertainty in the empty chamber could be attributed to inherent LI-6800 inaccuracies and/or the syringe pump, employed for the controlled injection of HCl. The latter could probably be due to mechanical malfunctions of the pump's motor, leading to deviations in the dispensed volume. In the non-empty chambers (containing dry and wet potting substrate), additional error sources could be due to existing C in the potting substrate that could be released due to the action of microbes in the wet substrate or upon contact with HCl during injection. In the wet substrate, a notable observation is the lingering delay in the CO_2 evolution signal returning to zero, persisting even after the cessation of HCl injection, pointing to a possible delay in CO_2 release due to slower diffusion (Figure 1.9). Other potential sources of error include diffusional leaks or bulk airflow leaks through the mass flow meter and fluctuations in the reference CO_2 (Kölling et al., 2015) or calibration drift of the reference and sample IRGA (Iersel and Bugbee, 2000). To minimize these errors in gas exchange experiments with plants, leak detection and prevention measures were carried out by routinely inspecting tubes and connectors and promptly addressing leaks. Furthermore, the reference and sample IRGAs were regularly calibrated to address calibration drift and ensure accuracy (LI-6800 matching procedure) carried out every thirty minutes.

1.6.2 Above and Below-Ground Fluxes in Real Plants

Utilizing semi-continuous measurements as previously described in Complete Growth Chamber Setup and Gas Exchange System, the robustness of the growth chamber to accurately measure daily CO_2 and H_2O fluxes along with the accompanying fluctuations and outliers as well as diurnal variations in the measured fluxes was demonstrated. This allowed for proper documentation of changes in these fluxes while maintaining a reasonably high experimental throughput.

The progression of data cleaning and the derivation of mean daily flux values successfully removed artifacts and outliers from the data without causing any damage to the trend of the results (Appendix Figure 1.12). The analysis of daily mean fluxes provided insights into the daily trajectory of the measured parameters. The mean daily assimilation and nocturnal respiration exhibited consistent correspondence throughout the experiment, aligning with expectations based on plant growth. As the plants grew, both assimilation and nocturnal respiration increased, with shoot assimilation eventually surpassing respiration and reaching values one order of magnitude higher by the end of the experimental period. This growth-related increase in assimilation is a well-documented phenomenon in plant physiology, reflecting the plants' ability to accumulate biomass and optimize their energy capture through photosynthesis. The higher shoot assimilation compared to respiration indicates a net gain in C fixation and biomass accumulation during the experimental period (Lawlor, 1995; Givnish, 1986). The results of this study highlight a notable deviation from previously reported values in the literature. Givnish (1986) suggests that nocturnal respiration typically constitutes around 7% of peak assimilation. In contrast, nocturnal respiration accounted for approximately 13% of the average daily assimilation in this study (Figure 1.12). It is crucial to emphasize that, unlike the referenced study, this investigation did not measure peak assimilation. Instead, the focus was on assessing nocturnal respiration relative to the average daily assimilation.

The incremental trend of above-ground nocturnal respiration as well as below-ground respiration is explained by the increasing metabolic demands of plants for maintenance and growth purposes (Iersel and Bugbee, 2000). The strong correlation ($R^2 = 0.94$ and 0.98) observed between the total plant biomass (dry mass) and the integrated LI-6800 net C fluxes underscores the suitability of the set-up to capture NPP in the test plants. This finding also suggests that the amount of C assimilated by the plants, as measured by the LI-6800 instrument, is a reliable measure of the overall plant productivity. Similar findings have also ben documented in other studies (Iersel and Bugbee, 2000; Salvatori et al., 2021). Above-ground day and night time transpiration increased daily as the plants grew in size (Appendix Figure 1.13). This may be attributed to the development of more leaves and/or expanding leaf area, which results in increased water uptake and subsequent transpiration. The significantly higher day time transpiration compared to night time transpiration is expected, as daytime conditions promote higher rates of photosynthesis and transpiration due to the availability of light and favorable environmental factors (Givnish, 1986). In contrast, below-ground evaporation showed a decrease over time. This trend indicates two things: first, a gradual drying of the soil surface over time, and second, a result of escalated root water uptake as the plants grew larger, potentially leading to a reduction in the available water for evaporation from the substrate.

Furthermore, the comparison between total evapotranspiration measured by the LI-6800 and independent gravimetric measurements provide insights into the accuracy of the LI-6800 instrument. The mean relative error of 11% suggests a slight underestimation of evapotranspiration by the LI-6800 compared to the gravimetric measurements. This difference may be attributed to various factors such as measurement limitations of the LI-6800 and uncertainties in sensor calibration among others. The weighing balance may also introduce errors due to its sensitivity to environmental conditions such as air currents, and vibration. These factors can lead to fluctuations in the

measured weight of the sample, consequently affecting the accuracy of gravimetric measurements.

Finally, the attempt to track the fate of C that did not contribute to plant biomass did not yield conclusive outcomes. This lack of meaningful results could be attributed to the possibility that C content of the sub-samples used for the C analysis might not have accurately represented the true C content in the samples, both for total C and dissolved organic C (DOC). Additionally, the inherent challenges in extrapolating these values to the entire mass of the experimental substrate for each below-ground cylinder is acknowledged. The quantification of total C and DOC involved multiple steps, each introducing its own degree of uncertainty. These uncertainties, when compounded through the process of scaling, could potentially amplify experimental errors. This highlights the need for methodological refinement in subsequent studies.

1.6.3 CO_2 Respiration in Custom Potting Substrate

The results of the basal respiration experiment conducted on the potting substrate unveiled daily average respiration rates spanning the range of 1 to 3 nmol s^{-1} (Figure 1.7). The respiration rates measured in this experiment are lower than those from previous studies on bare grassland soil (Dyukarev and Kurakov, 2023) and rootless reconstructed soils (Lei and Han, 2020). This observation suggests that "soil" respiration in the potting substrate is only a small fraction of the total below-ground respiration measured during the experiments. This proposition gains added strength when considering the distinct pattern observed in GC B, where initial "soil" respiration levels remained low but gradually increased as the plant established its presence and started growing. Moving forward, the insights gained from below-ground respiration in subsequent plant growth experiments will be interpreted within the framework of this initial observation.

1.7 Conclusion

A novel growth chamber was designed to comprehensively analyze plant gas exchange, with a particular focus on above and below-ground dynamics. This chamber enabled separate and simultaneous monitoring of CO_2 assimilation, nocturnal respiration, H_2O transpiration above-ground, and H_2O evaporation, CO_2 respiration below-ground. Calibration experiments using chemical agents demonstrated rapid and accurate responses within both compartments. The below-ground gas-exchange measurement revealed absolute error values of ± 10 nmol s^{-1} surpassing the uncertainties observed in a similar experiment, possibly due to combined error sources such as the syringe pump, inherent error from the measurement instrument and leaks. However, experiments excluding plants revealed narrower uncertainties (< 2 nmol s^{-1}), underscoring the system's capacity to measure fluxes despite the challenges posed by the combined error sources in the earlier accuracy tests.

The robust correlation of over 90% between the total plant biomass and the integrated LI-6800 net C fluxes highlights the effectiveness of the setup in accurately capturing net primary productivity (NPP) within the tested plants. The system revealed a possible C loss (up to 17%) to the potting substrate possibly as exudates. The inability to capture this loss highlights the need for methodological refinements in total C measurements in future studies.

The growth chamber can potentially be used in various plant centered applications from plant phenotyping, comparative species studies, root-soil interaction analysis to ecological investigations as well as understanding long-term flux dynamics under different conditions. Its extensive experimentation capacity positions it as a pivotal tool for advancing plant science, environmental research, and model validation.

Subsequent chapters of this thesis utilize the described growth chamber and experimental set-up to assess the cost and benefits of above and below-

ground processes across varying soil bulk densities and between distinct plant species.

1.8 Appendix

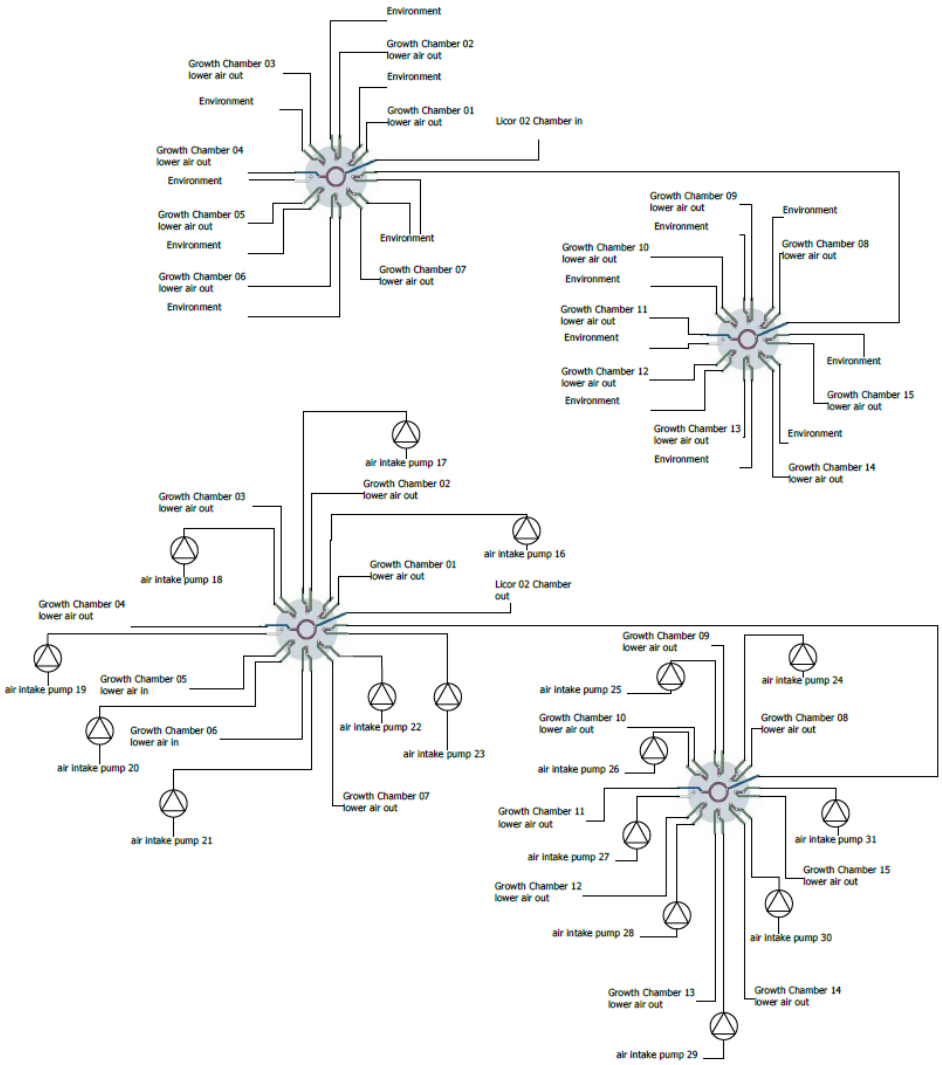

Figure 1.8: Below-ground multiplexer connecting scheme. Above ground scheme not shown as it is typically the same connection principle. Credit: Oliver O'Nagy.

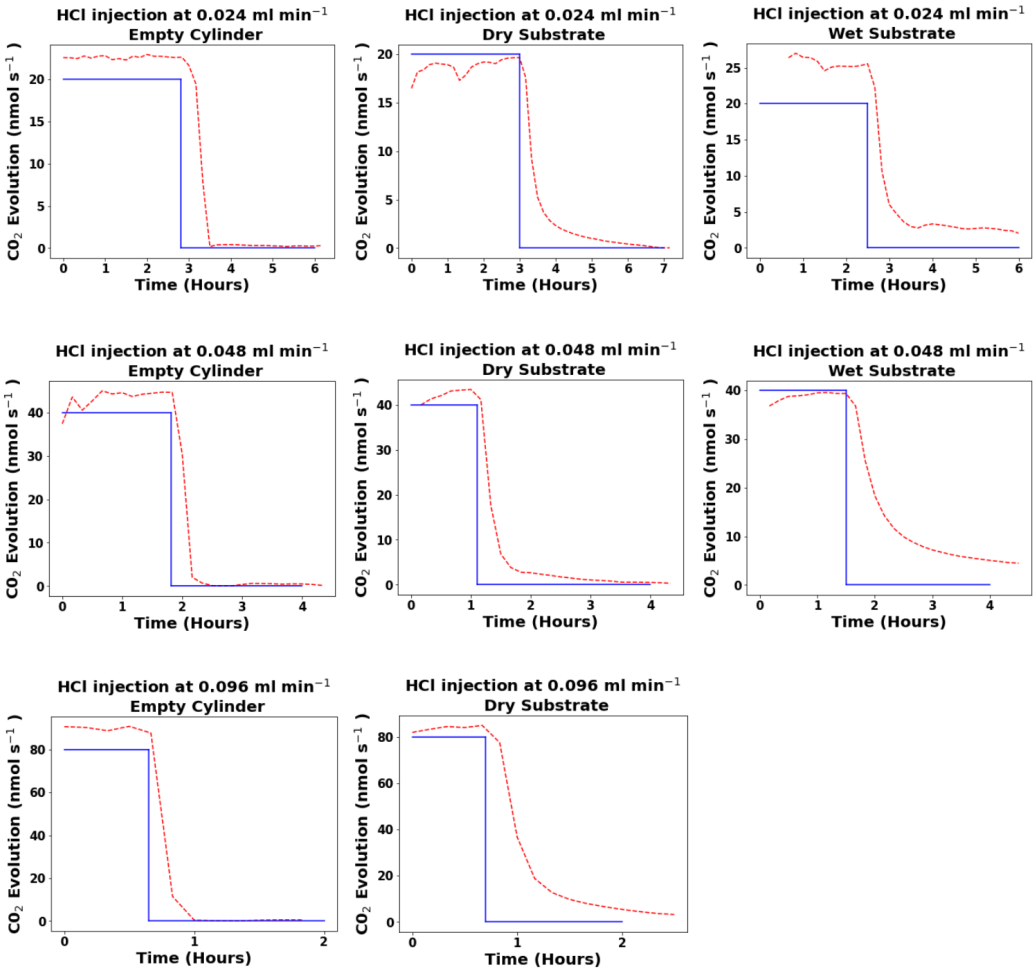

Figure 1.9: CO_2 evolution following HC*l* injection at different rates. **(Top)** HCl injection rate at 0.024 ml min^{-1} in an empty (right), dry (middle) and wet (left) potting substrate filled cylinder. **(Middle)** HCl injection rate at 0.048 ml min^{-1} in an empty (right), dry (middle) and wet (left) potting substrate filled cylinder respectively and **(Bottom)** HCl injection rate at 0.096 ml min^{-1} in an empty (right) and dry (middle) potting substrate filled cylinder. The blue line segment denotes the expected CO_2 evolution rate for each injection rate as well it's progression to zero.

Table 1.2: Complete Growth Chamber Setup Components with Manufacturers and Suppliers.

Model	**Manufacturer**	**Supplier**
LI-6800 Infrared Gas Analyzer	LI-COR, Lincoln, NE, USA	LI-COR Biosciences GmbH, Bad Homburg, Germany
Cree Xlamp CXA2520	Cree, Durham, USA	Vossloh-Schwabe Deutschland GmbH, Ettlingen, Germany
19K Gas Diaphragm Pump 24 V BLDC	Boxer GmbH, Ottobeuren, Germany	Boxer GmbH, Ottobeuren, Germany
Honeywell AWM5102VN Flow Sensor	Honeywell International Inc, Charlotte, NC, USA	Mouser Electronics, Mansfield, TX, USA
Vici 8-Port Multiposition Selector Valves on Standard Electric Actuators	Vici AG International, Schenkon, Switzerland	Macherey-Nagel GmbH & Co. KG, Düren, Germany
CPC PMC Series Valves and Connectors (PMC4204, PMC1002)	Colder Products Company, Minnesota, USA	AFT Systems, Kaiserslautern, Germany
Masterflex^{TM} 30621-32	Antylia Scientific, Illinois, USA	AFT Systems, Kaiserslautern, Germany
Legris 1025T Pneumatic Hose Fluoropolymer Transparent, Inner Ø 4mm / Outer 6mm x 25m up to 20 bar	Parker Hannifin, Cleveland, Ohio, USA	RS Components, Bruxelles, Belgium
1.510.1601.14 Polyamid Hose, DN17, Inner Ø 17mm	HUMMEL AG, Denzlingen, Germany	D.M.E. Distribution de Matériel Électrique, Ehlerange, Luxembourg
Keithley DAQ6510	Tektronics, Beaverton, Oregon, USA	C.N.Rood BV, Zoetermeer, Netherlands
Keithley 2614B	Tektronics, Beaverton, Oregon, USA	C.N.Rood BV, Zoetermeer, Netherlands

Table 1.3: Potting mixtures used in preliminary experiment to determine the best possible C-depleted mixture that allows plant growth. Lufa speyer 2.1 standard soil was used as control. Burnt soil = Lufa speyer soil subjected to burning at 600 °C. QB was eventually selected as the best option for the experiments.

Name of Potting Mixture	**Components**	**Proportions (%)**
BBU	Burnt soil: Bentonite: Unburnt soil	78:20:2
BBV	Burnt soil: Bentonite: Vermiculite	78:20:2
PC	Lufa Speyer 2.1, Unburnt	100
NC	Lufa Speyer 2.1, Burnt	100
QB	Quartz: Bentonite	80:20
QBV	Quartz: Bentonite: Vermiculite	78:20:2
QBU	Quartz: Bentonite: Burnt soil	60:20:20

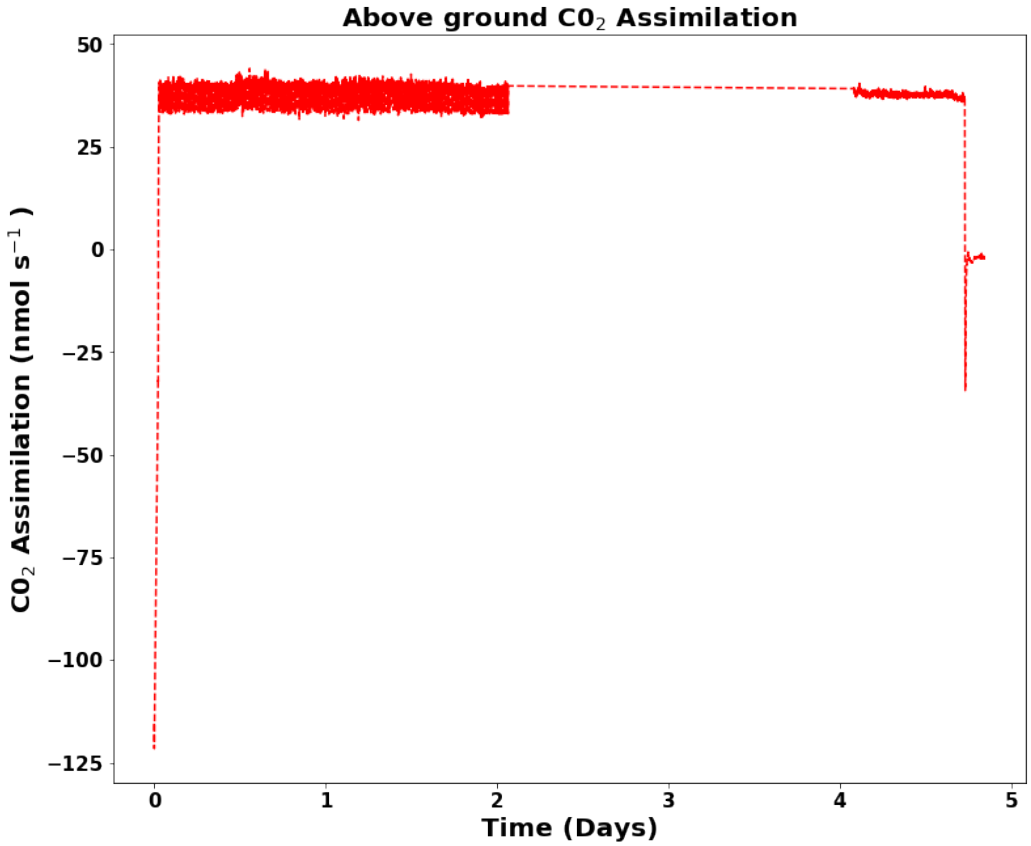

Figure 1.10: Time series of CO_2 absorption rate during a 4-days experimental period. Flux signal remained constant from start until the end of the experiment. Absorption experiment continued to run as air was continuously funneled through the LI-6800 to the sample throughout the experimental period but the LI-6800 malfunctioned and stopped logging between late hours of the second day and early hours of the fourth day hence the broken lines between these days (no data was stored). The gap was filled by taking the mean values of all the measurements.

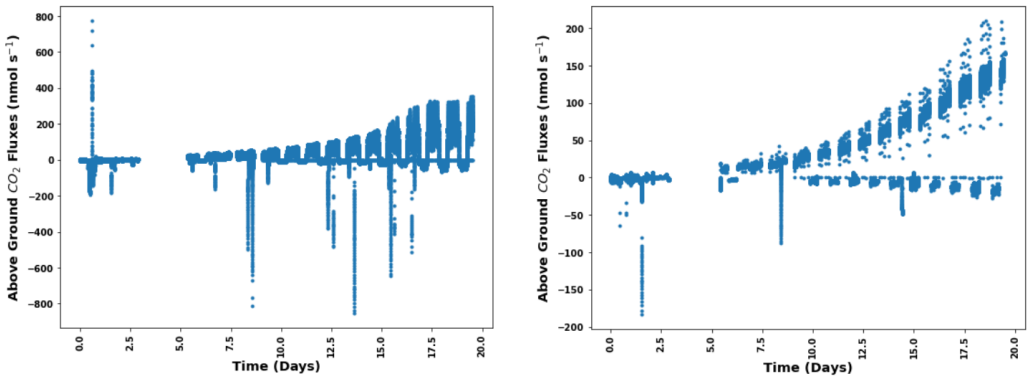

Figure 1.11: **(Left)** Time series of above-ground CO_2 fluxes for all growth chambers showing all fluctuations in the data as well as possible outliers and **(Right)** Diurnal variations in CO_2 fluxes in a typical growth chamber.

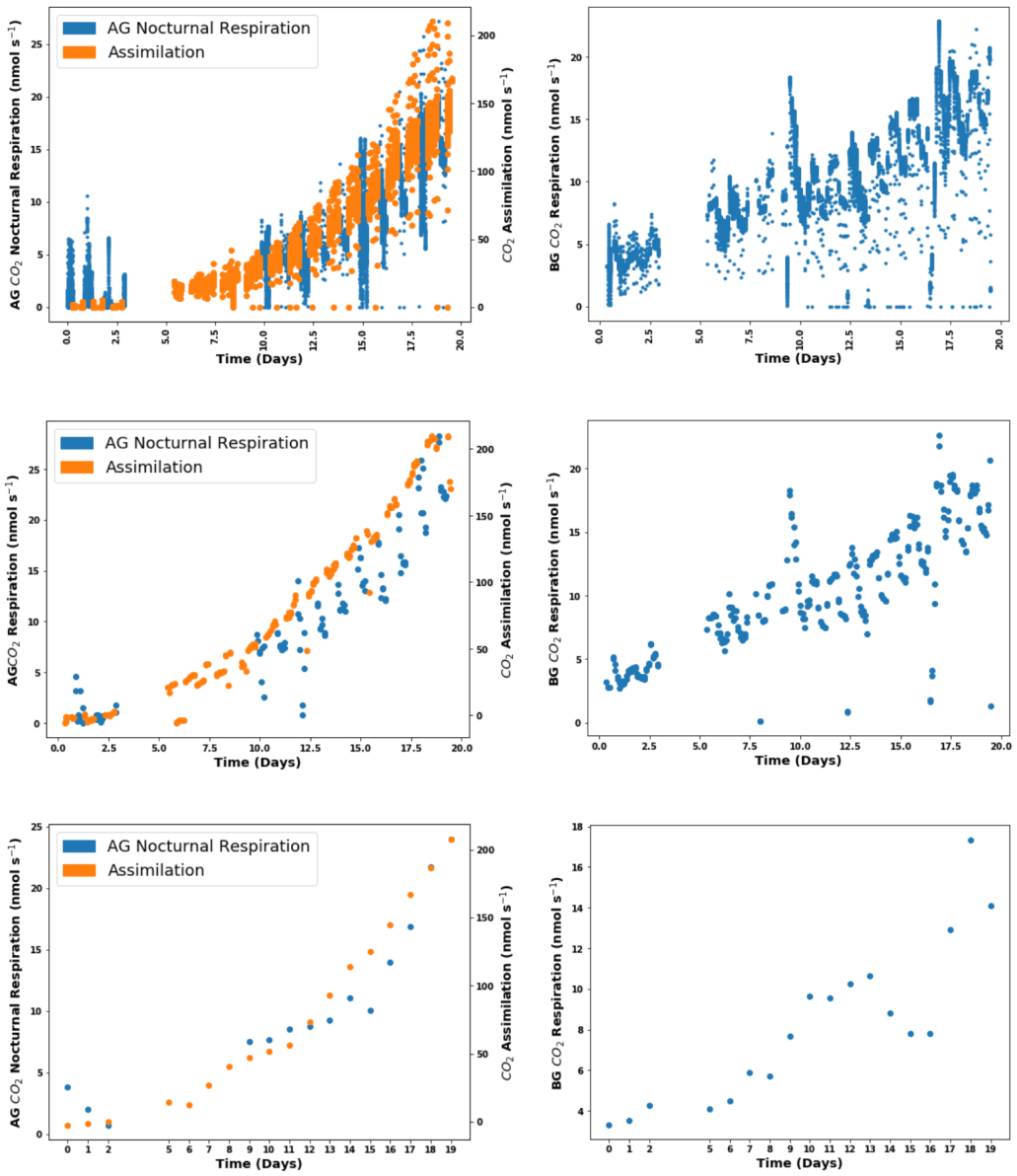

Figure 1.12: **(Top)** Semi-continuous measurements of CO_2 above and below ground fluxes, respiratory fluxes are plotted as positive for ease of comparison; **(Middle)** Data after medians values are calculated every 10 minutes and; **(Bottom)** mean daily fluxes. No data was recorded on day 3 and 4 due to a malfunction of the LI-6800 and data points for nocturnal respiration are missing up to day 8 due to continuous lighting during this time period.

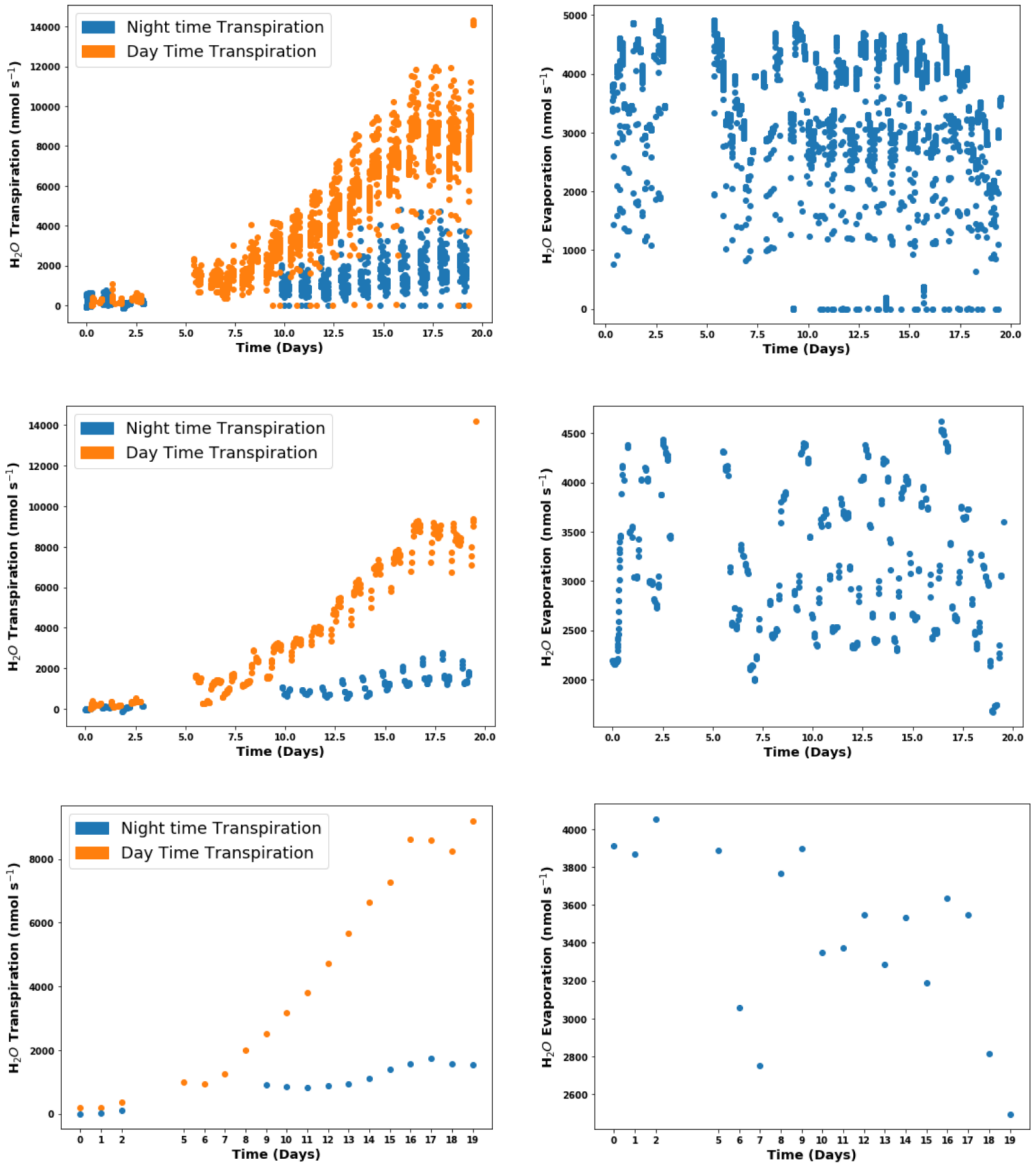

Figure 1.13: **(Top)** Semi-continuous measurements of H_2O fluxes above and below ground; **(Middle)** Data after medians values are calculated every 10 minutes and; **(Bottom)** Mean daily fluxes. No data was recorded on day 3 and 4 due to a malfunction of the LI-6800 and data points for night-time transpiration are missing up to day 8 due to continuous lighting during this time period.

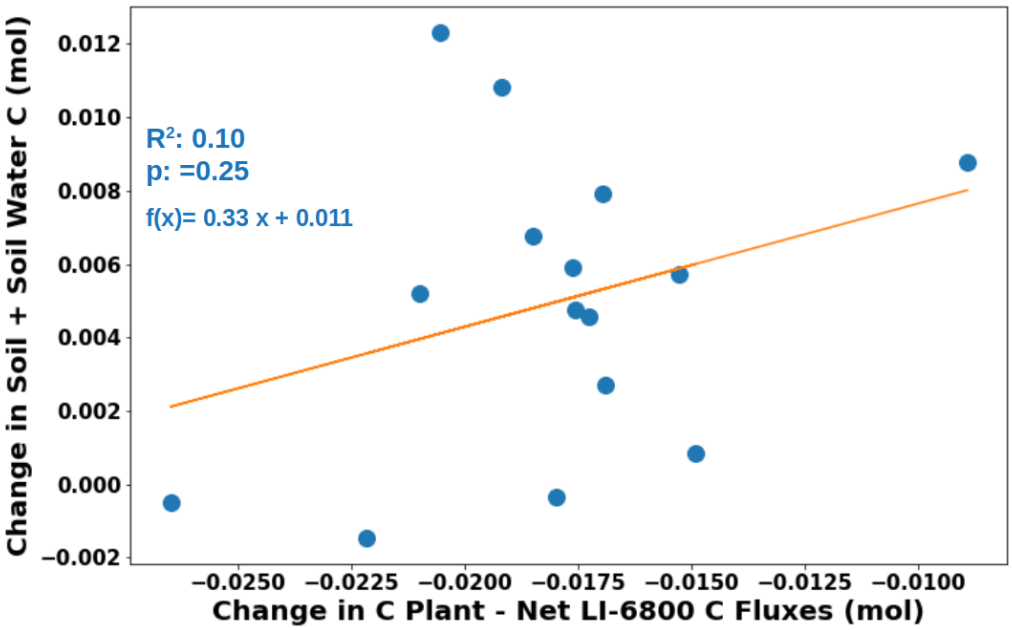

Figure 1.14: Relationship between the change in the C content of the plant - Net LI-6800 C Fluxes vs change in C substrate + change in C wash water. The linear regression p value for each independent variable tests the null hypothesis that the variable has no correlation with the dependent variable.

Chapter 2

Experimental assessment of the relation between above-ground and below-ground carbon investments in maize plants and their cost-benefit ratios

2.1 Abstract

Plant resource allocation is often thought to be guided by a cost-benefit relationship. These ratios represent the trade-offs that plants face in allocating resources to various competing demands, such as growth, reproduction, defense, and in response to environmental stresses. To quantitatively assess resource allocation in response to environmental stressors, carbon (C) allocation and above-ground and below-ground cost-benefit relationships were examined in maize plants exposed to two levels of soil bulk density/penetration resistance. The allocation proportions of assimilated C to above-ground biomass, dark respiration, and translocation to the root system were determined. The fate of translocated C below-ground was investigated, differentiating between biomass, respired, and exuded fractions. The relationship

between above-ground costs of C assimilation (shoot nitrogen (N) investment and transpiratory water loss) and below-ground costs of water and N uptake (respiration, root biomass, and exudates) was further analyzed.

The investigation indicated no differences in the above-ground C allocation patterns between the two bulk density treatments. Below-ground, there was a statistically significant reduced investment in root biomass, along with an indication of increased below-ground respiration in the high bulk density group. C allocation to root exudation remained comparable across both groups.

Maize plants grown under the high bulk density treatments had higher root respiration rates per root length (0.9 nmol m^{-1} s^{-1}) compared to the low bulk density treatment (0.4 nmol m^{-1} s^{-1}). Similarly, the root respiration rates per root growth rate were 374.05 and 656.59 nmol mm^{-1} for the maize pants grown in the low and high bulk density treatments respectively. Although there was an over 100% relative increase in the root respiration rate for plants cultivated under high bulk density, both groups achieved comparable levels of water (H_2O) and nitrogen (N) uptake. This similarity was also reflected in their photosynthetic H_2O and N use efficiency.

Nonetheless, due to the increased C cost associated with root development in plants cultivated under high soil bulk density, the below-ground cost of root uptake was greater within that particular group.

2.2 Introduction

Plants play a vital role in the global carbon (C) cycle, as they derive their entire biomass from atmospheric C through the process of photosynthesis. Their growth is linked to their ability to obtain and retain resources (C, water and nutrients) above-ground and below-ground. Following C assimilation by plant shoots, C translocation and partitioning within the plant is a tightly regulated process that determines the distribution of resources for

various functions. These investment decisions are crucial for plant survival, governing plant growth and development by determining how C resources are distributed among different plant organs and metabolic processes (Mooney, 1972; Poorter et al., 2012; Hartmann et al., 2020). Understanding C allocation is crucial for improving crop productivity, managing natural ecosystems, and predicting plant responses to changing environmental conditions (Jahnke et al., 2009; Hartmann et al., 2020). It also facilitates the estimation of C distribution across soil organic matter, above- and below-ground biomass, and ecosystems as a whole. This knowledge is crucial for determining ecosystem productivity, calculating C sequestration rates, and forecasting ecological responses to climate change (Brüggemann et al., 2011).

C allocation usually involves trade-offs due to the limited availability of resources and the diverse functions performed by different plant organs (Eissenstat, 1992; Givnish, 1988). It is also influenced by plants' physiological status and environmental conditions such as light, nutrient and water availability, biotic interactions, and potential threats (Hartmann et al., 2020; Atwell, 1990; Martínez et al., 2002; Redmond et al., 2019; Monson et al., 2022) and has been described in terms of a functional equilibrium between above-ground and below-ground biomass, investing resources at the most needed sites depending on environmental conditions (Brouwer, 1983).

Above-ground C investment involves C allocation into the construction and maintenance of the photosynthetic tissues (Mooney, 1972; Givnish, 1986). C acquisition above-ground is also associated with the loss of water (H_2O) through transpiration (Givnish, 1986) and so to satisfy the shoot transpiration demands, plants also need to invest in their roots to aid water and nutrient uptake (Martínez et al., 2002). Therefore, C cost below-ground includes the cost of building and maintaining the roots (uptake apparatus) and the energetic expenses incurred by plants during the uptake of H_2O and nutrients from the soil through their root systems. The proper quantification of C investments and potential benefits in plant systems requires an extensive

understanding of two major fluxes of C, namely assimilation and respiration.

Plants utilize chlorophyll and other pigments to capture sunlight and convert it into chemical energy. This energy is used to synthesize organic molecules used for construction of tissues, stored in the plant biomass or released to the environment as secondary materials (e.g. volatile organic carbon (VOC), exudates in roots) (Eissenstat, 1992) and also translocated to other tissues. Respiration on the other hand is the reverse process of photosynthesis. During respiration, sugars (such as glucose) are broken down to produce carbon dioxide (CO_2), H_2O, and energy in the form of adenosine triphosphate (ATP). This energy generated through respiration is essential for various cellular activities, including growth, maintenance, and other biochemical processes (Lambers, 1987). Shoot and root respiration are major sources of C loss in plants (Givnish, 1986; Lambers, 1987). Above-ground cost and benefits especially shoot gas exchange (assimilation, respiration and transpiration) has been studied extensively at various scales from leaf gas exchange experiments (Kennedy and Johnson, 1981; Schlüter et al., 2003; Kopczewski et al., 2020) to whole canopies (Kölling et al., 2015; Salvatori et al., 2021) in a bid to understand the functioning and response of plants and ecosystems to their environment.

Approximately half of above-ground gross primary production (GPP) are transported below-ground (Lambers, 1987). 30% to 60% of this below-ground translocated C is lost through root respiration (Lambers, 1987) while up to 20% is lost through exudation (Sasse et al., 2018). Root respiration drives essential metabolic processes for root maintenance, growth, uptake, transport, defense, and symbiotic interactions, while root exudation releases organic compounds that foster interactions with beneficial microorganisms, enhancing nutrient uptake, soil structure, and pathogen suppression (Sasse et al., 2018). Despite the significance of below-ground processes, investigating their costs and benefits has been relatively limited, possibly due to technical complexities associated with below-ground gas exchange measurements

(Kuzyakov and Larionova, 2005). Recently, innovative systems have emerged that enable the concurrent monitoring of below-ground gas exchange alongside above-ground gas exchange (Kläring et al., 2014; Kläring and Körner, 2020; Barthel et al., 2011), as well as the fist chapter of this thesis.

Leveraging advancements in gas-exchange systems, it is imperative to monitor below-ground cost and benefits under different environmental conditions as it is the case that most studies either focus on either costs or benefits under these conditions. For instance, root response to environmental stressors especially under drought conditions and high bulk density have been explored in multiple studies (Atwell, 1990; Burton et al., 1998; Ruiz et al., 2016; Bengough et al., 2006; Colombi et al., 2017). These studies have revealed that unfavorable below-ground conditions can result in a heightened demand for photosynthate to support the expansion of root systems, potentially diminishing the available C for above-ground plant growth. However, these studies have yet to elucidate the effects of these stressors on root acquisition, thereby not quantifying their impact on the cost-benefit ratios of these plants.

Experimental designs enabling the precise exploration and quantification of temporal dynamics in above-ground and below-ground C allocation across various environmental conditions are essential in understanding the expenses associated with plant metabolic processes and their susceptibility to environmental influences. This knowledge is crucial to understanding the adjustments necessary in maintaining the delicate balance of ecosystems that underpin our well-being. Furthermore, this will contribute to the progression of ecosystem prediction models, particularly optimality models (Schymanski et al., 2007, 2008) that seek to explain how plants allocate limited resources to different functions to maximize their fitness under different environmental conditions. For instance, existing ecosystem prediction models often neglect the energetic costs associated with the mechanical exploration of the soil volume by plant roots, potentially impacting the overall C balance of

plants. This may constrain the precision of these models in predicting plant responses. Therefore, incorporating accurate data on root-related costs and benefits into these models can lead to more accurate predictions of plant behavior and performance under various environmental scenarios and ultimately enhance our fundamental understanding of plant biology. This also has practical applications in agriculture and ecosystem management. Given this background, the current study aims to enhance our knowledge of C investment, resource allocation, and cost-benefit trade-offs in maize plants under different levels of soil penetration resistance. This is achieved through continuous gas exchange measurements and the assessment of C allocations to shoots and roots at the end of the experiment. The hypothesis posits that changes in soil penetration resistance will affect below-ground cost/benefit dynamics and influence the above-ground allocation patterns of maize plants. To test this hypothesis, experiments on maize plants were conducted with the following objectives:

1. Determine the proportions of assimilated C allocated to above-ground biomass and dark respiration and quantify C translocated into the root system.

2. Investigate the portion of translocated C that remains in the root biomass and the proportion that is respired.

3. Assess the relationship between root costs and benefits in terms of shoot transpiration and change in plant Nitrogen (N) status.

4. Assess the trade-off in shoot assimilation in terms of C gained per unit of H_2O and N translocated above ground.

5. Investigate the influence of soil mechanical properties on these costs and benefits.

To achieve these objectives, the setup and methodology outlined in the first chapter of this thesis were employed. Gas exchange of maize plants

was monitored from the seedling stage for a duration of 3 weeks, and the proportions of C biomass were quantified at the end of the experiment. The gas exchange setup facilitated real-time, non-destructive, and quantitative measurements of gas exchange rates throughout the experimental period. Subsequently, measurements of the biomass C pools at the experiments' conclusion provided insights into the C proportions of both above and below-ground biomass.

2.3 Materials and Methods

In this study, 15 maize plants were cultivated in the potting substrate described in the first chapter of this thesis and subjected to three different bulk densities. The penetration resistance for each bulk density was determined utilizing a low-cost, custom-made mini-penetrometer adapted according to the method outlined by Ruiz et al. (2017). The experimental plants were cultivated in the custom growth chambers designed to enable separate and simultaneous monitoring of above and below-ground gas fluxes using a gas analyzer (LI-6800, LI-COR, Lincoln, NE, USA), as detailed in the first chapter of this thesis. Additionally, the roots of the plants were periodically imaged using a Nuclear Magnetic Resonance Imaging device (NMR) to capture dynamic measurements of root lengths. At the conclusion of the experiment, the dry masses and C content of both above-ground and below-ground plant parts were measured.

2.3.1 Soil Substrate

The experimental plants were grown using a custom-made C-depleted potting mixture. The mixture's maximum water holding capacity (field capacity) was measured as 32.0 ± 2.2 g/100g using the method described by Blažka and Fischer (2014). It consisted of 4:1 quartz:bentonite, and 5 g/l of Peter's all-rounder fertilizer (20+20+20+TE, ICL Growing Solutions, Tel Aviv, Israel).

The %C content of the components of the potting mixture was 6.94 ± 1.31, 0.0020 ± 0.0008, and 0.06 ± 0.02 for Peter's allrounder, fertilizer, quartz, and bentonite, respectively as determined by a total C analysis using an elemental analyzer ((Vario MacroCube, Elementar, Hesse, Germany). 15 growth chambers were packed with three different bulk densities (1.40, 1.45, and 1.55 g cm^{-3}), 5 chambers for each bulk density. All growth chambers contained a volumetric "soil" water content of 20%.

2.3.2 Soil Packing

To achieve a consistent volumetric "soil" water content of 20% and avoid air pockets from forming in the below-ground cylinders, a precise procedure was adhered to in all growth chambers. Each below-ground cylinder contained 285 ml of water. A fertilizer solution was prepared by adding 5 g/l of fertilizer (Peter's allrounder fertilizer (20+20+20+TE, ICL Growing Solutions, Tel Aviv, Israel)) to 85.5 ml (30%) of the required total water volume (285 ml). This solution was mixed with the potting mixture and subsequently divided into three equal portions. Ensuring the right consistency of the mixture prevented the formation of air pockets as we packed the soil cylinders. The remaining water was also divided into three equal parts, each containing 66.5 ml. The entire quantity of potting mixture needed for the desired bulk density was weighed, thoroughly mixed, and then divided into three portions. Below-ground cylinders, marked at 3 equal heights, were packed with the potting substrate, compacted with a metal, and sprinkled with 66.5 ml of water. This process was repeated three times, each time adding the pre-mixed potting substrate portions to the column and sprinkling with water. Finally, all columns were securely sealed with cling film and aluminum foil and left undisturbed for 24 hours. This allowed some time for the uniform redistribution of water within the packed substrate before seed cultivation.

2.3.3 Determining Soil Penetration Resistance

A low-cost alternative to the mini-penetrometer designed by Ruiz et al. (2017) was developed. A 30 mm long conic penetrometer with a cone base radius of 2.5 mm, a 15° vertex angle and a recessed shaft (Figure 2.1) was mounted on a load cell (Omega LC703-25, OMEGA Engineering, Deckenpfronn, Germany) attached to a syringe pump (LEGATO 110, KD Scientific Inc, Holliston, MA, USA) that drives penetration to achieve a constant movement of 1 mm min^{-1}. This set-up was connected to a source meter (Keithley 2614B, Tektronics, Beaverton, Oregon USA) and a data logger (Keithley DAQ6510, Tektronics, Beaverton, Oregon, USA) (Figure 2.1). The entire set up was controlled through pyvisa (Python wrapper for the Virtual Instrument Software Architecture library).

The system was calibrated using 1 g to 3000 g weights (Kern and Son GmbH, Balingen, Germany). First, the offset value in millivolts (mV) of the mounted penetrometer needle was recorded. Subsequently, weights from 1 g to 3000 g were placed vertically on the load cell and the corresponding reading in mV were recorded. The output readings in mV were plotted against the calibrated weights to obtain a calibration curve. The curve fit parameters were used to convert the mV readings to Newton (N) (Appendix Figure 2.10).

To obtain the penetration resistance of the bulk densities employed in the experiments, two separate cylinders were packed for each bulk density in plexiglass cylinders with holes at three different heights of the soil cylinder (see Section Soil Packing). Penetration measurements were performed by driving the needle through the soil at a rate of 1 mm min^{-1}. Penetration resistance was measured at 250, 500 and 750 mm soil height and mean values obtained. Readings are expressed in Newton (N) units. The penetration depth was obtained by multiplying timestamps (in minutes) with the penetration rate. The resulting readings in mV were recorded individually for all soil layers and converted to N. The average N values were transformed into

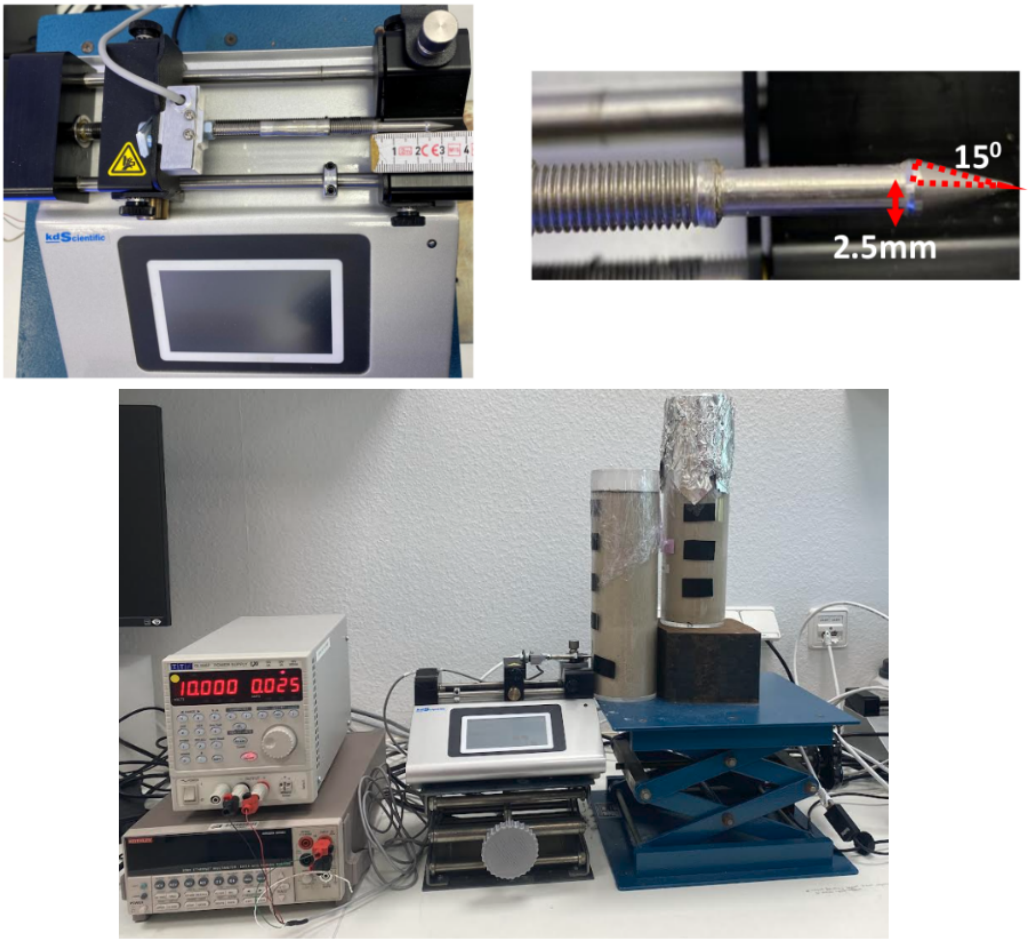

Figure 2.1: **(Above)** Penetrometer needle dimensions and **(Below)** Full penetrometer set-up.

penetration stress (Pa) by dividing the force value by the cross-sectional area of the base of the cone (2.5 mm).

The results of all bulk densities, along with their replicates, were aggregated, and mean penetration resistance values were calculated after the needle had been fully inserted. (Appendix Figure 2.11).

2.3.4 Plant Material

Maize seeds (Zea mays L. var. Badische gelbe) were weighed and sterilized in 70 % ethanol for 1 minute. Subsequently, the seeds were germinated on wet filter paper in covered petri dishes and placed in a dark cabinet at room temperature for seventy-two hours. After germination, the resulting seedlings were transferred to the substrate, buried at a depth of 3 cm in the central region of the seed chamber of the growth chamber.

2.3.5 Growth Conditions

Plants were grown for 19 days in the growth chamber described in Chapter 1. The separation of the above-ground and below-ground compartments was achieved by pouring melted palm fat at a temperature of 28 °C (semi-solid consistency) in the seed chamber, creating a 0.7 cm thick separation layer between the below and above-ground compartment, adapting the method of Koebernick et al. (2015). The growth chambers were placed in a climate chamber in a 14/10 hours, 20°C/ 16°C light/dark regime. Each growth chamber was equipped with the individual light cylinders described in Chapter 1. Between the second and ninth day of the experiment, the light was inadvertently left on continuously due to a malfunction of the timer.

Nutrition was supplied once to the plants during the soil cylinder packing step at the beginning of the experiment. Subsequently, in order to maintain a consistent moisture level, the plants were re-watered to constant weight every other day except during the weekends. This was accomplished by adding water at the top of the soil cylinder using the water supply tubes present in the growth chamber.

2.3.6 Growth Chamber Setup and Gas Exchange Measurements

Continuous and simultaneous measurements of CO_2 and H_2O exchange in each compartment of the growth chambers was monitored using two portable photosynthesis systems (LI-6800, LI-COR, Lincoln, NE, USA), with one system assigned to each compartment. Above and below-ground gas exchange of the fifteen maize plants was studied for nineteen days. The set-up was connected to a multiplexing system, (eight 8-way multiplexers (Vici 8-Port Multiposition Selector Valves, Vici AG International, Schenkon, Switzerland)) allowing for repetitive measurements on 15 growth chambers in rapid succession. Every chamber was measured for 10 minutes, about 10 times within a 24-hour period. Data acquisition was conducted using the LI-6800 gas exchange system, with measurements recorded at a frequency of five seconds throughout the entire experiment. To ensure data integrity and system stability, a custom background script was used on the LI-6800, automatically initiating a new file every twenty-four hours to prevent system crashes and data loss.

Upon completion of the experiments, the recorded data stored in an ASCII format on the LI-6800 were downloaded and analyzed. Flux measurements were assigned to the corresponding growth chambers based on the recorded switch time in the labview program of the multiplexers. To minimize the impact of extreme outliers, median values of the fluxes were calculated every 10 minutes. The above-ground A values were categorized as assimilation or nocturnal respiration based on the light on/off regime, while below-ground A values represented root respiration. E values corresponded to above-ground transpiration and below-ground evaporation. Daily mean assimilation, nocturnal respiration, and transpiration rates were obtained by calculating the mean value of the median fluxes for each chamber, both above-ground and below-ground.

The detailed description of the complete gas exchange set-up and data analysis protocol for the LI-6800 data is provided in the first chapter of this thesis.

2.3.7 Pre-experimental Total and Dissolved C and N Analysis

To measure the initial C content of the seeds before conducting the experiments, 10 maize seeds were chosen randomly. These seeds were subsequently oven dried at 65°C for 24 hours. This procedure aimed to eliminate any additional moisture that might have been absorbed by the seeds during storage. Once dried, the seeds were weighed, homogenized, and analyzed for total C and N content using an elemental analyzer (Vario MacroCube, Elementar, Hesse, Germany). The mass percentage of C present in the seeds was then calculated.

The pre-experimental total C content of the potting medium was obtained by measuring the total C content of sub-samples of the individual components (fertilizer, quartz and bentonite) using an elemental analyzer (Vario MacroCube, Elementar, Hesse, Germany) and scaling the values up using the mass percentages as described in the first chapter of this thesis.

Similarly, the initial dissolved organic carbon (DOC) content of each potting substrate component was determined by mixing sub-samples of each component with 250 ml of water and analyzing the filtrate (filtered using a 0.4 μm syringe filter) for DOC using a Torch TOC Combustion Analyzer (Teledyne Tekmar, Mason, OH, USA) as previously described in Chapter 1 of this thesis as well. The concentration of DOC in the filtered solution, measured in mg/l, was multiplied by the volume of wash water to estimate the pre-experimental DOC content of each chamber.

2.3.8 MRI Measurements

All experimental plants were imaged in a vertical 4.7T magnet equipped with an MR console (MR Solutions, Guildford, UK) at the Institute of Bio- and Geosciences, IBG-2: Plant Sciences, Forschungszentrum Jülich. The orientation of the borehole in the vertical direction allowed measurements of plants to be taken in their upright natural growth orientation. A radio-frequency coil with an inner diameter of 100 mm (Varian, Palo Alto, CA, USA) was employed for the study. The SEMS (Spin-Echo Multi-Slice) sequence provided by the vendor was utilized for image acquisition. As the roots grew in size, it took approximately 1 hour to measure a soil cylinder with outer length of 300 mm, inner diameter of 30 mm and total volume of 1464 cm^3. MRI measurements of the 15 growth chambers were measured in two batches, each batch was measured every third day over a 14-day period. Each pot was measured about five to six times, depending on which batch it belonged to.

2.3.9 Harvest and Post-Experimental Total C and DOC Analysis

At the conclusion of the gas-exchange and root imaging experiments, the above-ground plant shoots were collected. The length and width of the maize leaves were measured with a ruler and the leaf area was calculated following the method of Montgomery (1911) cited in McKee (1964). Leaf fresh mass was measured using a precision weighing balance. Subsequently, the lower portion of the soil cylinder was removed, and the soil was extricated using a piston. To disentangle the roots while preserving their integrity as much as possible, the soil was washed in a large bowl using up to 8 liters of water. This washing process involved placing a sieve with a mesh size of 2 mm atop a finer sieve with a mesh size of 0.5 mm, both positioned inside a large container. Roots that passed through the 2 mm sieve settled on the finer

sieve to prevent root loss. The washed roots were then patted dry with paper towels to remove excess moisture, and their fresh mass was measured. Any roots adhering to the paper towels were removed using tweezers. The fresh roots were then scanned using an EPSON V800 scanner and analyzed using WinRhizo Pro (Regent Instruments, Ottawa, Canada) using the following settings: Image type: Gray levels; Resolution: high, 600; Tray size: 20cm X 20cm; Surface area: 1464cm^{-3}.

Both the roots and above-ground shoots were subsequently dried in an oven at 65°C for 48 hours. The dry mass of the roots and shoots was measured, and sub samples (about 50 mg) were subjected to total C analysis using an elemental analyzer (Vario MacroCube, Elementar, Hesse, Germany). The percentage C by mass of the sub-samples was multiplied by the total mass of the samples to obtain an estimate of total C in the whole plant dry mass.

The water and soil mixture obtained from the root washing process was thoroughly mixed by hand, and the wash water was decanted from the soil. The decanted water was manually mixed once again, and a sub-sample was drawn using a 40 ml syringe. This sub-sample was then filtered through a 0.4 μm syringe filter and analyzed for dissolved organic carbon (DOC) using a Torch TOC Combustion Analyzer (Teledyne Tekmar, Mason, OH, USA).

Additionally, sub-samples (about 500 mg) of the washed soil were collected, dried at a temperature of 105 °C for 48 hours, and analyzed for total carbon using an elemental analyzer (Vario MacroCube, Elementar, Hesse, Germany). The percentage C by mass of the sub-samples was multiplied by the total mass of the soil samples to obtain an estimate of post experimental total C in the growth chamber below-ground cylinder.

2.3.10 Root Image Analysis

MRI data image segmentation was done using ilastik (Berg et al., 2019), a machine learning (bio)image analysis tool. With ilastik, we interactively trained a model to separate background from root voxels using two repre-

sentative MRI scans. The resulting model tested on additional columns and was then applied to all MRI scans in batch mode. For each voxel within the imaging data, ilastik software computed a probability indicating the likelihood of that voxel being associated with a root structure. Subsequently, the probability map instead of the conventional magnetic resonance imaging (MRI) signal image was analyzed using NMRooting analysis (a software tool designed for segmenting plant roots in MRI and analyzing various root traits) (Dusschoten et al., 2016).

2.3.11 Statistical Analysis

Descriptive statistics, including mean, minimum, maximum, and median, were calculated for the datasets. To evaluate the normality of the data distribution, the Shapiro-Wilk test was employed (Shapiro and Wilk, 1965). Given the absence of normality in the data distribution, a non-parametric Mann-Whitney U-test (Mann and Whitney, 1947) was employed in comparing pair-wise differences of the two experimental groups in the study. This statistical test allowed for the assessment of significant differences between Group A (1.40 - 1.45 gcm^{-3}, mean penetration resistance of 2.2 Newtons (N), (penetration stress = 0.11 MPa)) and Group B (1.60 gcm^{-3}, mean penetration resistance of 3.2 N, (penetration stress = 0.16 MPa)) with respect to the variable of interest.

The analysis involved the use of both ordinary linear regression based on ordinary least squares (OLS) (James et al., 2013) and robust linear regression models (RLM) (Yu et al., 2014) to account for outliers and small sized datasets. Minimal differences were observed between the two regression models when applied on data from daily flux measurements and dynamic root imaging, leading to the presentation of results exclusively from the OLS model. For datasets with fewer data points, particularly toward the conclusion of the experiments, the robust linear regression model (RLM) was also compared with the OLS. Given their similarity, the results from the OLS

model were ultimately presented.

To compare the slopes of the regression analysis in this study, a combination of fundamental concepts in statistical testing was employed (James et al., 2013). Slope estimates were derived from regression models fitted using group-specific data. The difference between the two slopes was determined, and to find the standard error of this difference, the square root of the sum of the squares of the standard errors for each slope was computed. The test statistic was computed as the ratio of the slope difference to the standard error of the difference. The degrees of freedom (df) for the t-test were then determined based on the lengths of the respective datasets for the groups. This was followed by a two-tailed t-test using the calculated test statistic and degrees of freedom. The p-value associated with the test statistic was obtained by evaluating the cumulative distribution function (CDF) of the absolute value of the test statistic using the t-distribution. The p-value was calculated as twice the complement of the CDF. Finally, the obtained p-value was compared to a chosen significance level ($p \leq 0.05$) to determine the statistical significance of the difference in slopes. A p-value below the significance level would indicate that the difference in slopes is considered statistically significant.

In every regression analysis presented in the results section, the slopes are calculated and compared among the experimental groups. The analysis assumes a linear relationship with a real intercept. In cases where the regression analysis is not significant or there are too few data points for a regression analysis, the y/x ratio is computed. In such instances, the ratio assumes that there is no intercept. Given the presence of intercepts in the regression analysis, the slope provides a quantitative measure of the cost/benefit relationship of the variables under consideration.

2.3.12 C allocation Above and Below-ground

C investments to biomass, respiration above ground and translocation to the roots were calculated as fractions of total assimilated C while C in the root was calculated as a sum of C translocated below-ground and initial C in seed. Any seed remnant below-ground was subtracted from the initial amount of C in seed. C investment to root biomass, respiration were then calculated as fractions of C in root. The C amount lost to the soil was determined by taking the sum of C in root biomass and C expended in respiration and subtracting it from total root translocation using the variables and expressions in Table 2.1.

2.4 Data Availability

All data and computations presented in this Chapter are found here:
https://doi.org/10.5281/zenodo.10384366 .

2.5 Results

In this study, experiments were conducted using 15 growth chambers and a single plant species, maize. The experiment lasted for about three weeks so the experimental plants were typically in the early stages of their vegetative growth period. Basic information regarding plant size, dry mass and leaf area is presented in Table 2.2.

To examine variations in cost-benefit ratios across different below-ground bulk density and penetration resistance levels, the growth chambers were categorized into two groups. Group A comprises GC 1-10 with bulk densities ranging from 1.40 to 1.45 g cm^{-3} and a mean penetration resistance of 2.2 Newtons (N), (penetration stress = 0.11 MPa), while Group B comprises GC 11-15 with a bulk density of 1.50 g cm^{-3} and a mean penetration resistance

Table 2.1: Relevant variables and expressions used to calculate biomass allocations above and below-ground. C investments to biomass, respiration above ground and translocation to the roots were calculated as fractions of total assimilated C while C in the root was calculated as a sum of C translocated below-ground and initial C in seed. In the case of any seed remnant below-ground, this was subtracted from the initial amount of C in seed. C investment to root biomass, respiration were then calculated as fractions of C in root. C exudation was calculated by taking the sum of C in root biomass and C expended in respiration and subtracting it from total root translocation.

Variables	**Description**	**Expressions (If applicable)**
$\mathrm{F}_{A\text{net, day}}$	Total Net above-ground daytime Assimilation (mol)	
$F_{R_{\text{night}}}$	Total Above-ground nocturnal respiration (mol)	
$F_{R_{\text{root}}}$	Total Below-ground respiration (mol)	
C_{rt}	C translocated below-ground (mol)	
C_i	C in seed (mol)	
$C_{i_{\text{remnant}}}$	C in seed remnant (mol)	
C_s	C in shoot (mol)	
C_r	C in root (mol)	
$C_{\text{r total}}$	C in root + C in seed	$C_{\text{rt}} + C_i$
C_e	C released into soil (mol)	$C_{\text{r total}} - C_r + F_{R_{\text{root}}}$
C_{s_F}	Shoot biomass proportion	C_s / $\mathrm{F}_{A\text{net, day}}$
C_{dr_F}	Shoot dark respiration proportion	$F_{R_{\text{night}}}$ / $\mathrm{F}_{A\text{net, day}}$
C_{rt_F}	Root translocation proportion	C_{rt} / $\mathrm{F}_{A\text{net, day}}$
C_{r_F}	Root biomass proportion	C_r / $C_{\text{r total}}$
C_{rr_F}	Root respiration proportion	$F_{R_{\text{root}}}$ / $C_{\text{r total}}$
C_{e_F}	Root exudation proportion	C_e / $C_{\text{r total}}$

of 3.2 N, (penetration stress = 0.16 MPa) (Appendix Figure 2.11).

C Allocation to Above and Below-ground Biomass and Respiration

The comparison between the proportion of cumulative C assimilates (mol) allocated to shoot biomass and root translocation in groups A and B revealed mean proportions of 44% and 39% for shoot biomass and 37% and 41% for root translocation, respectively. These allocation proportions showed no

Table 2.2: Relevant information about plants in the different growth chambers (GC1-GC15) for the two treatment groups. The average mass of cultivated seeds in each growth chamber was 0.45 g. GC 1-10 consists of 1.40 - 1.45 g cm^{-3} bulk density treatment while GC 11-15 consists of 1.50 g cm^{-3} bulk density treatment

	S/Name	Shoot Dry mass (g)	Root Dry Mass (g)	Leaf Area (cm2)	Root Length (mm)
Maize 0.112 mPa	GC1	9.22	0.35	249.59	20996.58
	GC2	14.10	0.46	434.31	31168.03
	GC3	13.02	0.26	339.23	26690.58
	GC4	13.43	0.25	417.53	30104.62
	GC5	17.96	0.35	466.03	34896.95
	GC6	9.26	0.19	317.28	19706.85
	GC7	9.66	0.37	294.83	19731.99
	GC8	12.65	0.30	343.30	30116.62
	GC9	10.43	0.35	285.53	31534.92
	GC10	8.74	0.20	262.18	25770.88
	Mean	**11.85**	**0.32**	**349.74**	**27216.35**
	Standard Deviation	**2.93**	**0.08**	**74.94**	**5408.45**
Maize 0.16 mPa	GC11	17.22	0.37	378.88	37056.22
	GC12	12.23	0.23	300.17	18632.77
	GC13	8.38	0.17	256.83	19627.61
	GC14	11.29	0.28	364.91	26709.49
	GC15	11.90	0.18	311.75	22772.51
	Mean	**12.20**	**0.25**	**322.51**	**24959.72**
	Standard Deviation	**3.19**	**0.08**	**49.76**	**7460.44**

statistically significant difference between the two bulk density groups for both parameters (p = 0.3 and 0.1 for groups A and B respectively) (Table 2.3, Figure

The comparison of C allocation to shoot respiration was done by examining the relationship between mean daily assimilation rates (nmol s^{-1}), mean daily above-ground nocturnal respiration rates (nmol s^{-1}), and the proportion of cumulative assimilates (mol) allocated to cumulative nocturnal respiration. In both groups A and B, no statistically significant differences were observed in either comparison (Table 2.3 and Figure 2.3, top). For both groups, the percentage proportion of cumulative C invested in shoot respiration was 20% while the proportion of mean daily assimilation invested in mean daily nocturnal respiration was 11% in both groups.

C investment below-ground was quantified by the taking sum of the C translocated from the shoots and the initial C content of the seeds (mol). Subsequently, the proportions of this below-ground C investment were com-

Table 2.3: Summary of above-ground (AG) C allocation proportions as a fraction of net cumulative daytime C assimilation above-ground to shoot biomass and translocated to the roots (formatted in %) for group A and B. GC 1-10 belong to group A with a bulk density of 1.40 - 1.45 g cm^{-3} and a mean penetration resistance of 2.2 Newtons (N), (penetration stress = 0.11 MPa) and GC 11-15 belong to group B with a bulk density of 1.50 g cm^{-3} and a mean penetration resistance of 3.2 N, (penetration stress = 0.16 MPa). The Mann-Whitney U test p-value for the % proportions tests whether there is a statistically significant difference in the distribution of a continuous dependent variable between the two independent groups A and B.

	Allocation Proportions of Total C Assimilation					
	Shoot Respiration		**Shoot Biomass**		**Root Translocation**	
	Group A (1.4 - 1.45 gcm^{-3})	**Group B (1.50gcm^{-3})**	**Group A (1.4 - 1.45 gcm^{-3})**	**Group B (1.50gcm^{-3})**	**Group A (1.4 - 1.45 gcm^{-3})**	**Group B (1.50gcm^{-3})**
No. of Cases	10	5	10	5	10	5
Min	5% (0.003 mol)	5% (0.005 mol)	30% (0.020 mol)	27% (0.018 mol)	29% (0.018 mol)	23% (0.016 mol)
Mean	20% (0.015 mol)	20% (0.014 mol)	44% (0.033 mol)	39% (0.030 mol)	37% (0.027 mol)	41% (0.031 mol)
Max	26% (0.026 mol)	49% (0.035 mol)	59% (0.044 mol)	46% (0.044 mol)	56% (0.037 mol)	51% (0.049 mol)
p value that Group A = B	p = 0.2		p = 0.3		p = 0.1	

pared in terms of its allocation to root biomass, root respiration, and the proportion released to the soil. There was a statistically significant reduced investment in root biomass for the higher bulk density plants (Group B) (19% against 25%, p = 0.03) along with a statistically insignificant indication for increased root respiration investment in group B plants (41% vs 34%, p = 0.06) (Table 2.4, Figure 2.4). There was no statistically significant difference between the two bulk density groups regarding the proportion of C released to the soil (41% and 40% for group A and B, p = 0.4).

Costs and Benefits of Plant Roots

To understand the physiological trade-offs and the cost/benefit ratio below-ground, the analysis of below-ground resource uptake per root length was first explored by examining the relationship between root length and resources uptake (root water uptake (represented by above-ground transpiration) and N uptake (represented by total N in plant dry mass)) as benefits. This was

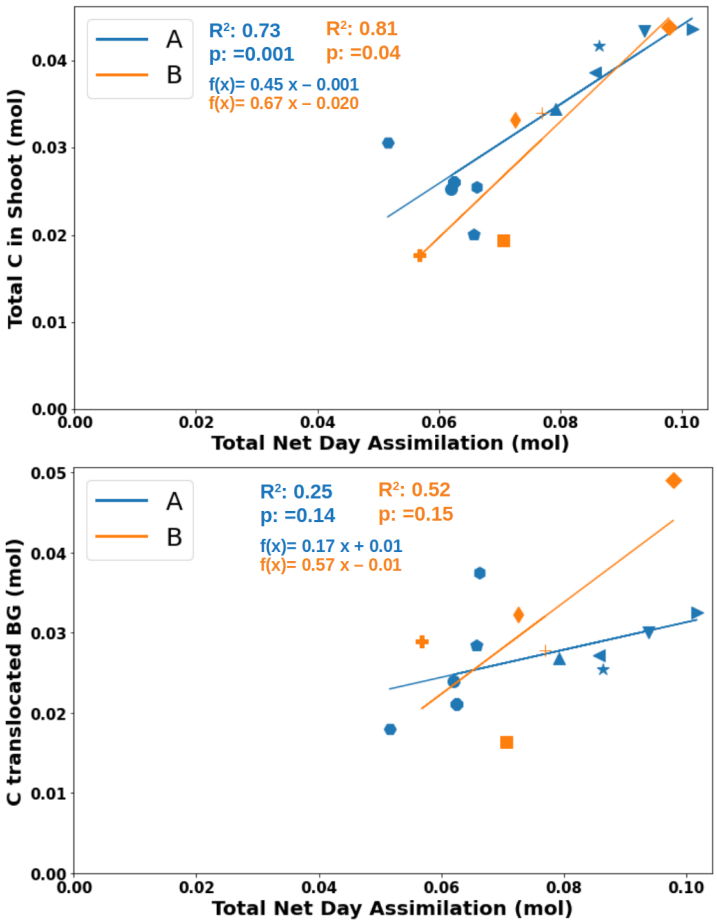

Figure 2.2: Above-ground (AG) fractions of cumulative assimilates allocated to **(Top)** shoot biomass and **(Bottom)** translocated to the root system. The orange and blue colours represent the groups while the markers represent different growth chambers in each group. Group A: low penetration resistance, and group B: high penetration resistance. The linear regression p value for each independent variable tests the null hypothesis that the variable has no correlation with the dependent variable.

followed by relating them to their root respiration, exudation and/or biomass costs.

The relationship between mean daily transpiration rates (nmol s^{-1}) per dynamic root length (mm) and N uptake (mol) per final root length (mm)

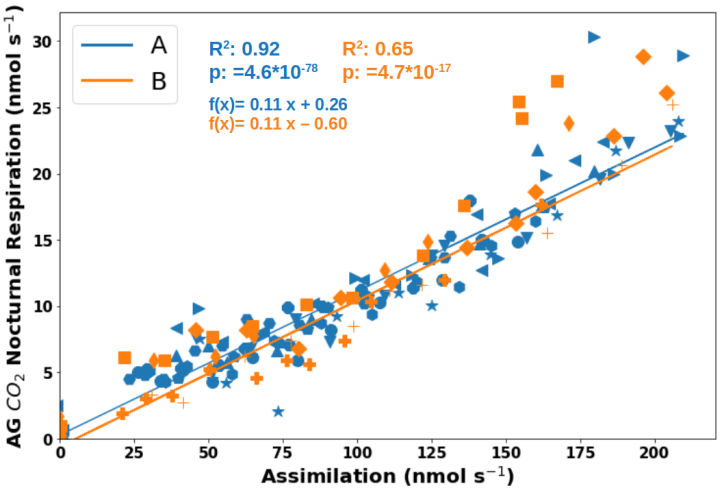

Figure 2.3: Relationship between mean daily assimilation rate and mean daily above-ground (AG) nocturnal respiration rate. The orange and blue colours represent the groups while the markers represent different growth chambers in each group. Group A: low penetration resistance, and group B: high penetration resistance. The linear regression p value for each independent variable tests the null hypothesis that the variable has no correlation with the dependent variable.

were examined across the two groups. N uptake was derived by calculating the difference between initial N content in the seeds and the N content of the plant biomass at the experiment's conclusion.

The relationship between dynamic root length (mm) and mean daily transpiration rates (nmol s^{-1}), showed a strong correlation ($R^2 > 0.90$) for both groups. The slopes of these relationships were similar, measuring 0.41 nmol mm^{-1} s^{-1} for group A and 0.45 nmol mm^{-1} s^{-1} for group B (Figure 2.5, top). Additionally, both groups exhibited similar specific root length (SRL) (1.17 * 10^{-5} and 9.88 * 10^{-6} g mm^{-1}, p = 0.3) for group A and B respectively.

The regression analysis between N uptake (mol) and final root length (mm) showed a significant correlation between both parameters in group A plants ($R^2 = 0.65$) but not in group B possibly due to fewer data points (Figure 2.5, bottom). Given the lack of significance in the regression analysis for

Table 2.4: Summary of below-ground (BG)(root translocation + C in seed) C investment allocated to root biomass, root respiration and lost to the soil (formated in %) for group A and B. GC 1-10 belong to group A with a bulk density of 1.40 - 1.45 g cm^{-3} and a mean penetration resistance of 2.2 Newtons (N), (penetration stress = 0.11 MPa) and GC 11-15 belong to group B with a bulk density of 1.50 g cm^{-3} and a mean penetration resistance of 3.2 N, (penetration stress = 0.16 MPa). The Mann-Whitney U test p-value for the % proportions tests whether there is a statistically significant difference in the distribution of a continuous dependent variable between the two independent groups A and B.

	Allocation Proportions of Total C Translocated to the Root					
	Root Respiration		**Root Biomass**		**C lost to the soil**	
	Group A (1.4 - 1.45 gcm^{-3})	**Group B (1.50gcm^{-3})**	**Group A (1.4 - 1.45 gcm^{-3})**	**Group B (1.50gcm^{-3})**	**Group A (1.4 - 1.45 gcm^{-3})**	**Group B (1.50gcm^{-3})**
Count	10	5	10	5	10	5
Min	27% (0.010 mol)	34% (0.015 mol)	18% (0.007 mol)	13% (0.006 mol)	32% (0.015 mol)	27% (0.009 mol)
Mean	34% (0.015 mol)	41% (0.019 mol)	25% (0.011 mol)	19% (0.009 mol)	41% (0.018 mol)	40% (0.019 mol)
Max	40% (0.019 mol)	54% (0.023 mol)	33% (0.015 mol)	23% (0.014 mol)	50% (0.022 mol)	45% (0.026 mol)
p value that Group A = B	p = 0.06		**p = 0.03**		p = 0.4	

group B, a comparison of their ratios, rather than the slopes of the regression analysis, was conducted. Both groups exhibited similar N uptake per root length ratios (1.5 vs 1.4 mol mm^{-1}, p = 0.2) for group A and B.

To examine the respiratory cost of root penetration and growth across the two groups, the relationship between below-ground respiration rate (nmol s^{-1}) and dynamic root length measurements (mm) as well as root growth rate (mm s^{-1}) across the two groups A and B was examined.

There was a strong linear relationship between root respiration and root length for group B (R^2 = 0.80) and a moderate yet significant relationship between both variables for group A (R^2 = 0.30). The slope of the relationship was 0.4 and 0.9 nmol m^{-1} s^{-1} (p = 4.3 * 10^{-5}) for group A and B respectively (Figure 2.6, top). It was also observed that group B was also associated with a statistically significant higher root respiration to root length ratio (15 nmol m^{-1} s^{-1}) mean ratio for group B compared to 7 nmol m^{-1} s^{-1} for group A (p = 0.04).

Similarly, the correlation between root growth rate (mm s^{-1}) and below-

ground respiration (nmol s^{-1}) exhibited a moderate (group A) to strong (group B) linear relationship across the two groups (R^2 = 0.42 and 0.70) with slope values of 374 and 657 nmol mm^{-1} (p = 0.007) for groups A and B, respectively (Figure 2.6, bottom).

As previously demonstrated, the water and N uptake per root length exhibited similarities between the two groups whereas group B plants expended more C in root respiration compared to group A plants. In the presented figures (Figure 2.7), the root respiration costs are juxtaposed with root benefits (water and N uptake) to highlight the respiratory costs of water and N uptake.

The analysis of the relationship between mean daily below-ground respiration and transpiration rates (nmol s^{-1}) (Figure 2.7, top) revealed a positive linear relationship for both group A and B; (R^2 = 0.35 and 0.71) respectively. The slope of the relationship was higher in group B (0.0015 nmol s^{-1} $nmol^{-1}$ s) compared to 0.0010 nmol s^{-1} $nmol^{-1}$ s in group A plants (p = 8.9 * 10^{-5}).

The analysis of the respiratory expenditure (total below-ground respiration, (mol)) associated with N uptake (total N in plant (mol)) (Figure 2.7, bottom), revealed no significant correlations. However, their ratio was notably higher in group B, (3.93 and 6.37 mol mol^{-1}, p = 0.04) for group A and B respectively.

Furthermore, the overall cost of root water uptake was obtained by taking the sum of cumulative below-ground respiration and C in root dry mass (mol) and compared with cumulative transpiration (mol). Significant correlations were not observed in their relationship (Appendix Figure 2.12). The ratios of total water uptake cost to cumulative transpiration (0.004 and 0.005 mol mol^{-1}, p = 0.1) for group A and B respectively were not significantly different between the two groups.

Additionally, the overall cost of N uptake was also obtained by taking the sum of cumulative below-ground respiration, C in root dry mass, and exudates (mol) and compared with the N content in the plant biomass (mol).

Significant correlations were not observed in their relationship (Appendix Figure 2.13). The ratios of total cost to total N in the plant biomass (11.55 and 15.11 mol mol^{-1}, p = 0.06) for group A and B respectively were not significantly different between the two groups.

Above-ground Costs and Benefits

The cost and benefits associated with above-ground processes were also investigated. This analysis specifically focused on the relationship between C assimilation as a benefit, water consumption (represented by above-ground transpiration) and total N in the shoot as a cost. Furthermore, the below-ground respiration cost of assimilation was also analyzed.

The relationship between mean daily above-ground assimilation and transpiration rates (nmol s^{-1}) revealed very strong positive correlations (R^2 = 0.94 and 0.93) for group A and B respectively. The slope of their relationship was considered as the water use efficiency (WUE). Both groups had identical slopes (WUE) (0.02 mol mol^{-1}, p = 0.2) (Figure 2.8, top).

The relationship between cumulative net assimilation (mol) and shoot N (mol) also displayed robust and similar correlations (R^2 = 0.85) for both groups (Figure 2.8, bottom). The slopes of their relationship was considered as the N use efficiency. There was no significant difference between the slopes (NUE) (9.04 and 15.01 mol mol^{-1}, p = 0.3) for group A and B respectively.

The relationship between mean daily above-ground assimilation rate and below-ground respiration rate (nmol s^{-1}) revealed moderate positive correlations (R^2 = 0.30 and 0.50) for group A and B respectively. The slope of the relationship was higher in group B (0.07 and 0.11 mol mol^{-1}, p = 0.01) for group A and B respectively (Figure 2.9).

2.6 Discussion

The aim of this study was to analyze various aspects of C allocation and above and below-ground cost-benefit ratios under 2 levels of "soil" penetration resistance. It involved determining the allocation proportions of assimilated C to above-ground biomass, dark respiration, and quantifying C translocation to the root system. Additionally, we investigated the fate of translocated C within the root biomass, assessing the proportions that remain and those that are respired or released into the soil as exudates. We further analyzed the relationship between above-ground costs of C assimilation (N invested in the shoot and H_2O lost during assimilation) and below-ground cost of water and N uptake (respiration, root biomass and exudates). The key focus was to explore the impact of soil mechanical properties on these different aspects of allocation and cost-benefit ratios and compare them between two experimental groups subjected to a low (1.40 - 1.45 gcm^{-3}) and high (1.50 gcm^{-3}) bulk density.

C Allocation to Above and Below-ground Biomass and Respiration

Soil compaction has been identified as a significant factor that can impede the growth and development of plant roots. It has been shown to reduce root elongation rate (Bushamuka and Zobel, 1998; Popova et al., 2016), hinder root penetration in extreme cases and ultimately restrict the ability of plants to access essential nutrients and water from the soil (Wang et al., 2019), ultimately affecting general plant growth and development. Under such conditions, it has been demonstrated that some plants allocate a larger proportion of assimilated C below-ground, specifically towards root growth (Masle, 1992). This finding is also supported by the concept of functional equilibrium in biomass allocation (Brouwer, 1983) where plants allocate more C resources to the organ with a limiting factor for growth. Contrary to these studies, this study unveiled no statistically significant differences in the al-

location patterns of C assimilates to the roots between group A (high bulk density) and group B (low bulk density) plants. This could either be because the selected bulk density treatments could not elicit any differences in the above-ground C allocation patterns of the experimental plants or that the duration of the experiment may not have been long enough to capture possible gradual adjustments in resource allocation strategies of the experimental plants.

The observed positive correlation between above-ground nocturnal respiration, assimilation, and total C content in shoot biomass for both group A and group B (Figure 2.3) is potentially due to the interdependence of these processes, as photosynthesis provides the substrates essential for respiration (Givnish, 1988; Ridge, 2002). The observed similarity in the proportion of C allocated to shoot respiration in both groups is unsurprising, considering their comparable shoot biomass C (Table 2.3, Figure 2.2). This aligns with the established understanding that shoot respiration tends to scale allometrically with size, as documented in previous studies (Reich et al., 2008; Wang et al., 2021b). Both groups allocated about 13% of mean daily assimilation to mean daily above-ground nocturnal respiration. This finding reveal a significant departure from values previously reported in the literature. Nocturnal respiration is typically estimated to constitute around 7% of peak assimilation (Givnish, 1986). Unlike the referenced study, this investigation did not measure peak assimilation; rather, the focus was on assessing nocturnal respiration relative to the mean daily assimilation.

In the examination of below-ground C allocation patterns, a statistically significant difference in the allocation of C to root biomass was identified between plants in group A and group B. Specifically, it was observed that group A allocated a greater proportion of C to their root biomass compared to group B plants. This finding is consistent with prior research results (Tubeileh et al., 2003), which demonstrated that maize plants subjected to a bulk density of 1.30 gcm^{-3} exhibited higher root biomass than those grown

under 1.45 gcm^{-3}. The higher C allocation to root biomass in group A plants corresponds to lower soil resistance and possibly reduced root respiration demands compared to group B plants which had a marginally higher (statistically insignificant) root respiration, potentially reflecting an adaptation to counteract the physical constraints imposed by their compacted soil environment (Table 2.4, Figure 2.4).

Despite reports indicating an increase in root exudation in compacted soils, contributing to the penetration of compacted layers (Tubeileh et al., 2003) and recognized for its crucial role in enhancing nutrient acquisition under such conditions (Dakora and Phillips, 2002; Lynch et al., 2005), this study did not reveal any significant difference in C allocation to exudation between the low bulk density group A plants and high bulk density group B plants (Table 2.4, Figure 2.4). It is important to note that exudation was not measured here, but inferred from the mass balance, so the uncertainty is likely large, as it could sum up all the uncertainties of the other measurements.

The C allocation proportions described in this study in the same order of magnitude as those in other studies (Zagal, 1994; Tubeileh et al., 2003; Meng et al., 2013; Sun et al., 2018) (Appendix Table 2.5).

Costs and Benefits of Plant Root Uptake

The cost/benefit analysis of water and N uptake in this study highlights comparable water uptake rates and total N uptake per root length (Figure 2.5) across the two bulk density groups. However, higher rates of root respiration per root length and root growth rate are evident (Figure 2.6). Comparing respiratory costs with water and N uptake provides a clearer insight. Due to the elevated cost of root penetration in group B plants, the acquisition of water and N is more expensive for this group compared to group A plants (Figure 2.7).

Previous research has highlighted the importance of root length in facilitating both root water and nutrient uptake (Eissenstat, 1992; Moroke et al.,

2005; Lynch et al., 2005; Mokhele et al., 2012; Hodgkinson et al., 2017; Xie et al., 2021; Lyzenga et al., 2023). In line with this perspective, this study reveals a significant correlation between root length and both transpiration and N uptake (Figure 2.5). Furthermore, both bulk density groups A and B achieved comparable rates of transpiration and N uptake per unit root length. While this finding diverges from some studies (Atwell, 1990; Lipiec and Stepniewski, 1995; Tubeileh et al., 2003) that have emphasized reduced water and nutrient uptake in compacted soils, it aligns with observation from other studies (Masle and Passioura, 1987; Hoffmann and Jungk, 1995).

The observed similarity in transpiration rates may be attributed to a well-developed root system effectively accessing water resources (Green et al., 2006; Guswa, 2010), or a water-saving approach achieved through the controlled adjustment of stomatal conductance (Rawson et al., 1977), or a combination of both mechanisms. Similarly, plants in both groups likely exhibit comparable N uptake rates or N use efficiency.

This study demonstrated that both group A and B plants shared similar specific root lengths (SRL). Consequently, both high and low bulk density plants demonstrated equally high SRL values, consistent with findings from previous studies (Eissenstat, 1992; Lynch et al., 2005; Ho et al., 2005), which highlight the role of high SRL values in enhancing water and nutrient uptake, especially under adverse soil conditions. This suggests that the high bulk density treatment for group B plants, while increasing root respiratory costs, did not compromise their efficiency in soil penetration and water/nutrient acquisition. This finding challenges the expected decrease in root water uptake per unit root length, often associated with potentially reduced hydraulic conductivity linked to soil compaction (Tubeileh et al., 2003; Correa et al., 2019). The reasons for this finding are usually due to diminished root length (Grzesiak et al., 2014), or reduced root hair surface (Atwell, 1990), both of which were not the case in the current experiment.

The relationship between root water uptake and C costs has been a fo-

cal point of inquiry in plant physiology and ecology. Researchers have employed diverse methodologies to unravel how plants navigate the trade-off between soil water acquisition and C resource investment. These methodologies include studies on C allocation to roots, modeling studies as well as root respiration measurements. Root growth necessitates substantial energy and carbohydrate expenditure, especially in compacted soils characterized by high penetration resistance (Colombi et al., 2017). This prompts an increased allocation of C below-ground from above-ground tissues to support below-ground processes. This slightly higher C allocation pattern was observed for the high bulk density group B plants (Table 2.3).

To further understand the respiratory investment related to root growth, the relationship between root length, root growth rate and root respiration rates across the different bulk density groups was examined. Contrary to previous studies (Atwell, 1990; Bengough et al., 2011; Colombi et al., 2017), higher soil penetration resistance did not lead to a statistically significant decrease in root growth rate (Figure 2.6, bottom). However, similar to a study on energy cost of root growth, (Colombi et al., 2017), root respiration per root length increased with increasing soil penetration resistance. Group B plants exhibited a stronger correlation and a steeper slope compared to Group A plants (Figure 2.6); 0.4 and 0.9 nmol m^{-1} s^{-1} for group A and B respectively (Figure 2.6, top). The root respiration values measured in this study are similar to those reported in previous studies (Bloom et al., 1992; Bouma et al., 1997; Bryla et al., 2001) (Appendix Table 2.6). The difference in the measured root respiration rates per root length signifies a relative increase of over 100% in the respiratory rate of Group B plants compared to Group A, despite only a 37% difference in penetration resistance between the two groups. This relative increase exceeds those reported in a prior study, where a 90% difference in penetration resistance led to only a 35% increase in energy cost (Colombi et al., 2017).

The root respiration rates per root growth rate were 374.05 and 656.59

nmol mm^{-1} for groups A and B, respectively. Converting these rates into energy expenditure involved applying a conversion factor of 455 kJ mol^{-1} based on a study by (Hansen et al., 2004). This allowed for a meaningful comparison with measurements reported by Colombi et al. (2017). By measuring the heat dissipation of growing wheat roots under 3 penetration resistance treatments (0.14, 0.45, and 0.89 MPa), energy expenditure of root penetration was determined to range from 0.2 to 0.8 J mm^{-1} in the referenced study. Similarly, this present study calculated energy expenditure values of 0.17 J mm^{-1} for group A and 0.29 J mm^{-1} for group B under similar penetration resistances (measuring 0.11 and 0.16 MPa) when converted from Newton (N) to MPa using the cross-sectional area of the penetrometer (cone radius = 2.5 mm). This finding highlights that root growth requires more energy under higher penetration resistance emphasizing the substantial impact of soil conditions on the energetic demands associated with root development possibly due to heightened metabolic effort. The finding also suggests that the energetic cost of root penetration is determined by below-ground soil conditions rather than the species. It is important to highlight that no distinctions were made between growth and maintenance respiration in this current study.

Also worth highlighting is the distinct variance observed between the slope values characterizing the relationships between root respiration and root length, as well as root growth rate, when examined separately from their mean ratios. For instance, the root respiration to root length ratio (15 nmol m^{-1} s^{-1}) for group B and (7 nmol m^{-1} s^{-1}) for group A is atleast one order of magnitude higher than the reported slopes (Figure 2.6, top). This discrepancy could stem from the dispersion of data points relative to the regression line, as well as the contribution of a substantial intercept. The intercept may encompass an element of background respiration that is not directly attributed to root activity. This could potentially emanate from initial seed respiration and microbial respiration in the potting substrate contributing to extra release of CO_2.

Furthermore, comparing root respiration costs with water uptake rates and N content in plants (Figure 2.7) further highlights the elevated C respiratory cost associated with below-ground resource acquisition by plant roots, particularly in the high bulk density Group B plants. This observation aligns with established scientific literature that emphasizes the heightened metabolic costs linked to root system expansion under constrained soil conditions (Atwell, 1990; Bengough et al., 2011; Colombi et al., 2017). It provides valuable insights into the sensitivity of root-related metabolic processes to alterations in soil structure.

It's noteworthy to highlight that taking the sum of cumulative respiration, C in root biomass and exudates and comparing it with total transpiration, revealed no differences between the two groups (Appendix Figure 2.12). This implies that, when considering the overall cost in the roots, both groups exhibit a similar cumulative expenditure over the studied period. However, this observation prompts a critical examination of whether amount of C in the plant biomass should be categorized as a cost, given its inclusion of both structural and non-structural C. This leads to an important consideration for future experiments, where a more detailed analysis of the various components of biomass C becomes imperative. Distinguishing between structural and non-structural C will provide a finer-grained understanding of their respective contributions to the overall C budget.

Above-ground Costs and Benefits

Photosynthetic water use efficiency (WUE) represents a crucial aspect of plant performance, as it reflects the efficiency with which plants utilize water to carry out photosynthesis and produce biomass. Similarly, photosynthetic nitrogen use efficiency (NUE) is a measure of how efficiently plants utilize N absorbed from the soil to create the pools of enzymes and pigments needed to sustain high rates of CO_2 assimilation (Field and Mooney, 1986).

The investigation into the relationship between mean daily assimilation

and transpiration rates and the relationship between total N in shoot and net assimilation among plants subjected to low (group A) and high bulk density (group B) revealed a comparable WUE between both groups despite varying below-ground conditions (Figure 2.8). This similarity can be explained by the similar root water and N uptake rates between the two groups (Figure 2.5) and implies that both groups of plants exhibited comparable capacities in terms of water and N acquisition and utilization.

Consistent with similar correlations in prior investigations and comprehensive reviews conducted across a diverse array of plant species and environmental contexts (Givnish, 1988; Byrd et al., 1992; Lawlor, 1995, 2002), this study substantiates the fundamental role of N availability in influencing plant growth and overall productivity. Although soil compaction has been implicated in constraining root penetration and subsequent nutrient accessibility by plant roots (Field and Mooney, 1986; Correa et al., 2019), this study deviates from this expectation, as the high bulk density treatment did not impede root penetration.

The literature on WUE in compacted soil presents divergent findings. For instance, reduced WUE was observed in pickling cucumbers grown at high bulk densities (Smittle and Williamson, 1977), while increased WUE was recorded in rice plants under compacted soil conditions (Singh et al., 1980). It is noteworthy that these studies were conducted using bulk densities higher than those applied in our current investigation. Therefore, the interplay between soil compaction levels and WUE necessitates further exploration to establish a comprehensive understanding of the relationship between photosynthetic WUE and soil compaction.

The positive linear relationship observed between mean daily assimilation and below-ground respiration rates (Figure 2.9) highlights the direct connection between the amount of assimilated C by the plant and the energy expended in root respiration (Brüggemann et al., 2011). The higher below-ground respiration rates per assimilation observed in the higher bulk

density group B plants, in contrast to group A plants, further strengthens the supporting evidence that soil bulk density increases C expenditure in root respiration possibly due to heightened metabolic effort to sustain both root growth and maintenance (Lambers et al., 1983; Lambers, 1987).

2.7 Conclusion

In summary, the investigation focused on resource allocation strategies in plants under diverse soil conditions, particularly exploring C allocation patterns in maize plants subjected to varying soil bulk densities and penetration resistances. The study examined allocation dynamics concerning above-ground biomass, dark respiration, root system translocation, and below-ground C utilization. Additionally, it explored the relationship between above-ground costs, (shoot N investment and water loss), and below-ground costs (root biomass, respiration, exudates) of resource acquisition.

Despite the differences in soil conditions, above-ground C allocation exhibited no significant variations between the two groups. The below-ground analysis revealed reduced C investment in root biomass and indications of increased below-ground respiration in the high bulk density group. Notably, C allocation to root exudation remained consistent across both groups.

Root respiration, both per root length and growth rate, exhibited a significant increase under high bulk density conditions. High bulk density group B plants exhibited a steeper slope compared to the low bulk density group A plants; 0.4 and 0.9 nmol m^{-1} s^{-1} for group A and B respectively. The calculated energy cost of root penetration 0.17 J mm^{-1} for group A and 0.29 J mm^{-1} for group B measured in this study was similar to those measured in a previous study under similar penetration resistances (Colombi et al., 2017). Despite an over 100% relative increase in root respiration rate for high bulk density plants, both groups attained similar levels of water and N uptake. This similarity extended to photosynthetic WUE and NUE. However, due to

the higher C cost associated with root development in high soil bulk density plants, the cost of below-ground root uptake was greater in this group.

To conclude, this study highlights that increase in soil penetration resistance and bulk density elevates root respiration costs and affects cost-benefit ratios. Furthermore, the study challenges the notion that higher costs correspond to reduced benefits, emphasizing the need to assess C costs and benefits simultaneously.

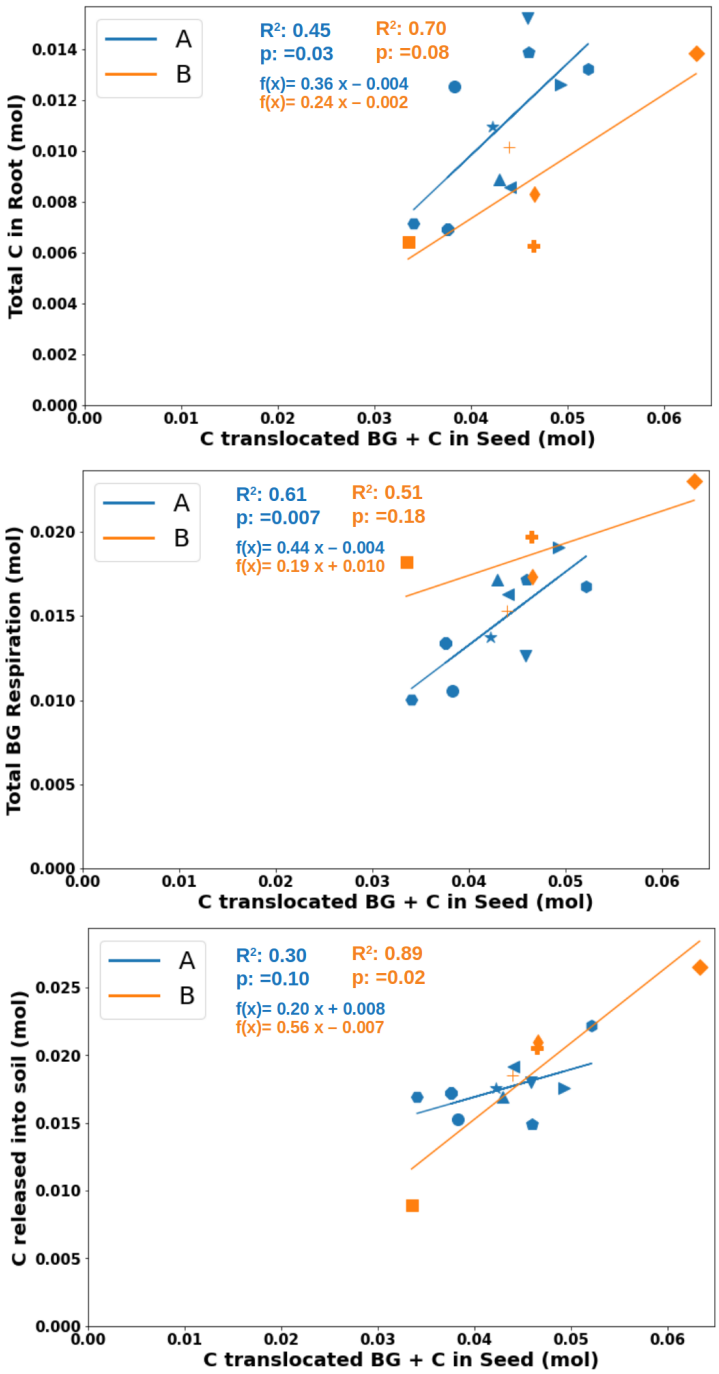

Figure 2.4: Below-ground (BG) fractions of C investment allocated to **(Top)** root biomass, **(Middle)** root respiration and **(Bottom)** lost to the soil. The orange and blue colours represent the groups while the markers represent different growth chambers in each group. Group A: low penetration resistance, and group B: high penetration resistance. The linear regression p value for each independent variable tests the null hypothesis that the variable has no correlation with the dependent variable.

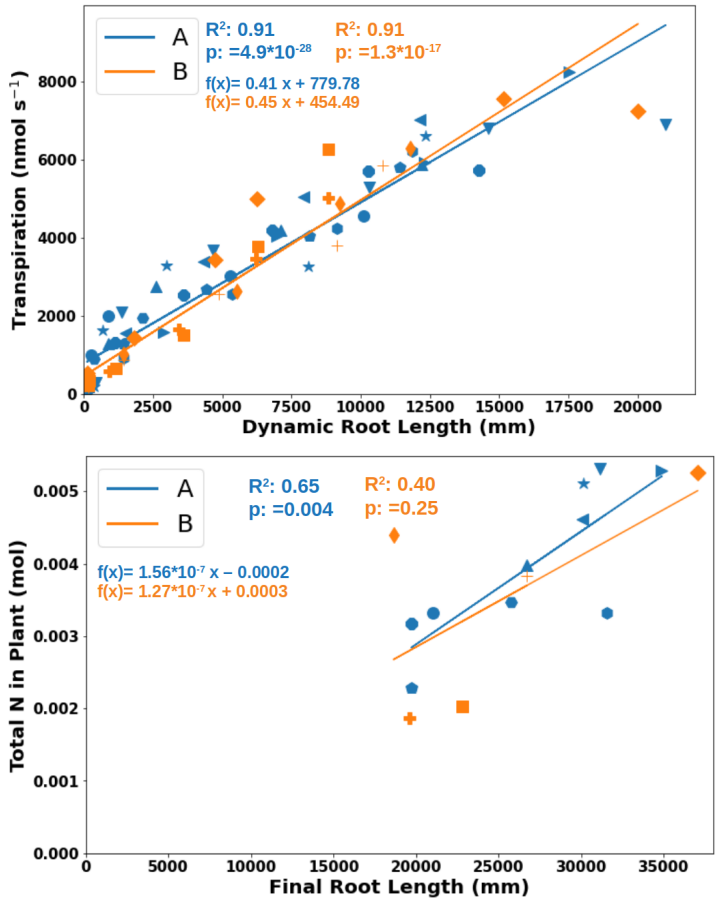

Figure 2.5: Relationship **(Top)** dynamic root length (mm) and daily transpiration rates (nmol s^{-1}) and **(Bottom)** N uptake (mol) per final root length (mm). The orange and blue colours represent the groups while the markers represent different growth chambers in each group. Group A: low penetration resistance, and group B: high penetration resistance. The linear regression p value for each independent variable tests the null hypothesis that the variable has no correlation with the dependent variable.

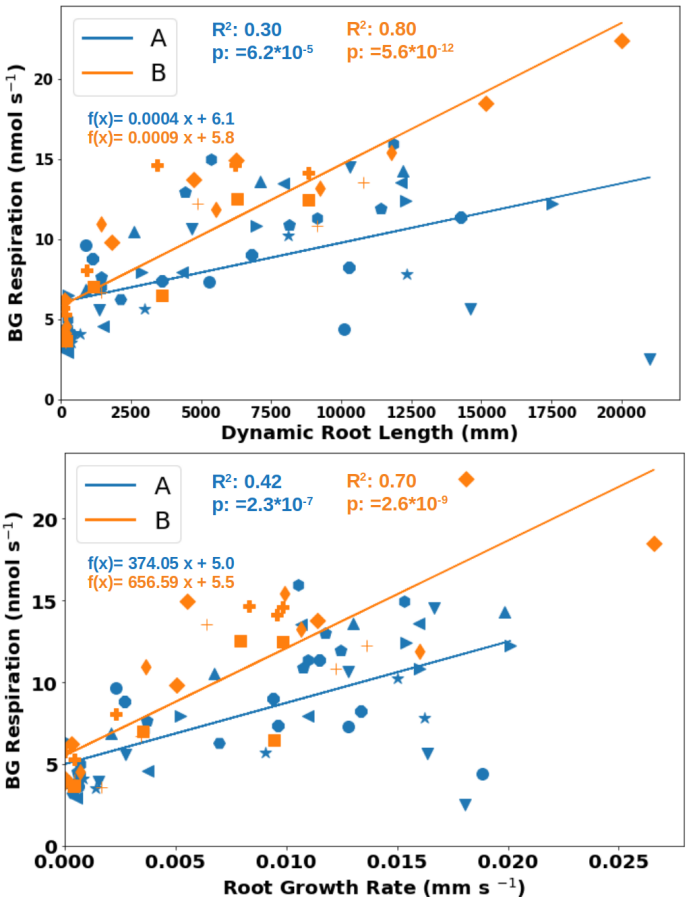

Figure 2.6: Relationship between below-ground (BG) respiration and **(Top)** dynamic root length and **(Bottom)** root growth rate. The orange and blue colours represent the groups while the markers represent different growth chambers in each group. Group A: low penetration resistance, and group B: high penetration resistance. The linear regression p value for each independent variable tests the null hypothesis that the variable has no correlation with the dependent variable.

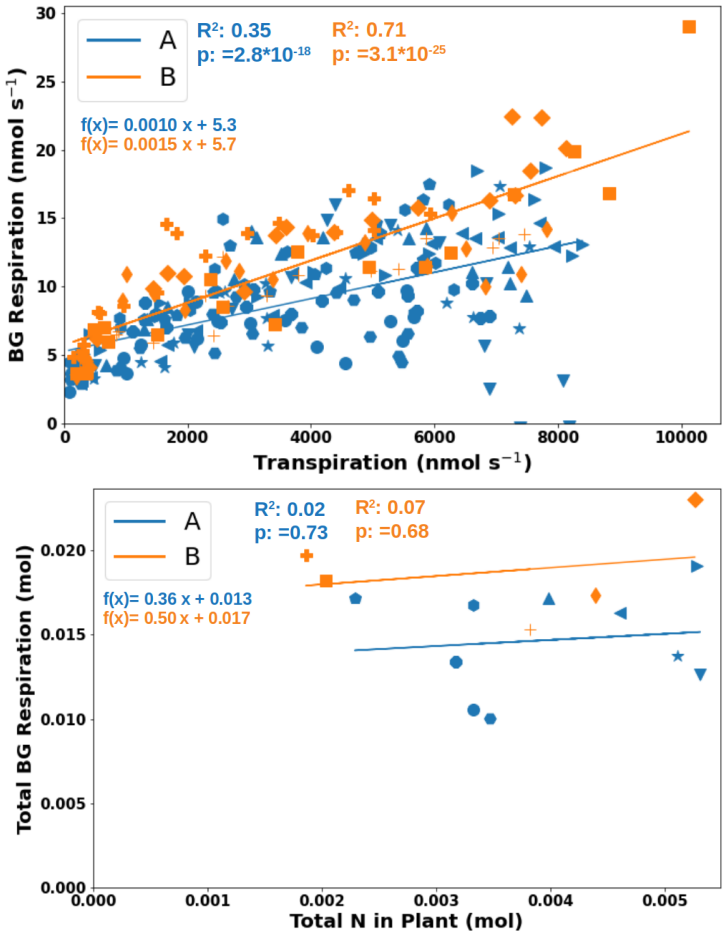

Figure 2.7: Relationship between below-ground respiration and **(Top)** below-ground (BG) transpiration and **(Bottom)** Nitrogen (N) in plant. The orange and blue colours represent the groups while the markers represent different growth chambers in each group. Group A: low penetration resistance, and group B: high penetration resistance. The linear regression p value for each independent variable tests the null hypothesis that the variable has no correlation with the dependent variable.

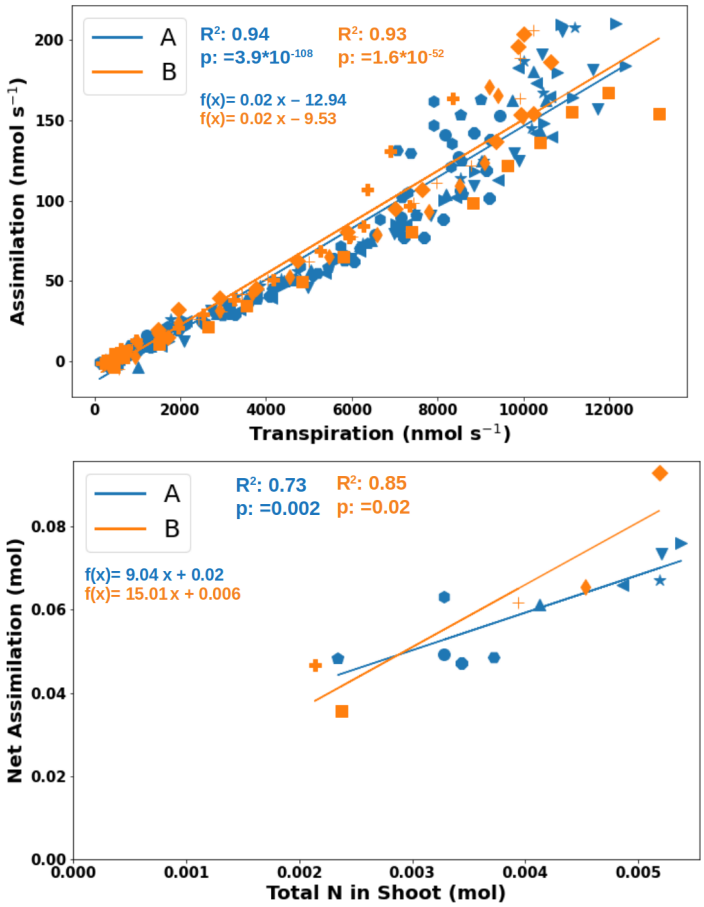

Figure 2.8: Relationship between **(Top)** mean daily assimilation and mean daily transpiration rate **(Bottom)** Cumulative net assimilation and N in shoot. The orange and blue colours represent the groups while the markers represent different growth chambers in each group. Group A: low penetration resistance, and group B: high penetration resistance. The linear regression p value for each independent variable tests the null hypothesis that the variable has no correlation with the dependent variable.

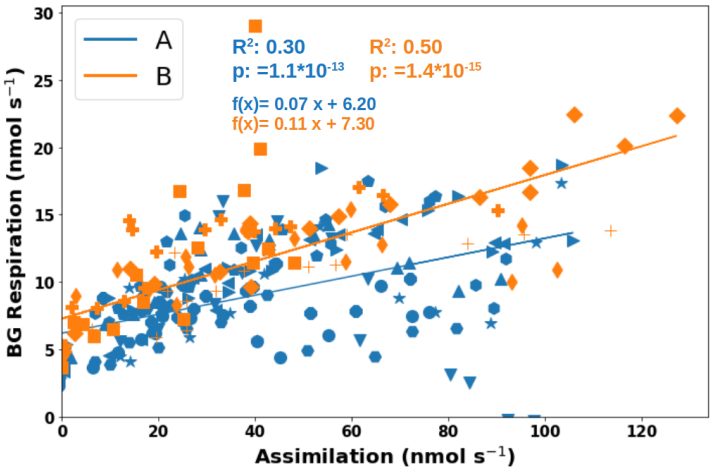

Figure 2.9: Relationship between mean daily assimilation rate and mean daily below-ground (BG) respiration rate. The orange and blue colours represent the groups while the markers represent different growth chambers in each group. Group A: low penetration resistance, and group B: high penetration resistance. The linear regression p value for each independent variable tests the null hypothesis that the variable has no correlation with the dependent variable.

Table 2.5: % C allocation of assimilated C to shoots, roots and soil as determined following ^{14}C labelling in the literature

Plant	Plant age (days)	Shoots	Roots	Soil	References
Wheat	23	36	10.8	52.9	Sun et al., 2018
Barley	25	62.3	15.3	22.4	Zagal et al., 1994
Maize	21	80 - 83	6 - 11	6 - 14	Tubeileh et al., 2003
Maize	27	53.5	46.5	3.8	Meng et al., 2013

2.8 Appendix

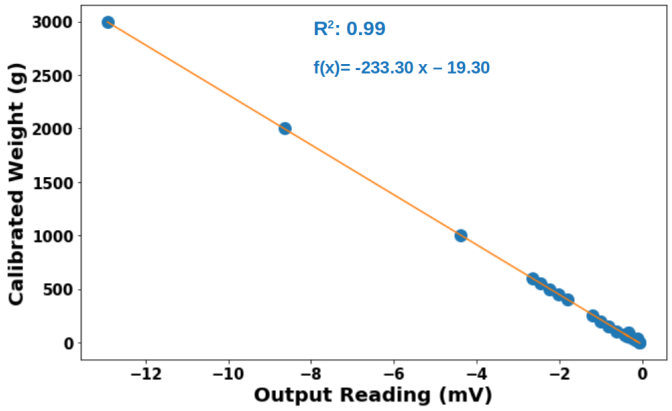

Figure 2.10: Penetrometer load cell was calibrated using 1 g to 3000 g weights (Kern and Son GmbH, Balingen, Germany). The output readings (mV) of the offset value of the mounted load cell and the calibrated weights are plotted against the calibrated weights to obtain a calibration curve. The curve fit parameters were used to convert the mV readings to Newton (N).

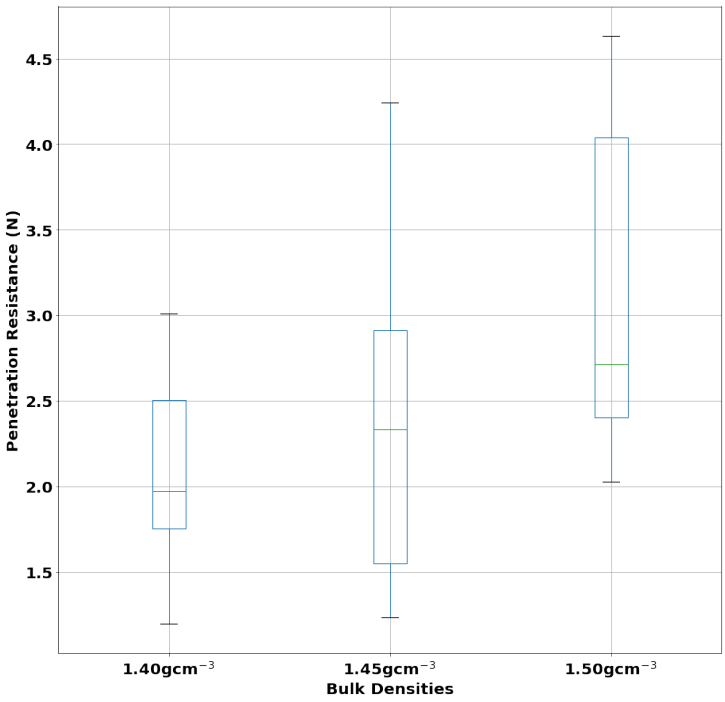

Figure 2.11: Penetration resistance of the three different bulk densities used in the experiment. GC 1-5 has a bulk density of 1.40 g cm^{-3} and a mean penetration resistance of 2.0 N, GC 6-10 has a bulk density of 1.45 g cm^{-3} and a mean penetration resistance of 2.2 N, while GC 11-15 has a bulk density of 1.50 g cm^{-3} and a mean penetration resistance of 3.2 N, (penetration stress = 0.16 MPa). GC 1-10 combined has a mean penetration resistance of 2.2 N (penetration stress = 0.11 MPa) and were grouped under one penetration resistance as their mean values were similar. The penetration cone base radius was 2.5 mm. Penetration resistance for each bulk density was measured at 250, 500 and 750 mm soil height and mean values obtained. Each bulk density had two replicates.

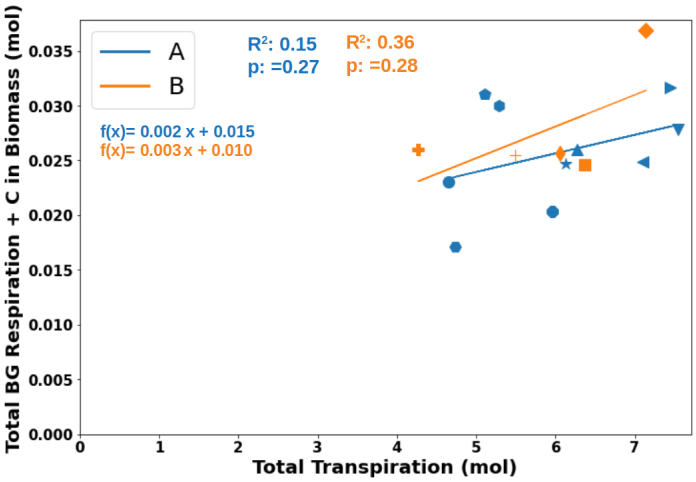

Figure 2.12: Relationship between total transpiration and the sum of biomass and cumulative below-ground (BG) respiration. The orange and blue colours represent the groups while the markers represent different growth chambers in each group. Group A: low penetration resistance, and group B: high penetration resistance. The linear regression p value for each independent variable tests the null hypothesis that the variable has no correlation with the dependent variable.

Table 2.6: Some root respiration rates reported in the literature. Root density of 0.01 g/m of root (as obtained from present study) was assumed. Measurements with Barley plants (Bloom et al., 1992), Common bean and Citrus plants (Bouma et al., 1997), Citrus plants (Bryla et al., 2001).

Reference	**Measurement Unit**	**Measured Respiration Rate**	**nmol s^{-1} m^{-1}**
Bloom et al., 1992	μmol min^{-1} g^{-1}	1.5 - 3.5	0.25 - 0.58
Bouma et al., 1997	nmol $s^{-1}g^{-1}$	3.0 - 17.5	0.03 - 0.175
Bryla et al., 2001	nmol $s^{-1}g^{-1}$	5 - 20	0.05 - 0.2

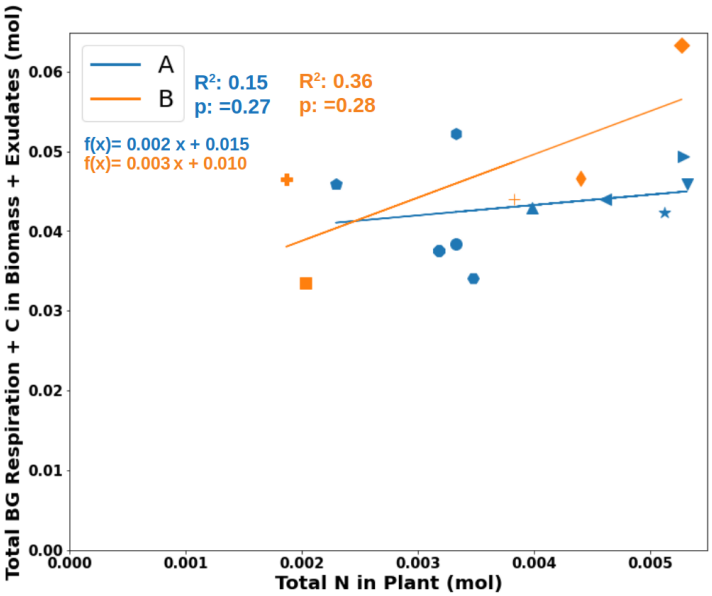

Figure 2.13: Relationship between total N in plant biomass and the sum of biomass, cumulative below-ground (BG) respiration and exudation. The orange and blue colours represent the groups while the markers represent different growth chambers in each group. Group A: low penetration resistance, and group B: high penetration resistance. The linear regression p value for each independent variable tests the null hypothesis that the variable has no correlation with the dependent variable.

Chapter 3

Evaluating cost-benefit ratios of carbon allocation across species and environmental conditions

3.1 Abstract

The cost and benefits of above and below-ground resources acquisition have been studied separately across different species and environmental conditions. Yet a direct comparison of the relative influence of species traits and environmental conditions on these cost-benefit ratios is unavailable. Using the custom growth chamber described in Chapter 1, this study investigated the dominant factors shaping the cost-benefit relationships in resource allocation strategies of maize and barley plants grown in soils with two bulk densities; (1.40 and 1.60 g cm^{-3}). To achieve spread in the growth rates of the experimental plants, three light/dark regimes (long: 18/6, medium: 14/10 and short: 10/14 hours) were employed. CO_2 and H_2O fluxes were monitored from the seedling stage until the experiment's conclusion after two weeks. Cumulative fluxes, plant dry mass, carbon (C) content of plant roots and

shoots as well as final root lengths through destructive analysis were determined at the end of the experiment. Subsequently, the experimental plants were grouped based on species and bulk density to compare the differences in cost-benefit ratios between species and bulk densities.

Maize plants allocated more C to shoot biomass and less to roots translocation, while barley invested significantly more C in the root biomass below-ground. Maize plants were characterized with higher respiration rates compared to barley. Both species showed similar relationships between day-time assimilation rates and nocturnal respiration rates (0.07 vs. 0.06 mol mol^{-1}) as well as similar water uptake per root length. Maize demonstrated nearly double the water use efficiency compared to barley (0.01 vs. 0.006 mol mol^{-1}), however, the root respiration cost per water uptake was higher (0.007 mol mol^{-1}) for maize compared to barley (0.003 mol mol^{-1}). Maize also achieved significantly higher assimilation rates (up to 140 nmol s^{-1}), three times that of barley (up to 40 nmol s^{-1}), but at the cost of higher nitrogen (N) demand, leading to elevated root respiration costs. Interesting, the slopes observed between cumulative below-ground respiration and total N content in plant biomass at the experiment's conclusion were comparable for both maize and barley (1.79 and 1.70 mol mol^{-1}). The total cost of water and nutrient uptake encompassing the sum of total C in root biomass, cumulative respiration and exudation in mols was similar for both species, however, a detailed analysis of the different components of root biomass C is necessary to isolate the pure cost of the root architecture (structural C).

The analysis of the rate of root respiration per root length across the species separately revealed elevated respiration costs for the high bulk density treatments across the species separately. Maize exhibited respiratory cost of 1 vs 0.4 nmol m^{-1} s^{-1} for high and low bulk density respectively while barley exhibited 0.3 vs 0.1 nmol m^{-1} s^{-1} for the high and low bulk density treatments respectively. Higher bulk density treatment in barley was also associated with higher transpiration rate in contrast to the low bulk

density treatment. However, the high soil bulk density treatments were also associated with higher respiration rates per root length ratio in both species (2 vs 0.4 nmol m^{-1} s^{-1}) for high and low bulk density maize and (0.5 vs 0.2 nmol m^{-1} s^{-1}) for high and low bulk density barley respectively.

The findings of this study highlights increased root respiration costs incurred by plant roots under adverse soil conditions. However, increased resources uptake under this conditions suggest a coordinated approach by plants to overcome the limitations imposed by soil compaction. Furthermore, while different species vary in their different uptake strategies, the environment imposes the cost for resource acquisition. The similarity in the cost/benefit ratio of N acquisition in maize and barley highlight the fundamental costs associated with resource uptake, and underscores their species-independent nature.

3.2 Introduction

Resource allocation in plants is a fundamental process involving the distribution of limited resources among competing demands of above and below-ground structures and processes (Mooney, 1972; Givnish, 1986; Poorter et al., 2012; Hartmann et al., 2020). Plants must balance investments in above and below-ground structures and processes for carbon (C) assimilation through photosynthesis as well as water and nutrient uptake (Bazzaz et al., 1987; Poorter et al., 2012; Hartmann et al., 2020). Plant resource allocation is usually invested in the context of above-ground/below ground ratios or assimilation/resource use ratios. These ratios represent the trade-offs that plants face in allocating resources and the potential benefits they can gain from these allocations (Givnish, 1986).

Allocation of resources to above-ground structures is crucial for photosynthesis. The economics of resource acquisition above-ground involves the investment of the C resources into the construction and maintenance of the

photosynthetic tissues (Mooney, 1972; Givnish, 1986). For instance, species with higher specific leaf area (SLA) have been shown to allocate more resources to leaf construction, maximizing their photosynthetic capacity (Reich et al., 1997). Thick leaves requiring more C investment have longer leaf lifespans allowing plants to recoup their C investment over a longer period through extended photosynthesis (Westoby et al., 2002) while highly productive leaves require large inputs of nitrogen (N), phosphorus (P), and other mineral nutrients to create the pools of enzymes and pigments needed to sustain high rates of CO_2 uptake (Givnish, 1986). Furthermore, C acquisition above-ground is also associated with the loss of water (H_2O) through transpiration. To satisfy the shoot transpiration demands, plants also need to invest in their roots to aid water and nutrient uptake. The interaction between shoot photosynthetic capacity, H_2O loss and the C expenses involved in constructing and sustaining tissues for high photosynthetic rates (Field and Mooney, 1986; Mooney, 1972) therefore calls for weighing any photosynthetic benefit against the cost of shoot tissue construction and maintenance as well as H_2O loss.

Below-ground allocation of resources towards roots and root processes is critical for resource acquisition, including H_2O and nutrient uptake. C cost below ground includes the cost of building and maintaining the roots (uptake apparatus) and the energetic expenses incurred by plants during the active uptake of water and nutrients from the soil through their root systems. Root system development, including root length, branching patterns, and architecture, influences below-ground cost-benefit ratios (Nielsen et al., 1994). Different rooting strategies (root morphologies and associations) allow plants to adapt to specific soil conditions and maximize resource acquisition strategies (Hodgkinson et al., 2017). For instance, root systems with extensive branching (Lynch, 1995) or specialized cluster roots (Shane and Lambers, 2005) aid effective soil exploration due to increase in the surface area for resource absorption thereby maximizing resource uptake efficiency while others

may form mycorrhizal associations to enhance nutrient uptake (Lynch et al., 2005). These strategies are associated with varying below-ground cost and benefit ratios.

Research on plant cost-benefit ratios have mostly been dedicated to examining the influence of environmental conditions on above-ground, with limited attention given to below-ground. Majority of these studies have primarily focused on above-ground factors, such as light intensity (Hikosaka et al., 1998; Avola et al., 2008; Field and Mooney, 1986; Bebre et al., 2022), humidity (Rawson et al., 1977), temperature (Dusenge et al., 2019) and CO_2 concentration (Avola et al., 2008), investigating their impact on photosynthetic water-use efficiency (WUE) and nitrogen-use efficiency (NUE). These studies have demonstrated the remarkable adaptability of plants under these specific environmental conditions. For instance, it has been shown that plants in shaded environments allocate more resources to leaf expansion to optimize light capture (Hikosaka et al., 2006). Furthermore, reduction of stomatal conductance under water limited environments increases water use efficiency in plants at the expense of C assimilation (Rawson et al., 1977), while the reduction in photo-respiration under elevated CO_2 levels benefits C3 plants by increasing their Nitrogen Use Efficiency (NUE) (Wong et al., 1992). The emphasis on investigating the effects of above-ground environmental conditions on cost-benefit ratios and photosynthetic efficiency aligns with the ecological significance of photosynthesis in plant growth and ecosystem functioning, as well as the need to understand above-ground resource acquisition in a changing environment. Nevertheless, it is crucial to complement this research with studies exploring the effect of below-ground conditions on the cost and benefits of above and below-ground C investments. For instance, it has been found that limited nutrient availability constrains leaf growth (Reich et al., 2003). As leaves are the primary sites of photosynthesis, the reduced leaf growth leads to a decrease in the overall photosynthetic capacity of the plant. Consequently, the benefit obtained from C assimilation per

unit of investment in leaf growth decreases, affecting the cost-benefit ratio for photosynthesis. This example among others underscores the significance of further investigations into below-ground conditions and their impact on both above and below-ground cost and benefits.

Studies investigating root resource acquisition have provided valuable insights into how below-ground conditions, such as water availability, nutrient levels, and soil compaction, influence the cost and benefits of water and nutrient uptake in plants (Drew, 1975; Grzesiak et al., 2014; Atwell, 1990; Reich et al., 2003; Bengough et al., 2006; Hodgkinson et al., 2017; Colombi et al., 2022) as well as the second chapter of this thesis. These studies consistently show that plants increase their investment in the root system, allocating more C to below-ground structures as well as root respiration to optimize resource uptake especially under challenging conditions. Optimal water and nutrient uptake is contingent on effective exploration of the soil volume. Therefore, soil compaction and the corresponding increase in penetration resistance plays a role in below and above ground cost-and benefits. For instance, the cost of root elongation varies in different soil bulk densities. High bulk densities hinder root elongation in various plant species, potentially leading to decreased access to water and nutrients (Bushamuka and Zobel, 1998; Bengough et al., 2006; Colombi et al., 2017). In response, some plants invest more into the root system, developing thicker roots to cope with the higher soil pressure (Bengough et al., 2011). Furthermore, there has been documented evidence of increased energetic costs with increasing soil penetration resistances (Atwell, 1990; Herrmann and Colombi, 2019). The studies discussed above focused primarily on costs accrued without considering potential benefits.

The second chapter of this thesis addressed this gap through a cost-benefit analysis of C resource allocation using maize plants. Root C respiration cost was compared alongside its associated benefits in terms of water and N uptake. The findings revealed that increased respiratory cost observed in maize

plants grown under high soil bulk density did not result in a corresponding decrease in water uptake. It is important to note that this study was carried out using a single species. Besides environmental conditions, species-specific traits, encompassing morphological, physiological, and biochemical characteristics, play a crucial role in determining plant allocation and trade-offs (Evans, 1989; Poorter et al., 2012). Notably, Evans (1989) demonstrated significant variation in photosynthetic capacity per unit of N across different species. Additionally, Grassi and Bagnaresi (2001); Wang et al. (2021a) share these views and emphasized that plants possess adaptive flexibility through phenotypic plasticity. This allows them to adjust their species-specific traits in response to changing environmental conditions and biological interactions, dynamically altering their structure and function to better adapt to diverse and ever-changing habitats (Matesanz et al., 2010).

It is still however an unsolved question in how far the costs and benefits of C-investment into the root system are species-specific, or determined by environmental conditions. In this third chapter, I aim to test the hypothesis that cost-benefit ratios vary more between environmental conditions (soil bulk density in this context) than species.

3.3 Materials and methods

To test these hypotheses, the set-up and methodology described in the first chapter of this thesis was employed. Above and below-ground fluxes were monitored in 8 maize and 8 barley plants for 15 days. Both plants were divided into two groups and subjected to low ($1.40 g cm^{-3}$) and high ($1.60 g cm^{-3}$) bulk densities. The maize plants in the study were grown in GC 1-4 for low bulk density treatment (1.40 g cm^{-3}) and GC 5-7 for high bulk density treatment (1.60 g cm^{-3}). Similarly, the barley plants were grown in GC 12-15 for low (1.40 g cm^{-3}) and GC 8-10 for high (1.60 g cm^{-3}) bulk density treatments respectively. The mean penetration resistance for GC 1-4 and GC 12-15 was

2.2 N, while for GC 5-7 and GC 8-10, it was 7.4 N (Appendix Figure 3.11). To increase the spread of the values, three different day lengths were used to help the plants grow at different rates. At the end of the experiment, the amount of C in the above and below-ground biomass were quantified.

3.3.1 Soil Substrate

The experimental plants were cultivated utilizing the custom-made potting mixture already described in the first two chapters of this thesis with a maximum water holding capacity of 32.0 ± 2.2 g/100g using the measurement technique established by Blažka and Fischer (2014). The potting mixture was supplemented with 5 g/l of Hakaphos Grün fertilizer (20-5-10(+2), Dünger Experte, Kipfenberg/Attenzell, Germany). The %C content of the components in the potting mixture as determined through an elemental analysis of the individual components was 0.50 ± 0.17 for Hakaphos Grün fertilizer, 0.0020 ± 0.0008 for quartz, and 0.06 ± 0.02 for bentonite. 6 chambers were packed with the potting substrate at 1.60gcm^{-3} bulk density and was cultivated with 3 maize and 3 barley plants, one plant in each chamber. 8 chambers were packed at 1.40gcm^{-3} and contained 4 maize and 4 barley plants, with each chamber containing one plant each. The last chamber was used as a seedless control and packed at 1.40gcm^{-3}. All growth chambers contained an initial volumetric "soil" water content of 20%.

3.3.2 Soil Packing

To achieve a volumetric "soil" water content of 20% in the below-ground cylinder, 285 ml of water was packed into each cylinder. A fertilizer solution was prepared by adding 5 g/l of Hakaphos Grün fertilizer to 85.5 ml (30%) of the total water volume required. The potting mixture, mixed with the fertilizer solution, was divided into three equal portions. Its appropriate consistency prevented the formation of air pockets during packing. The

remaining water was divided into three equal portions (66.5 ml each). The total amount of potting mixture needed for the desired bulk density was weighed, mixed, and divided into three portions. Below-ground cylinders, marked at 3 equal heights, packed with one third of the potting substrate, then compacted with a metal hammer down to the marking, and sprinkled with 66.5 ml of water. This process was repeated thrice until all the portions of the pre-mixed potting substrate were packed into the cylinder. All cylinders were sealed with cling film and aluminum foil and left for 24 hours to allow water redistribution before seed cultivation.

3.3.3 Determining Soil Penetration Resistance

The soil penetration resistance of the two bulk densities used in this study were determined using the custom soil penetrometer described in the second chapter of this thesis. Penetration resistance was measured at 250, 500 and 750 mm soil height and mean values obtained (Appendix Figure 3.11). The penetration forces, measured in Newtons (N), were transformed into penetration stress (Pa) by dividing the force value by the cross-sectional area of the base of the cone (2.5 mm)

3.3.4 Plant Material

Maize (Zea mays L. var Badische gelbe) and barley (Hordeum vulgare L. var Barke) seeds were weighed and subjected to sterilization by immersion in seventy percent ethanol for one minute. The sterilized seeds were then germinated on moist filter paper in sealed petri dishes and placed in a dark cabinet at room temperature for a duration of seventy-two hours. After germination, the resulting seedlings were transplanted into the soil substrate, planted 3 cm deep in the central region of the seed chamber of the growth chamber described in Chapter 1 of this thesis.

3.3.5 Growth Conditions

The plants were cultivated for a period of 15 days in the growth chambers described in the first chapter of this thesis. The separation of the above-ground and below-ground compartments was achieved by pouring melted palm fat at a temperature of 28 °C (semi-solid consistency) in the seed chamber, creating a 0.7 cm thick separation layer between the below and above-ground compartment, adapting the method of Koebernick et al. (2015). The growth chambers were placed in a laboratory with of 24°C / 22°C light/dark temperature. To vary plant growth and increase the spread, three different day lengths were used across the two bulk density treatments. The chambers were grouped into three light regimes (light/dark regime of 10/14, 14/10 and 18/6 hours).

Each growth chamber was equipped with the custom individual LED lamp described in the first chapter of this thesis, supplying light at 600 μmols m^{-2} s^{-1} photosynthetic photon flux density (PPFD).

3.3.6 Growth Chamber Setup and Gas Exchange Measurements

In this study, continuous and simultaneous measurements of CO_2 and H_2O exchange in each compartment of growth chambers were carried out using the gas exchange system described in Chapter 1. The set-up included two portable photosynthesis systems (LI-6800, LI-COR, Lincoln, NE, USA), with one system assigned to each compartment. The investigation focused on eight maize plants and eight barley plants, along with one seedless control chamber, totaling fifteen growth chambers. The experiment spanned fifteen days. To facilitate efficient measurements, the set-up was connected to a multiplexing system comprising eight 8-way multiplexers (Vici 8-Port Multiposition Selector Valves, Vici AG International, Schenkon, Switzerland). This arrangement enabled repetitive measurements on all fifteen growth chambers

in rapid succession. Each chamber underwent measurements for a duration of 10 minutes, about 10 times within a 24-hour period.

Data acquisition was done on the LI-6800 gas exchange system, recording measurements at a frequency of five seconds throughout the entire experiment. To ensure data integrity and system stability, a custom background script was opened on the LI-6800, which automatically initiated a new file every twenty-four hours to prevent system crashes and data loss. Subsequent to the experiments, the recorded data stored in ASCII format on the LI-6800 were downloaded and analyzed. The flux measurements were appropriately assigned to the corresponding growth chambers based on the recorded switch time in the labview program of the multiplexers. To prevent system crashes and data loss, a new file was automatically initiated every twenty-four hours.

It is important to note that during this experiment, fluctuations in the concentration of CO_2 in the incoming air posed challenges in achieving a steady state in the system. To address this, different calculations were adopted from those reported in previous chapters, as detailed by Schymanski and Osuebi-Iyke (2023). Specifically, incoming and outgoing fluxes were averaged, and from these, a net exchange was calculated, deviating from the approach in previous chapters, which utilized instantaneous fluxes.

When retrieving data from the LI-6800, CO_2 fluxes are presented as positive for CO_2 uptake and negative for CO_2 release. The separation of assimilation and nocturnal respiration fluxes during data analysis is done using the light on/off regime. For below-ground measurements, all negative fluxes are classified as respiration. In the above-ground context, when the light is off, negative values are attributed to respiration, while positive values represent above-ground net shoot assimilation. In data analysis, respiration is depicted as positive CO_2 release, whereas assimilation is denoted as positive CO_2 uptake. The addition of H_2O to the airstream is recorded as a positive value by the LI-6800, and this convention is consistently maintained both during data analysis and in the figures. Subsequently, daily mean values of assimilation,

nocturnal respiration, transpiration, and evaporation rates were calculated for the experimental conditions.

3.3.7 Pre-experimental Total and Dissolved C and N Analysis

The pre-experimental total C content of the potting medium was obtained by measuring the total C content of sub-samples of the individual components (fertilizer, quartz and bentonite) using an elemental analyzer (Vario MacroCube, Elementar, Hesse, Germany) and scaling the values up using the mass percentages as described in the first chapter of this thesis. Similarly, the initial dissolved organic carbon (DOC) content of each potting substrate component was determined by dissolving sub-samples of each component in 250 ml of water and analyzing the filtrate for DOC using a Torch TOC Combustion Analyzer (Teledyne Tekmar, Mason, OH, USA) as previously described in Chapter 1 of this thesis as well. The concentration of DOC in the filtered solution, measured in mg/l, was multiplied by the volume of wash water to estimate the pre-experimental DOC content of each chamber.

3.3.8 Harvest and Post-Experimental Total C and DOC Analysis

Upon completion of the gas-exchange, the above-ground shoots of the plants were harvested. The dimensions of the leaves, were measured using a ruler. Leaf area was then calculated using the method described by Montgomery (1911) as cited in McKee (1964). Leaf fresh mass was determined using a precision weighing balance.

To retrieve the roots from the below-ground cylinder, the soil was gently pushed out using a piston and washed in a large bowl using approximately 8 liters of water. This process involved placing a 2 mm mesh sieve on top of a finer 0.5 mm mesh sieve, both positioned inside the bowl. The roots

that passed through the 2 mm sieve were collected on the finer sieve to prevent loss. After washing, the roots were dried with paper towels to remove excess moisture, and their fresh mass was measured. Roots adhering to the paper towels were removed using tweezers. The fresh roots were then scanned using an EPSON V800 scanner and analyzed using WinRhizo Pro (Regent Instruments, Ottawa, Canada) using the following settings: Image type: Gray levels; Resolution: high, 600; Tray size: 20cm X 20cm; Surface area: 1464cm^{-3}.

Subsequently, both the roots and above-ground shoots were subjected to oven drying at 65°C for 48 hours, the dry mass was measured and sub-samples (about 50 mg) of the dried plant material were analyzed for total C and N using a Vario MacroCube elemental analyzer (Elementar, Hesse, Germany). By multiplying the mass percentage of C in the sub-samples by the total mass of the corresponding samples, an estimation of the total C content in the entire plant dry mass was obtained.

After the root washing process, the DOC content of the wash water was determined using a Torch TOC Combustion Analyzer (Teledyne Tekmar, Mason, OH, USA). In addition, dried (105°C for 48 hours) sub-samples (about 500 mg) of the washed soil were also analyzed for total C using a Vario MacroCube elemental analyzer (Elementar, Hesse, Germany). A full description of the methodology is described in Chapter 1 of this thesis.

3.3.9 C allocation Above and Below-ground

C allocations to biomass, above-ground respiration, and root translocation were determined as proportions of total assimilated C, while C in the roots was assessed as the sum of C translocated below-ground and the initial C present in the seed. Any remaining seed remnants below-ground were subtracted from the initial seed C content. Furthermore, C allocation to root biomass and respiration was calculated as fractions of the C content in the roots. The amount of C lost to the soil was derived by subtracting the sum

of C in root biomass and expended in respiration from the total root translocation, employing the variables and expressions provided in Table 3.1.

3.3.10 Statistical Analysis

Descriptive statistics, including mean, minimum, maximum, and median, were calculated for the datasets. To assess the normality of the data distribution, the Shapiro-Wilk test (Shapiro and Wilk, 1965) was employed. As the Shapiro-Wilk test did not indicate normality of data distribution, non-parametric tests were used to examine differences between groups. In instances where extreme outliers (for instance, positive assimilation values during the night possibly due to a malfunction in the timer) significantly impact mean values, median values are presented in the text instead.

When comparing pair-wise differences between species and bulk densities, the non-parametric Mann-Whitney U-test was utilized (Mann and Whitney, 1947). For cases where there were more than two groups, such as the light groups, the Kruskal-Wallis test (Kruskal and Wallis, 1952) was used to determine if there were significant differences between the groups. Additionally, the Conover-Iman test (Conover and Iman, 1981) was used as a post hoc test to further investigate the differences between pair-wise combinations within the light groups. These non-parametric tests are suitable for datasets that do not meet the assumptions of normality of distribution and provide robust results for comparing group differences.

The analysis involved the use of both ordinary linear regression based on ordinary least squares (OLS) (James et al., 2013) and robust linear regression models (RLM) (Yu et al., 2014) to account for outliers and small sized datasets. Minimal differences were observed between the two regression models. Given their similarity, the results from the OLS model are presented.

To compare the slopes of the regression analysis in this study, a combination of fundamental concepts in statistical testing was employed (James et al., 2013). Slope estimates were obtained from the regression models fitted

Table 3.1: Relevant variables and expressions used to calculate biomass allocations above and below-ground. C investments to biomass, respiration above ground and translocation to the roots were calculated as fractions of total assimilated C while C in the root was calculated as a sum of C translocated below-ground and initial C in seed. In the case of any seed remnant below-ground, this was subtracted from the initial amount of C in seed. C investment to root biomass, respiration were then calculated as fractions of C in root. C exudation was calculated by taking the sum of C in root biomass and C expended in respiration and subtracting it from total root translocation.

Variables	**Description**	**Expressions (If applicable)**
$\mathrm{F}_{A\text{net, day}}$	Total Net above-ground daytime Assimilation (mol)	
$F_{R_{\text{night}}}$	Total Above-ground nocturnal respiration (mol)	
$F_{R_{\text{root}}}$	Total Below-ground respiration (mol)	
C_{rt}	C translocated below-ground (mol)	
C_i	C in seed (mol)	
$C_{i_{\text{remnant}}}$	C in seed remnant (mol)	
C_s	C in shoot (mol)	
C_r	C in root (mol)	
$C_{\text{r total}}$	C in root + C in seed	$C_{\text{rt}} + C_i$
C_e	C released into soil (mol)	$C_{\text{r total}} - C_r + F_{R_{\text{root}}}$
C_{s_F}	Shoot biomass proportion	C_s / $\mathrm{F}_{A\text{net, day}}$
C_{dr_F}	Shoot dark respiration proportion	$F_{R_{\text{night}}}$ / $\mathrm{F}_{A\text{net, day}}$
C_{rt_F}	Root translocation proportion	C_{rt} / $\mathrm{F}_{A\text{net, day}}$
C_{r_F}	Root biomass proportion	C_r / $C_{\text{r total}}$
C_{rr_F}	Root respiration proportion	$F_{R_{\text{root}}}$ / $C_{\text{r total}}$
C_{e_F}	Root exudation proportion	C_e / $C_{\text{r total}}$

using the data specific to each group. The difference in the two slopes were obtained and to find the standard error of the difference in slopes, the square root of the sum of the squares of the standard errors for each slope was taken. The test statistic was computed as the ratio of the slope difference to the standard error of the difference. The degrees of freedom (df) for the t-test were then determined based on the lengths of the respective data sets for the groups. This was then followed by a two-tailed t-test performed using the calculated test statistic and degrees of freedom. The p-value associated with the test statistic was obtained by evaluating the cumulative distribution function (CDF) of the absolute value of test statistic using the t-distribution. The p-value was calculated as twice the complement of the CDF. Finally, the obtained p-value was compared to a chosen significance level, ($p \leq 0.05$), to determine the statistical significance of the difference in slopes. A p-value below the significance level would indicate that the difference in slopes is considered statistically significant.

Similar to the convention in the second chapter of this thesis, in each presented regression analysis in the results section, the slopes are computed and compared between the experimental groups. Here, a linear relationship is assumed and the intercept real. Where the regression analysis is not significant or the data points are too few for a regression analysis to be carried out, the y/x ratios were computed. In this case, the ratio assumes that there is no intercept. Due to the presence of intercepts in the regression analysis, the slope offers a quantitative measure of the cost/benefit relationship of the variables under consideration.

3.4 Data Availability

All data and computations presented in this Chapter are found here:

https://doi.org/10.5281/zenodo.10386962 .

3.5 Results

In this study, experiments were conducted using 14 + 1(empty) growth chambers and two plant species, maize and barley. The experiment lasted for about two weeks so the experimental plants were typically in the early stages of their vegetative growth period. Basic information regarding plant dry mass and leaf area is presented in Table 3.2.

Table 3.2: Relevant information about plants in the different growth chambers for different treatment groups. The average mass of cultivated seeds in each growth chamber was 0.31 g for Maize and 0.05 g for Barley.

	S/Name	Shoot Dry mass (g)	Root Dry Mass (g)	Leaf Area (cm2)	Root Length (mm)
Maize 1.40 g cm^{-3}	GC1	0.47	0.11	146.16	16274.83
	GC2	0.49	0.12	136.77	10020.19
	GC3	0.75	0.13	232.34	22042.14
	GC4	0.90	0.20	166.89	26548.44
	Mean	**0.65**	**0.14**	**170.54**	**18721.40**
	Standard Deviation	**0.21**	**0.04**	**43.08**	**7164.42**
Maize 1.60 g cm^{-3}	GC5	0.18	0.05	47.33	1120.54
	GC6	0.29	0.06	78.79	1815.30
	GC7	0.15	0.06	28.91	1175.01
	Mean	**0.20**	**0.06**	**51.68**	**1370.28**
	Standard Deviation	**0.07**	**0.01**	**25.22**	**386.36**
Barley 1.60 g cm^{-3}	GC8	0.14	0.05	34.78	2815.87
	GC9	0.11	0.07	30.60	2815.87
	GC10	0.18	0.11	38.25	3483.74
	Mean	**0.14**	**0.08**	**34.54**	**3038.50**
	Standard Deviation	**0.03**	**0.03**	**3.83**	**385.59**
Barley 1.40 g cm^{-3}	GC12	0.10	0.06	28.19	4877.68
	GC13	0.19	0.13	44.31	20278.47
	GC14	0.18	0.14	39.79	14632.73
	GC15	0.26	0.19	42.32	26158.44
	Mean	**0.73**	**0.52**	**154.60**	**65947.31**
	Standard Deviation	**0.07**	**0.05**	**7.22**	**9057.71**

To test whether cost-benefit ratios exhibit greater variations across environmental conditions than across species, the experimental plants were grouped based on their species and bulk density. This resulted in two main groups: one for each bulk density (1.40 g cm^{-3} and 1.60 g cm^{-3}), consisting of both maize and barley plants, and another group for each species (maize and barley), comprising plants grown under both bulk densities. The penetration resistance was 0.11 and 0.38 MPa for the low and high bulk density

treatments respectively. The two species were also analyzed separately across the two bulk densities. Due to the limitation of the experimental setup to 15 plants at a time, each group contained only 7 plants. Due to this small sample size, interactions between soil compaction and species, i.e. whether the different species responded differently to the compactions, were not investigated.

C Allocation to Above and Below-ground Biomass and Respiration

The comparison between the proportion of cumulative C assimilates (mol) allocated to shoot biomass, shoot respiration and root translocation revealed that maize allocated a larger fraction of assimilates to shoot biomass (69% for maize and 53% for barley, $p = 0.001$) and a lower fraction to the root system compared to barley (20% for maize and 38% for barley $p = 0.004$). There was no observed statistically significant difference in the shoot respiration proportion (11% for maize and 9% for barley, $p = 0.2$) between the two species (Table 3.3, Figure 3.1). The same analysis was done as grouped by penetration resistance (bulk density), but no statistically significant difference was observed between groups for the fractions of assimilates allocated to shoot respiration, shoot biomass or the root system for all three proportions (Figure 3.1). Also within each species, no significant differences in C allocation to shoot respiration, shoot biomass or the root system were observed between compaction treatments (Figure 3.1).

The analysis of the below-ground allocation proportions, categorized by species (maize and barley), showed statistically significant differences in C allocation patterns between the two species in the root respiration and root biomass proportion. Specifically, maize allocated a higher proportion of below-ground C to root respiration (43% for maize and 33% for barley, $p = 0.005$) and a lower proportion to root biomass compared to barley (30% for maize and 40% for barley, $p = 0.003$). Additionally, there was no observed statistically significant difference in C released to the soil between the

Table 3.3: Summary of above-ground (AG) C allocation proportions as a fraction of net cumulative daytime C assimilation above-ground to shoot respiration, biomass and translocated to the roots (formatted in %) for the two species, maize and barley. Each species group consists of both low (1.40 g cm^{-3}) and high bulk density (1.60 g cm^{-3}). The Mann-Whitney U test p-value for the % proportions tests whether there is a statistically significant difference in the distribution of a continuous dependent variable between the two independent groups.

	Allocation Proportions of Total C Assimilation					
	Shoot Respiration		**Shoot Biomass**		**Root Translocation**	
	Maize	**Barley**	**Maize**	**Barley**	**Maize**	**Barley**
Count	7	7	7	7	7	7
Min	6% (0.0008 mol)	5% (0.0006 mol)	60% (0.006 mol)	46% (0.003 mol)	10% (0.0009 mol)	26% (0.002 mol)
Mean	11% (0.003 mol)	9% (0.0009 mol)	69% (0.017 mol)	53% (0.006 mol)	20% (0.005 mol)	38% (0.005 mol)
Max	19% (0.005 mol)	14% (0.001 mol)	80% (0.034 mol)	60% (0.010 mol)	32% (0.012 mol)	49%(0.010 mol)
p value that maize = barley	p = 0.2		**p = 0.001**		**p = 0.004**	

two species (27% for maize and 27% for barley, p = 0.1). (Table 3.4, Figure 3.2).

There was no statistically significant difference between the two bulk density groups concerning the three below-ground C allocation proportions: root respiration, root biomass, and C released to the soil. Within each species, no significant differences in C allocation to to root respiration, root biomass, or released to the soil were observed between compaction treatments for maize. However, for barley, There was a statistically increased C investment (p = 0.03) to root biomass for the low compaction treatment (45%) compared to the high compaction treatment (33%) (Figure 3.2).

Costs and Benefits of Plant Roots

To understand the C expenditure below-ground, the analysis of root respiration per root growth as well as the below-ground cost of water uptake (using transpiration as a proxy) and N uptake was analyzed. N uptake was determined as the difference between initial N content in the seed and in the plant biomass at the end of the experiment.

The relationship between root length (mm) and above-ground transpira-

Table 3.4: Summary of below-ground (BG)(root translocation + C in seed) fractions of C investment allocated to root biomass, root respiration and released to the soil (formatted in %) for the two species, maize and barley. Each species group consists of both low (1.40 g cm^{-3}) and high bulk density (1.60 g cm^{-3}). The Mann-Whitney U test p-value for the % proportions tests whether there is a statistically significant difference in the distribution of a continuous dependent variable between the two independent groups. Summary of below-ground C allocation for the two species, maize and barley. Each species group consists of both low (1.40 g cm^{-3}) and high bulk density (1.60 g cm^{-3}).

	Allocation Proportions of Total C Translocated to the Root					
	Root Respiration		**Root Biomass**		**C Released to the Soil**	
	Maize	**Barley**	**Maize**	**Barley**	**Maize**	**Barley**
Count	7	7	7	7	7	7
Min	39% (0.002 mol)	22% (0.001 mol)	26% (0.002 mol)	31% (0.001 mol)	21% (0.001 mol)	-19% (-0.001 mol)
Mean	43% (0.005 mol)	33% (0.002 mol)	30% (0.003 mol)	40% (0.002 mol)	27% (0.003 mol)	27% (0.002 mol)
Max	48% (0.008 mol)	54% (0.003 mol)	38% (0.007 mol)	65% (0.004 mol)	32% (0.004 mol)	46% (0.005 mol)
p value that maize = barley	**p= 0.005**		**p = 0.003**		p = 0.1	

tion (nmol s^{-1}) (as a proxy for root water uptake) was examined for maize and barley. For the comparison, the maximum transpiration rate was utilized instead of that of the last day in relation to the final root length due to a system malfunction on the last day of the LI-6800 measurements.

A significant linear relationship was observed between the two variables for the two species (R^2 = 0.81 and 0.65) for maize and barley respectively. There was no statistically significant difference between the slopes of the relationship between the two species (0.16 and 0.34 nmol mm^{-1} s^{-1}, p = 0.07) for maize and barley respectively (Figure 3.3, top). Analyzing the relationship for the species separately across the bulk density treatments, it was observed that higher bulk densities were associated with increased transpiration per root length ratio for maize plants (0.60 and 2.02 nmol mm^{-1} s^{-1}, p = 0.03) for low and high bulk density maize respectively. Although a tendency of higher transpiration per root length was observed for barley, it was not statistically significant across the two bulk densities (0.53 and 1.18 nmol mm^{-1} s^{-1}, p = 0.06) for the low and high bulk density treatments respectively.

The regression analysis between N uptake (mol) and final root length (mm) showed a significant correlation between the two variables for the two species ($R^2 = 0.94$ and 0.87) for maize and barley respectively. The slope of the relationship was higher for maize than for barley ($1.0 * 10^{-7}$ and $3.3 * 10^{-8}$ mol mm^{-1}, $p = 0.0005$) (Figure 3.3, bottom). Analyzing the relationship for the species separately across the bulk density treatments, it was observed that higher bulk densities were associated with increased N uptake per root length ratio for barley plants ($6.3 * 10^{-8}$ and $1.8 * 10^{-7}$ mol mm^{-1}, $p = 0.03$) for low and high bulk density barley respectively. Although a tendency of N uptake per root length was observed for maize, it was not statistically significant across the two bulk densities ($1.2 * 10^{-7}$ and $2.5 * 10^{-7}$ mol mm^{-1}, $p = 0.2$) for the low and high bulk density treatments respectively.

To examine the respiratory cost of the root length across maize and barley, the relationship between root length and root respiration was examined across the species first without distinguishing the bulk densities. In a second step, the control experiment was added to each of the bulk densities across the species separately to compare the effect of the two bulk densities on root respiration.

At the absence of dynamic root length measurements, the final root length (mm) at the end of the experiment was compared to below-ground respiration on the last day (nmol s^{-1}) across the two species. A strong linear relationship was observed between the two variables for maize and barley ($R^2 = 0.85$ and 0.78) respectively (Figure 3.4, top). The slope of the relationship was significantly higher for maize in contrast to barley (0.3 nmol m^{-1} s^{-1} and 0.1 nmol m^{-1} s^{-1}, $p = 0.01$). No distinction was made between the two bulk densities in this regression analysis. In both plant species, it was observed that higher bulk densities were associated with statistically significantly higher root respiration per root length ratios. For maize, the mean root respiration per root length ratio was 2 nmol m^{-1} s^{-1} for the high bulk density and 0.4 nmol m^{-1} s^{-1} for the low bulk density group, ($p = 0.03$). Similarly, in barley, the mean

root respiration to root length ratio was 0.5 nmol m^{-1} s^{-1} for the high bulk density and 0.2 nmol m^{-1} s^{-1} for the low bulk density, ($p = 0.03$).

Adding the control to each bulk density and analyzing the species separately across the bulk densities, a linear relationship was observed for each of the species across the two bulk densities, ($R^2 = 0.88$ and 0.74) for low and high bulk density maize respectively. The regression for the high bulk density maize was not significant ($p = 0.14$) whereas it was significant for the low bulk density maize ($p = 0.02$) (Figure 3.4, middle). Similarly, a significant linear relationship was also observed for barley across both bulk densities ($R^2 = 0.82$, $p = 0.03$ and 0.91, ($p = 0.05$))) for the low and high bulk density treatment respectively (Figure 3.4, bottom). Calculating the slopes separately for each of the species across the different bulk densities, maize exhibited slopes of 0.4 nmol m^{-1} s^{-1} and 1 nmol m^{-1} s^{-1} whereas barley exhibited slopes of 0.1 nmol m^{-1} s^{-1} and 0.3 nmol m^{-1} s^{-1} for the low and high bulk density treatments respectively. A statistical test for the significance of the differences in slopes was not conducted due to the insufficient amount of data available for each compaction level.

Furthermore, the relationship between average daily below-ground respiration and above-ground transpiration rates (nmol s^{-1}) was analyzed. A significant linear relationship was observed between the two variables for the two species ($R^2 = 0.47$ and 0.32) for maize and barley respectively (Figure 3.5, top). The slope of the relationship was higher for maize than for barley (0.0007 and 0.0004 mol mol^{-1}, $p = 5.7*10^{-5}$) for maize and barley respectively. It was observed that the low bulk density treatments for the two species were associated with higher respiration rates (Figure 3.5, top). Analyzing the species separately across the bulk densities, the slope of the relationship was 0.0005 and 0.0002 mol mol^{-1} for low and high bulk density maize plants. Since the regression analysis for the high bulk density maize plants was not significant ($p = 0.06$), the ratio rather than the slope of their relationship was compared. The mean daily below-ground respira-

tion per transpiration ratio was similar between the two bulk densities (0.004 mol mol^{-1}, p = 0.08). For the barley plants, the difference in the slopes of the relationship between the low and high bulk density treatment was not significant (0.0003 and 0.0001 mol mol^{-1}, p = 0.06).

The analysis of the respiratory expenditure (total below-ground respiration, (mol)) associated with N uptake (total N in plant (mol)) (Figure 3.5, bottom), revealed significant linear correlations for the two species (R^2 = 0.92 and 0.70) for maize and barley respectively. The slopes of the relationship for the two species was not statistically different (1.79 vs 1.70 mol mol^{-1}, p = 0.8). Analyzing the respiration per N uptake ratio for the species separately across the two bulk density treatments, there was no statistically significant difference for the respiration per N uptake for barley plants (2.51 and 2.80 mol mol^{-1}, p = 0.4) for the low and high bulk density treatment respectively. For maize, the respiration per N uptake ratio was higher for the high bulk density treatment compared to the low bulk density treatment (13.0 and 3.05 mol mol^{-1}, p = 0.03) respectively.

The overall cost of root water uptake was obtained by taking the sum of cumulative below-ground respiration and C in root dry mass (mol) and compared with cumulative transpiration (mol). A significant linear relationship was observed between the two variables for the two species (R^2 = 0.93 and 0.86) for maize and barley respectively (Figure 3.6, top). There was no statistically significant difference between the slopes of the relationship between the two species (0.003 and 0.002 mol mol^{-1}, p = 0.98) for maize and barley respectively. Similarly, the overall cost of N water uptake was also obtained by taking the sum of cumulative below-ground respiration, C in root dry mass (mol) and exudates (mol) and compared with cumulative transpiration (mol). A significant linear relationship was observed between the two variables for the two species (R^2 = 0.90 and 0.70) for maize and barley respectively (Figure 3.6, bottom). There was no statistically significant difference between the slopes of the relationship between the two species

(4.22 and 7.23 mol mol^{-1}, p = 0.2) for maize and barley respectively.

Above-ground Costs and Benefits

The investigation of above-ground C uptake centered on the relationship between C assimilation (nmol s^{-1}) as the benefit and above-ground transpiration (nmol s^{-1}) as the cost. The slope of the relationship was considered the water use efficiency (WUE). When considering the species-level grouping (Figure 3.7), there was a significant correlation between the two variables across both groups, (R^2 = 0.99) for maize and (R^2 = 0.96) for barley. The slope of the relationship (WUE) was higher for maize than barley (0.012 vs 0.006 mol mol^{-1}, p = 0.0001).

Analyzing the plant species separately, it was observed that higher bulk densities were associated with steeper slopes (higher WUE) in the regression analysis of net daily mean assimilation vs transpiration rate for barley (Figure 3.7). The WUE for barley plants grown under high soil bulk density was significantly higher (0.006 mol mol^{-1}) than those grown under low soil bulk density (0.005 mol mol^{-1}, p = 0.007).

The relationship between mean daily above-ground assimilation rate and below-ground respiration rate (nmol s^{-1}) revealed moderate positive correlations (R^2 = 0.41 and 0.30) and similar slopes (0.07 and 0.06 mol mol^{-1}, p = 0.9) for maize and barley respectively.

Additional Findings: Day Length effect on Nocturnal Respiration and WUE

Although different day lengths were only simulated to increase the range of plant sizes within a treatment, separate regression analyses were curiously conducted between daily mean assimilation and nocturnal respiration rates (nmol s^{-1}) for maize plants across three different day lengths: short day: 10/14 light/dark regime (R^2 = 0.54), medium day: 14/10 light/dark regime (R^2 = 0.41), and long day: 18/6 light/dark regime (R^2 = 0.97). The rela-

tionship between assimilation and respiration was positively correlated for all day lengths, with the highest slope observed in plants grown under the long day (0.15 mol mol^{-1}). Maize plants grown under the medium and short day length had similar slopes (0.12 mol mol^{-1}) (Figure 3.9, top).

To compare the nocturnal respiration/assimilation ratio across the different day lengths, a non-parametric Kruskal-Wallis test was used. The median ratio was 0.17, 0.13 and 0.11 mol mol^{-1} for the long, medium and short day length maize plants respectively. The post-hoc Conover-Iman test revealed that the ratio was significantly higher in plants grown under the long day compared to the other two day lengths, ($p = 0.0001$ for a pairwise comparison with 14/10) and ($p = 0.0006$ for a pairwise comparison with 10/14 light/dark regime). However, there was no statistically significant difference between the medium and short day length plants ($p = 0.6$).

For barley plants, the regression analysis examining the daily mean assimilation and nocturnal respiration rates revealed significant correlations (Figure 3.9, bottom). However, the regression coefficients were lower compared to maize, mainly due to the presence of considerable noise in the data. Consequently, the mean daily respiration/assimilation ratio rather than the slopes were compared between the different day lengths for a more meaningful assessment.

The post-hoc Conover-Iman test indicated that the respiration/assimilation ratio was significantly higher in plants grown under the long day length compared to the short day length (median ratio = 0.14 and 0.10 mol mol^{-1}, $p = 0.003$) respectively. However, there were no statistically significant difference between the long and medium day length (0.12 $^{-1}$ mol^{-1}) day length, ($p = 0.2$).

Similarly, a non-parametric Kruskal-Wallis test was conducted to compare water use efficiency (WUE) across different day lengths above-ground. For maize plants, there was similar WUE among different day lengths (0.01, $p = 0.3$) (Figure 3.10, top).

However, for barley plants, the Kruskal-Wallis test revealed statistically significant differences in WUE across different day lengths. Subsequently, pairwise post-hoc Conover-Iman tests were performed. The results showed that the WUE of barley subjected to long days (0.006 mol mol^{-1}) was significantly higher than those subjected to medium and short days (0.006 mol mol^{-1}) p = 0.0001 and 0.003) for comparisons with medium and short days (Figure 3.10, bottom).

3.6 Discussion

Building upon the insights obtained from the second chapter of this thesis, the scope of the investigation was expanded to explore the impact of soil mechanical properties, specifically bulk density and penetration resistance, on two distinct plant species, namely maize and barley. The aim was to assess whether the cost-benefit ratios exhibit greater variation across environmental conditions than across different plant species, utilizing similar bulk density treatments as employed in the second chapter. The low bulk density treatment was maintained at 1.40 gcm^{-3}, while the high bulk density treatment was increased to 1.60 gcm^{-3}. As a result, the corresponding penetration resistances for the low and high bulk density treatments were 0.11 MPa and 0.38 MPa respectively.

C Allocation to Above and Below-ground Biomass and Respiration varies more across Species

Abiotic stressors, such as soil compaction, exert a significant impact on plant growth, development, and yield, by increasing soil bulk density and penetration resistance. In response to these stressors, plants modify their C allocation patterns to prioritize the most constrained organ. For instance, when faced with soil compaction, there may be a need to allocate more photosynthates for root system expansion, potentially resulting in reduced C

availability for above-ground growth (Atwell, 1990). This adaptive strategy aligns with the concept of functional equilibrium (Brouwer, 1983), wherein plants reallocate C to address the organ that is most limited by the stress.

In the context of the current investigation encompassing two plant species, maize and barley, exposed to distinct soil bulk densities (low: 1.40 gcm^{-3}, high: 1.60 gcm^{-3}) treatments, statistically significant differences were not identified in the allocation of assimilates toward shoot biomass, shoot respiration, and below-ground allocation between the high and low bulk density treatments (Figure 3.1). This outcome is in agreement with the findings from the second chapter, where the two bulk density treatments did not lead to any statistically significant differences in above-ground C allocation patterns. However, contrasting strategies for above-ground C allocation emerge quite distinctly when comparing the two species (Table 3.3, Figure 3.1). Maize notably displays a tendency to direct a greater portion of assimilates towards its shoot system. This propensity could be rooted in maize's rapid growth approach, which requires a substantial leaf area to enhance photosynthetic efficiency (Irving, 2015). Similar allocation pattern have been observed by Meng and colleagues (Meng et al., 2013). The findings pertaining to barley suggest a conservative strategy, where it allocates a greater proportion of resources to its root system. This approach, common among C3 plants (Irving, 2015), might be imperative for barley to establish a comprehensive root system that facilitates effective water and nutrient uptake during its growth stage. This root-focused allocation pattern aligns with other observations in C3 plants, such as wheat (Atwell et al., 2002), as well as in barley (Swinnen et al., 1995a,b).

C3 plants require higher nitrogen (N) levels compared to C4 plants due to differences in their photosynthetic pathways. C3 plants directly fix CO_2 using the Calvin cycle in mesophyll cells, which requires more Rubisco enzyme with lower catalytic efficiency. This results in a substantial investment of leaf N (20% to 30%) in C3 plants (Irving, 2015). This suggests increased

maintenance cost for C3 plants due to the substantial energy expenditure associated with the turnover of organic N compounds (Irving, 2015). However, contrary to this position, there was no statistically significant difference in the dark respiration rates as well as relative allocation of assimilates to nocturnal respiration for both species (Table 3.3 and Figure 3.9). This outcome is in line with the findings of Byrd and colleagues, who conducted a comparative study on C3 and C4 plants (Byrd et al., 1992).

The analysis of below-ground allocation patterns between the maize and barley yielded significantly different allocation patterns of C below-ground. Specifically, maize allocated more root C to respiration, further reinforcing the previous submission of a heightened metabolic demand in contrast to barley. This is consistent with the understanding that faster-growing plants necessitate elevated energy expenditure for sustaining their growth and physiological processes Saglio et al. (1983).

The allocation patterns of the two species examined individually across the two bulk densities (1.40 and 1.60 gcm^{-3}), showed no significant differences between their respective allocation patterns for maize (Figure 3.2, top). A plausible explanation for this is the potential insufficiency of the duration of exposure to these bulk densities to induce observable shifts in allocation patterns. A similar experiment with longer duration (3 weeks) in Chapter 2 of this thesis vs 2 weeks in the current experiment yielded significant differences in below-ground allocation patterns of maize plants with a bulk density of 1.50 g cm^{-3}. Furthermore, the maize plants in the previous experiment also exhibited overall larger sizes (mean root length = 26 m and mean root dry mass = 0.30 g) compared to the current experiment (mean root length = 11 m and 0.10 g mean root dry mass). Therefore, it is plausible that the response of maize plants to environmental stressors, such as soil compaction, may necessitate more time to become fully evident. In contrast, barley plants exhibited a significant disparity in C allocation to root biomass between the two bulk density treatments. The low compaction treatment demonstrated a

statistically significant increase ($p = 0.03$) in C investment, allocating 45%, compared to the high compaction treatment, where the allocation was 33% (Figure 3.2). This finding diverges from the observations made on maize plants in the second chapter of this thesis and a prior research investigation. In the latter study (Tubeileh et al., 2003), maize plants displayed an increase in root biomass C allocation when grown under high soil bulk density compared to the low bulk density treatment (1.45 gcm^{-3} vs 1.30 gcm^{-3}). Given that the bulk densities used in both studies were lower than the higher bulk density treatment in the current study, it is conceivable that the bulk density applied in this study was excessively high, potentially resulting in the suppression of root growth. This hypothesis is supported by the observation that the root length in the higher bulk density treatment in the current study was significantly shorter than that in the lower bulk density treatment for both species (Table 3.2). Decrease in root growth rate and root length have been documented in previous studies (Atwell, 1990; Bengough et al., 2011; Colombi et al., 2017).

The C allocation proportions described in this study are in the same order of magnitude as those in other studies (Zagal, 1994; Tubeileh et al., 2003; Meng et al., 2013; Sun et al., 2018) (Appendix Table 3.5).

Taken together, these findings suggest the predominant role of species-specific traits in C allocation patterns. However, to arrive at definitive conclusions, extended experimental duration and potentially a refined choice of bulk density ranges would be necessary to effectively delineate the species' responses.

Cost and Benefit of Root Uptake

The C cost of resources acquisition was compared between the two species. In this species comparison, both bulk densities for each species were considered in the regression analysis and in the slope calculation because they fell along the same regression line. There was no statistically significant difference in

the transpiration per root length between maize and barley (Figure 3.3, top). However, despite achieving similar water uptake rates, maize plants exhibited higher respiration (double) per root length (0.3 nmol m^{-1} s^{-1} vs 0.1 nmol m^{-1} s^{-1}, Figure 3.4, top) and per transpiration rates (0.0007 vs 0.0004 nmol s^{-1} $nmol^{-1}$ s, Figure 3.5, top) compared to barley. However, looking at the N uptake per root length, maize plants achieved a higher N uptake rate per root length compared to barley (Figure 3.3, bottom), indicating that the higher respiration rates in maize were associated with higher nutrient uptake rates. Previous studies have found that maize plants require substantial nutrients to support their growth rate and increase their yield (Rutkowska et al., 2014; Zhang et al., 2016; ChunLi et al., 2018; Aliyu et al., 2021) with barley having lower uptake rates (Aliyu et al., 2021). The respiration rates measured for maize in this study is similar to those measured and reported in the second chapter of this thesis (Figure 2.6, top). Barley's lower root respiration rates as well as lower N uptake per unit root length could reflect its different growth strategy, which may not require the same level of nutrient acquisition and metabolic activity as maize during early stages.

Interestingly, the slopes between cumulative below-ground respiration and total N found in the plant biomass at the end of the experiment were similar for both maize and barley (1.79 and 1.70 mol C per mol N respectively (Figure 3.3, bottom)), with no significant difference ($p = 0.8$). This indicates that the environment imposes the costs for resource acquisition (water and N in this case), whereas different plant species vary in their resource uptake strategies while meeting these universal costs. The universality of the costs would not be apparent if only water uptake were considered, as maize would have seemed to incur significantly higher root respiration costs for water uptake than barley. The comprehensive analysis of both water and N uptake, however, revealed that both resources come with separate costs for their uptake.

The higher bulk density treatments limited root growth in both plant

species. This decrease in root growth rate has been documented in previous studies (Atwell, 1990; Bengough et al., 2011; Colombi et al., 2017). It is also conceivable that the measurement of root length may have slightly underestimated values in the high compaction treatments for both species. This could be attributed to the increased difficulty in completely extracting roots from the soil under conditions of higher compaction. Analyzing the species separately across the bulk densities, higher bulk densities were shown to be associated with statistically significantly higher transpiration rates per root length in maize (2.02 vs 0.60 nmol mm^{-1} s^{-1}) and higher N uptake per root length ($6.3 * 10^{-8}$ and $1.8 * 10^{-7}$, $p = 0.03$) for low and high bulk density barley respectively. However, the high soil bulk density treatments were also associated with higher respiration rates per root length in both species (2 vs 0.4 nmol m^{-1} s^{-1}) for high and low bulk density maize and (0.5 vs 0.2 nmol m^{-1} s^{-1}) for high and low bulk density barley respectively. This finding is a sharp contrast from the second chapter of this thesis where the high bulk density groups achieved similar levels of water uptake per root length as the low bulk density treatment albeit with higher root respiration rates. Adding the control to each bulk density and analyzing the species separately across the bulk densities, the slope of the relationship also revealed higher respiration rates per root length for the high bulk density treatments across both species with maize exhibiting slopes of 1 vs 0.4 nmol m^{-1} s^{-1} (Figure 3.4, middle) whereas barley exhibited slopes of 0.3 vs 0.1 nmol m^{-1} s^{-1} for the high and low bulk density treatments respectively (Figure 3.4, bottom). The root respiration values (regression slopes) measured in this study are similar to those reported in previous studies (Bloom et al., 1992; Bouma et al., 1997; Bryla et al., 2001) (Appendix Table 2.6) as well as the second chapter of this thesis. Particularly, the respiration per root length (slope) measured for the 1.40 g cm^{-3} in this experiment is identical to that measured in Chapter 2 for the same bulk density (Figure 2.6, top). More intermediate data points would be needed for each compaction in subsequent experiments in order to

establish reliable quantitative measurements of the respiratory cost of root growth.

The increased respiration rates per root length could be due to the increased metabolic demand and physical effort required for the roots to grow through the compacted soil resulting in heightened energy costs (Colombi et al., 2017) and hence increased C expenditure. In the context of elevated transpiration rates per root length ratio in the high bulk density group, it could be that roots in the compacted soil have more root hairs and/or better contact to the soil matrix. The presence of root hairs for instance in maize has been associated with enhanced resource accessibility in soils with high penetration resistance by improving soil penetrability and anchoring maize root to the soil (Bengough et al., 2016). However, they may also be related to higher respiration as they have been shown in a previous study to increase root C allocation (Holz et al., 2018). Perhaps, in loose soil, roots may experience reduced water and nutrient uptake per root length due to frequent disconnectedness. Consequently, plants may need to develop longer roots to attain equivalent water and nutrient uptake levels. Since soil penetration is cheaper at low bulk density, cost-benefit ratio of water uptake could then be similar between the two groups as typified by the lack of statistically significant difference in the respiration per water uptake ratios across the low and high bulk densities for maize and barley separately. This findings challenge the expected decrease in root water uptake per unit root length due to reduced hydraulic conductivity linked to soil compaction (Correa et al., 2019). However, it corresponds with the well-documented adaptive responses of root systems to optimize resource acquisition under constrained conditions (Tubeileh et al., 2003; Grzesiak et al., 2014). Nonetheless, the parallel patterns of increased root respiration and transpiration suggest a coordinated approach by plants to overcome the limitations imposed by soil compaction. It is crucial however, to take into account the increased root respiratory cost of N uptake for the high bulk density maize plants (13.0 and 3.05 mol mol^{-1},

p = 0.03), which aligns with the second chapter of this thesis as well as established scientific literature that emphasizes the heightened metabolic costs linked to root system expansion in compacted soils (Atwell, 1990; Bengough et al., 2011; Colombi et al., 2017). This suggests that even with a coordinated approach by plants to overcome the limitations imposed by adverse environmental conditions (soil compaction in this context), the cost/benefit ratios may still be higher under adverse below-ground conditions. Further experiments with a wide range of bulk density treatments are required in order to fully elucidate these cost/benefit relationships.

The root respiration to root length ratios in this current study are a similar order of magnitude to the slopes of their regression analysis (Figure 3.4). However, these ratios are lower than similar ratios reported in the second chapter of this thesis (Figure 2.6, top). For instance, root respiration per root length in low bulk density maize in Chapter 2 (7 nmol m^{-1} s^{-1}) was higher than the slope of the regression analysis (0.4 nmol m^{-1} s^{-1}), whereas in this current study, the ratio of root respiration to root length for the low bulk density maize (0.2 nmol m^{-1} s^{-1}) is similar to the slope of their relationship (0.1 nmol m^{-1} s^{-1}). This might be attributed to a lower intercept in this current study compared to Chapter 2, possibly resulting from clustering of data points around the regression line, a smaller contribution of microbial respiration in the substrate due to a shorter experimental duration.

This study revealed higher mean daily respiration per transpiration rates in the low bulk density treatment compared to the high density treatment especially for maize (Figure 3.5). This observation could be attributed to a potential incomplete measurement of respiration, influenced by the reduced diffusibility of CO_2 in the high bulk density treatment, which exhibited a fourfold increase in penetration resistance compared to the lower bulk density (Appendix Figure 3.11). Despite the elevated respiration rates for low bulk density treatments in maize, as indicated in Figure 3.5, the corresponding respiration per transpiration ratio did not reveal any significant differences

between the two bulk densities for maize and barley respectively. This finding contrasts with those in the second chapter of this thesis where the slopes of respiration per transpiration rate were higher for the high bulk density maize plants. This similarity in the cost-benefit ratio emerges as a consequence of the increased water uptake rate in the high bulk density group when compared to the lower bulk density group despite the increase in root respiration per root length. This is also supported by the comparable ratio of total cost of water uptake (total respiration + C in biomass (mol)) to cumulative transpiration across the bulk densities for the two species separately. It could also be that the potential underestimation of respiration rates in the high bulk density treatments contributed to these similarities.

Finally, the comparison of the ratio of total water uptake cost (total respiration + C in biomass (mol)) per cumulative transpiration across both maize and barley (Figure 3.6, top) and total N uptake cost (total respiration + C in biomass + exudation (mol)) per total N in plant across both maize and barley (Figure 3.6, bottom) revealed no difference between the two plant species. This finding further corroborates the initial assertion that the fundamental costs of resource uptake are independent of species. However, the total costs calculated here encompass root C in its totality, including structural and non-structural C. Since only the structural C component of plant roots is a cost, a more detailed analysis of the various components of biomass C is necessary in future experiments. Additionally, it is crucial to acknowledge that the C exudates calculated here were inferred from the mass balance and may include errors arising from the different measurements used in the mass balance calculation.

Above-ground Costs and Benefits

Maize and barley, both important cereal crops, demonstrate variability in their water use efficiency (WUE) due to their distinct photosynthetic pathway. Notably, maize, categorized as a C4 plant, typically exhibits superior

WUE compared to C3 plants like barley because their C4 photosynthesis facilitates efficient C capture and less water loss (Vogan and Sage, 2011; Sage et al., 2012). In line with this, the WUE for maize was statistically higher than those of barley (0.01 vs 0.005 mol mol^{-1}) respectively (Figure 3.7). Additionally, the findings indicated that in barley, the high bulk density treatment was associated with a statistically significantly higher WUE (Figure 3.7). Similar to the previous results on different plants, the high soil bulk density treatments were associated with shorter root lengths due to the effect of high soil penetration resistance on their root elongation rate (Bengough et al., 2006; Popova et al., 2016). As a consequence of this stress condition, the plants may respond by reducing their leaf area or stomatal conductance to minimize water loss (Rawson et al., 1977; Harper et al., 2021), improving their WUE but also reducing their assimilation rate. In this study, the high bulk density barley plants had a lower leaf area compared to the high bulk density treatment. This difference was however not statistically significant (34 vs 39 cm^{-2}, $p = 0.2$) for the high and low bulk density treatments respectively.

The positive linear relationship observed between mean daily assimilation and below-ground respiration rates (Figure 3.8) highlights the direct relationship between the amount of assimilated C by the plant and the energy expended in root respiration (Brüggemann et al., 2011). This relationship was not significantly different between maize and barley as both species exhibited similar slopes (0.07 and 0.06 mol mol^{-1}, $p = 0.9$). This implies that, regardless of the plant species, the energy investment in below-ground respiration is proportionate to the assimilated C.

Additional Findings: Discussing Day Length effect on Nocturnal Respiration and WUE

Day Length affects Nocturnal Respiration in Maize and Barley

By employing three distinct light/dark regimes (short day: 10/14, medium

day: 14/10 and long day: 18/6 light/dark cycles), this study suggests that for similar assimilation rates, nocturnal respiration exhibits an upward trend corresponding to the increase in day length for both species. This relationship is particularly evident in the longest day length (Figure 3.9). This phenomenon, observed in both species, implies a universal influence of day length on nocturnal respiration. This finding is in line with a previous study involving bent grass grown in growth chambers set at 20/15 °C (day/night) and 14-hour photoperiod for 60 days, and then exposed to a day/night temperature of 33/28 °C (heat stress) with three different light durations: 14, 18, and 22 h of light during each 24-hour cycle for 30 days. This study demonstrated that whole plant dark respiration rates scaled with increasing day length (Xu et al., 2004). However, this discovery sharply contrasts with a previous investigation where rye grass, exposed to continuous lighting, demonstrated lower dark respiration rates under darkness compared to those under a 16/8 light/dark cycle (Lehmeier et al., 2010). This finding suggests that long days and hence shorter nights could necessitate intensive shoot respiration for growth and maintenance within a condensed time period. Further investigations that explore the physiological, biochemical, and molecular aspects of plant responses to varying day lengths, across a range of plant species, has the potential to provide valuable insights into the underlying mechanisms influencing the observed patterns.

Divergent Effects of Day Length on WUE in Maize and Barley

The investigation into the impact of day length on maize and barley revealed significant differences in the WUE of barley across different light regimes. Specifically, the group exposed to long days exhibited higher WUE in comparison to the other light regimes. This phenomenon can be contextualized by considering that day length directly regulates the duration of light when cells can accumulate C through photosynthesis (Hobson et al., 1979). As such, it is reasonable to hypothesize that the extended light period poten-

tially facilitated elevated net photosynthesis rates thereby improving their WUE. Moreover, it is well-documented that barley plants have undergone acclimatization to long days due to their growth in regions characterized by extended photo-periods (Nishida et al., 2013). This natural adaptation might further contribute to the enhanced WUE observed in the long days, as the prolonged light exposure aligns with the species' evolutionary background. Conversely, investigation yielded no significant influence of varying light regimens on the WUE in maize. Maize, acknowledged for its day-neutral nature (unaffected by changes in day length) (Mascheretti et al., 2015; Alter et al., 2016) is probably poised to remain largely unaffected by fluctuations in light exposure.

3.7 Conclusion

In this study, the impact of two levels of soil penetration resistance was studied across two species - maize and barley. The primary aim was to assess whether the variation in cost-benefit ratios is greater across environmental conditions than across species.

This investigation highlights fundamental costs associated with resource uptake, demonstrating their species-independent nature. Despite maize showcasing nearly double the water use efficiency compared to barley (0.01 vs. 0.006 mol mol^{-1}), both species exhibited analogous relationships between day-time assimilation rates and nocturnal respiration rates (0.07 vs. 0.06 mol mol^{-1}). While maize achieved markedly higher assimilation rates (up to 140 nmol s^{-1}), three times that of barley (up to 40 nmol s^{-1}), it incurred higher nitrogen (N) demand, attributed to elevated root respiration costs. The slopes observed between cumulative below-ground respiration and total N content in plant biomass at the experiment's conclusion were comparable for both maize and barley (1.79 and 1.70 mol mol^{-1}).

The analysis of root respiration per root length across the species sepa-

rately revealed elevated respiration costs for the high bulk density treatments across the species separately. The results were similar to those in previous literature studies as well as in the second chapter of this thesis. Maize exhibited respiratory cost of 1 vs 0.4 nmol m^{-1} s^{-1} for high and low bulk density respectively while barley exhibited 0.3 vs 0.1 nmol m^{-1} s^{-1} for the high and low bulk density treatments respectively. Due to fewer data in this study, future studies with more data points per treatment are required to establish more reliable quantitative measurements of root respiration costs.

The total cost of water and nutrient uptake encompassing the sum of total C in root biomass, cumulative respiration and exudation (mol) was similar for both species, due to the increased investment in root biomass C for barley, highlighting a possibly different root investment in terms of structural C compared to maize plants. A detailed analysis of the different components of root biomass C is necessary to isolate the pure cost of the root architecture (structural C). This will aid the understanding of the complete picture of C investment in plant root systems.

Furthermore, the study indicated the influence of day lengths on the nocturnal respiration rates and water use efficiency (WUE) in the studied plants. Results revealed that longer day lengths led to increased nocturnal respiration rates, potentially due to an increase in photosynthetic capacity due to higher return for investment in longer day lengths and its concomitant increase in respiration rates to carry out metabolic activities over a short night period. WUE demonstrated divergent effects on maize and barley. While WUE was increased in barley at the long day length, possibly due to reduced stomatal conductance to adjust for extended exposure to long days, maize plants remained unaffected probably due to their day neutral nature.

In this investigation, the discernible impact of varied bulk densities on the parameters under examination did not manifest conclusively. This lack of clear distinction might be attributed to the relatively brief duration of the experimental period. It is plausible that the short-term nature of the

study may have limited the manifestation of discernible effects, and a more protracted experimental timeline could potentially unveil more explicit trends or differentiations associated with distinct bulk densities.

Nonetheless, these findings suggest that the environment imposes universal costs for resource acquisition (C, water, and N, in this context), while different plant species exhibit variations in their resource uptake strategies to meet these universal costs.

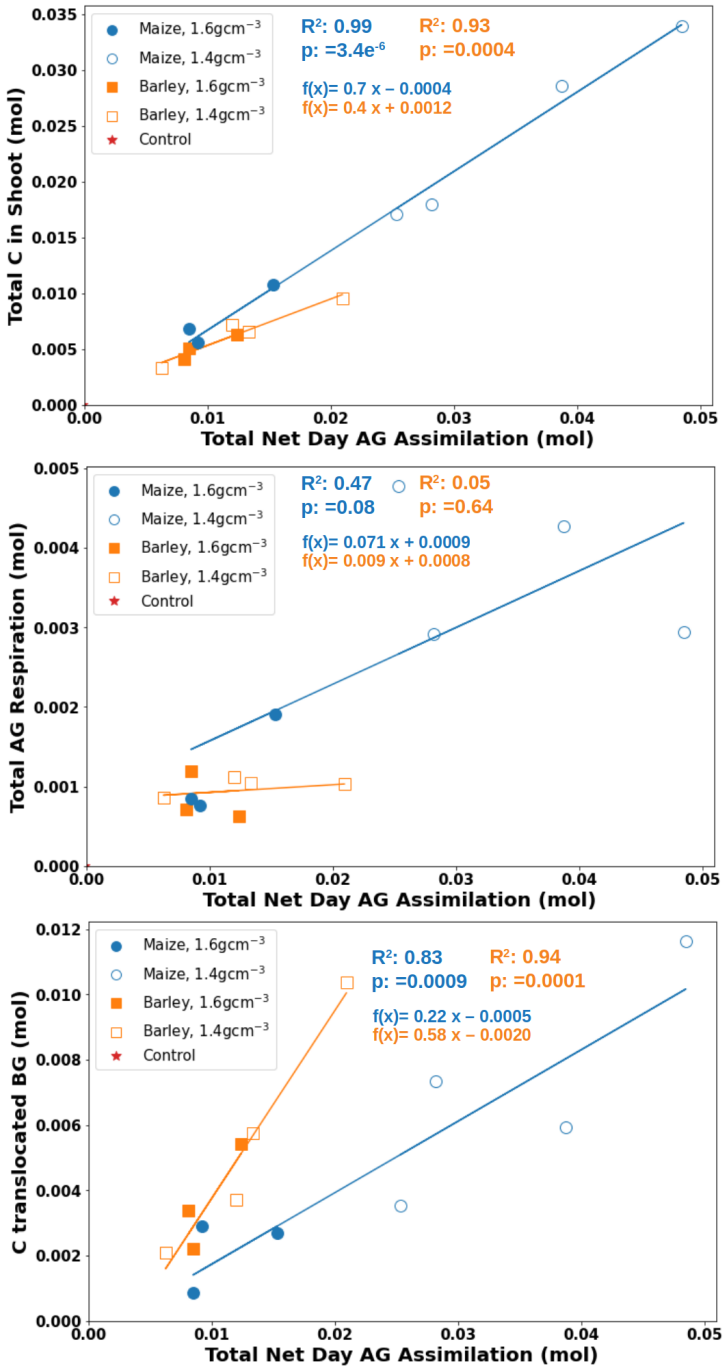

Figure 3.1: Above-ground (AG) fractions of assimilates allocated to **(Top)** shoot biomass, **(Middle)** shoot respiration and **(Bottom)** translocated to the root system. The marker colours represent the different species (blue: maize, orange: barley). Filled markers represent the high bulk density group (1.60 g cm^{-3}) while the empty markers represent the low bulk density group (1.40 g cm^{-3}). The linear regression p value for each independent variable tests the null hypothesis that the variable has no correlation with the dependent variable.

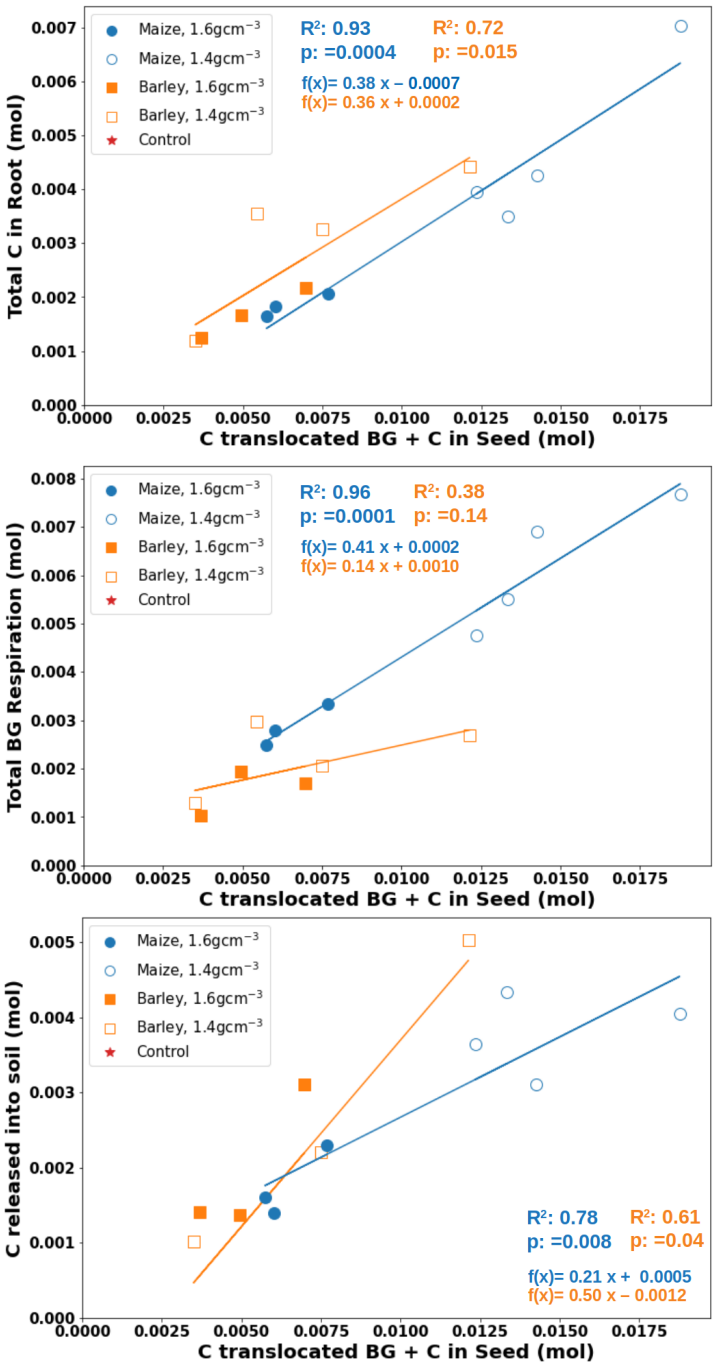

Figure 3.2: Below-ground (BG) fractions of C investment allocated to **(Top)** root biomass, **(Middle)** root respiration and **(Bottom)** released to the soil. The marker colours represent the different species (blue: maize, orange: barley). Filled markers represent the high bulk density group (1.60 g cm^{-3}) while the empty markers represent the low bulk density group (1.40 g cm^{-3}). The linear regression p value for each independent variable tests the null hypothesis that the variable has no correlation with the dependent variable.

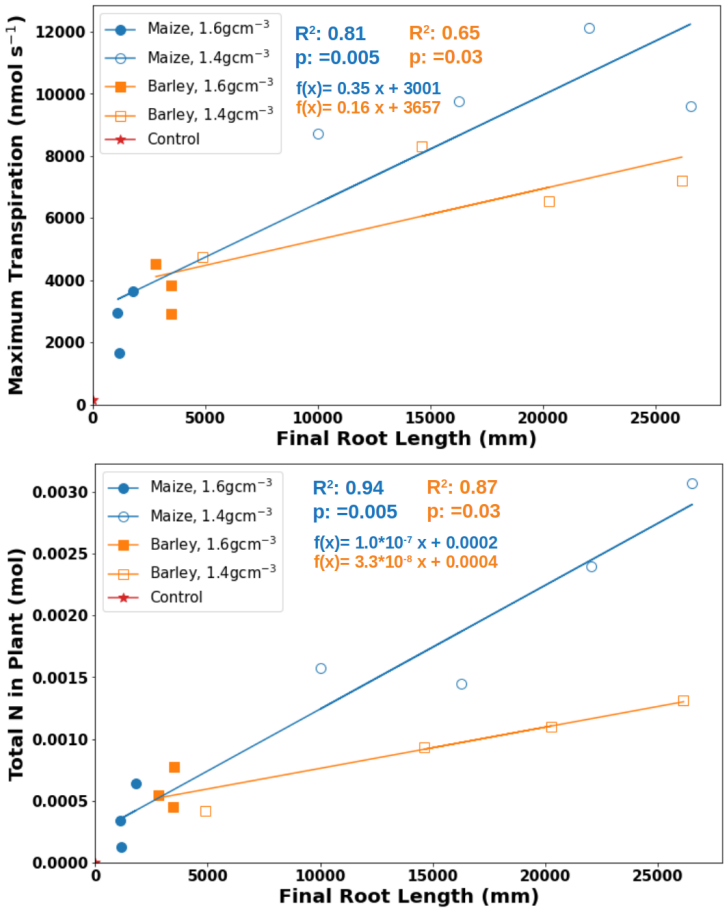

Figure 3.3: **(Top)** Relationship between final root length (mm) and maximum above-ground (AG) transpiration (nmol s^{-1}) . Due to a malfunction in the measurement on the last day, it is assumed that the maximum transpiration rate is the closest to those of the last day. **(Bottom)** Relationship between final root length (mm) and N uptake (mol). The marker colours represent the different species (blue: maize, orange: barley). Filled markers represent the high bulk density group (1.60 g cm^{-3}) while the empty markers represent the low bulk density group (1.40 g cm^{-3}). The linear regression p value for each independent variable tests the null hypothesis that the variable has no correlation with the dependent variable.

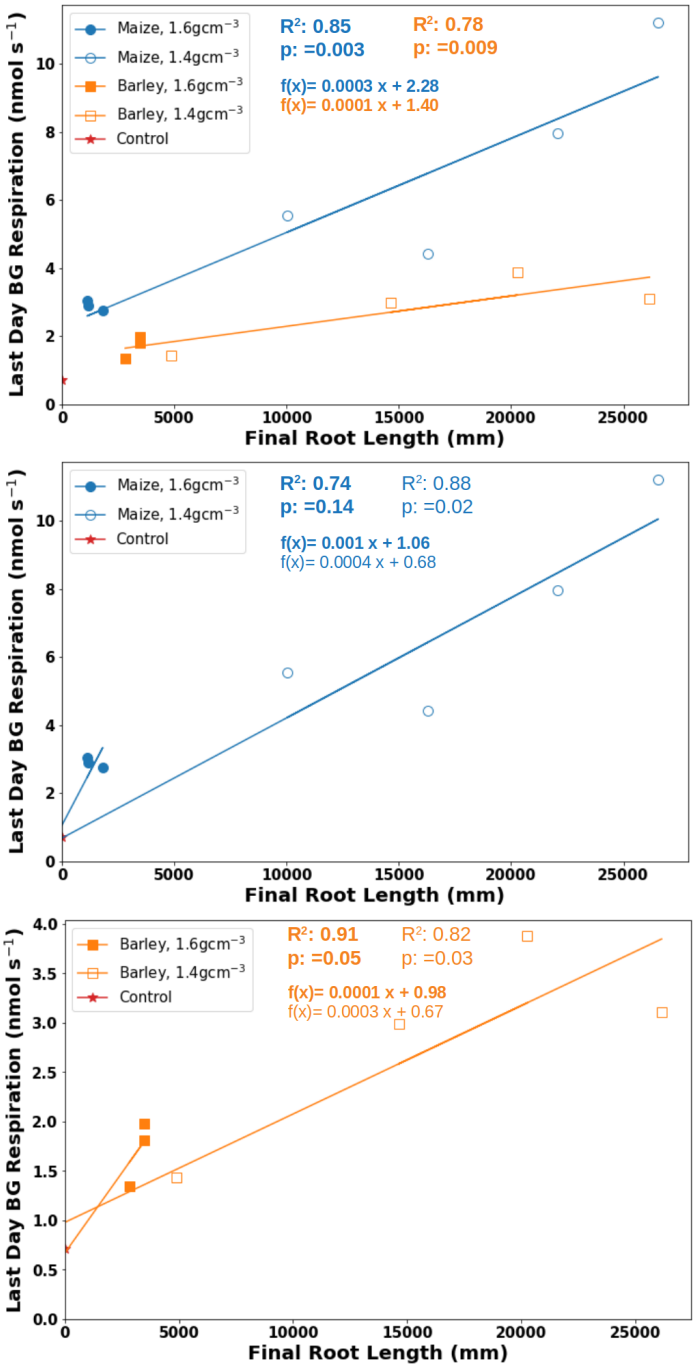

Figure 3.4: Relationship between Last day below-ground (BG) respiration and final root length **(Top)** for maize and barley (both bulk densities), **(Middle)** for maize alone and **(Bottom)** barley alone across the two bulk densities. The marker colours represent the different species (blue: maize, orange: barley). Filled markers represent the high bulk density group (1.60 g cm^{-3}) while the empty markers represent the low bulk density group (1.40 g cm^{-3}). The linear regression p value for each independent variable tests the null hypothesis that the variable has no correlation with the dependent variable.

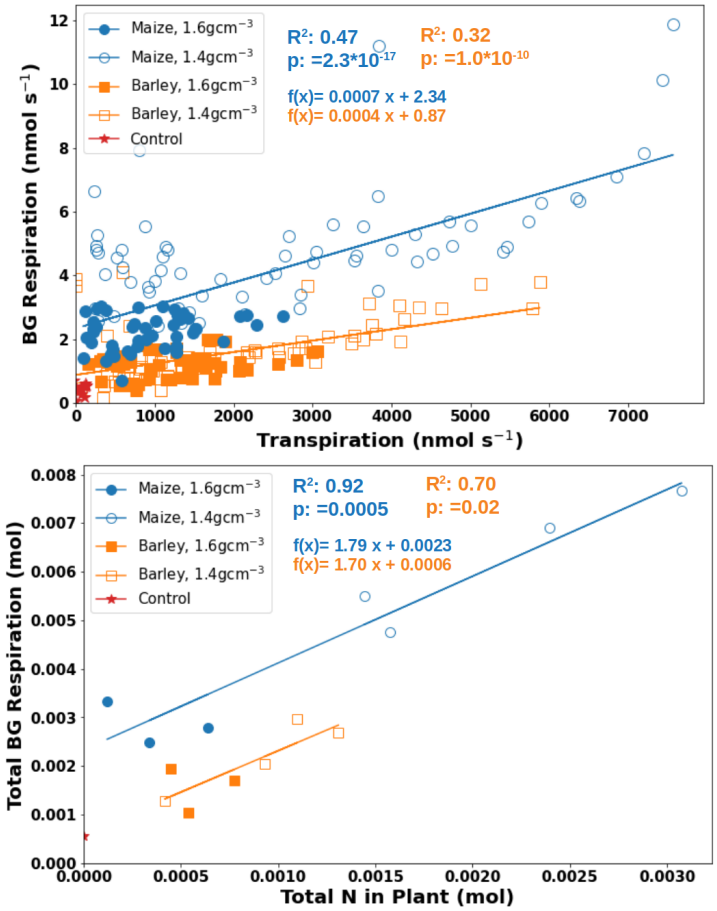

Figure 3.5: **(Top)** Relationship between daily average below-ground (BG) respiration and average above-ground (AG) transpiration rate (nmol s^{-1}). **(Bottom)** Relationship between total below-ground (BG) respiration and N uptake (mol). The marker colours represent the different species (blue: maize, orange: barley). Filled markers represent the high bulk density group (1.60 g cm^{-3}) while the empty markers represent the low bulk density group (1.40 g cm^{-3}). The linear regression p value for each independent variable tests the null hypothesis that the variable has no correlation with the dependent variable.

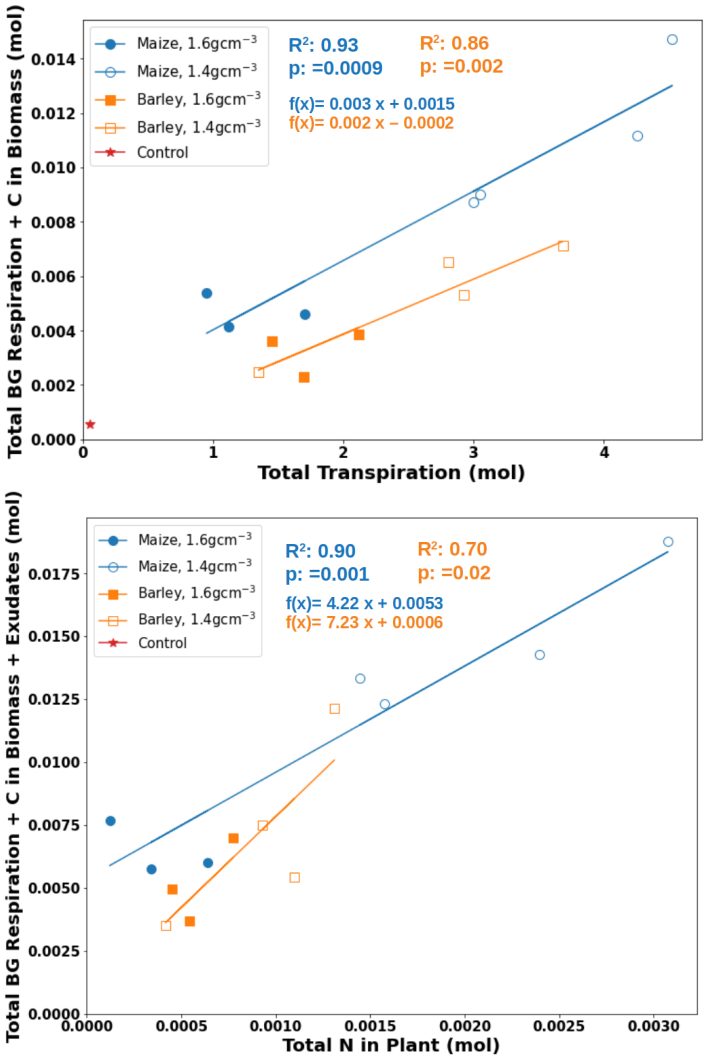

Figure 3.6: **(Top)** Relationship between total root water uptake cost (total respiration + C in root dry mass) (mol) and cumulative (AG) transpiration (mol). **(Bottom)** Relationship between total N uptake cost (total respiration + C in root dry mass + exudates) (mol) and N in plant (mol). The marker colours represent the different species (blue: maize, orange: barley). Filled markers represent the high bulk density group (1.60 g cm^{-3}) while the empty markers represent the low bulk density group (1.40 g cm^{-3}). The linear regression p value for each independent variable tests the null hypothesis that the variable has no correlation with the dependent variable.

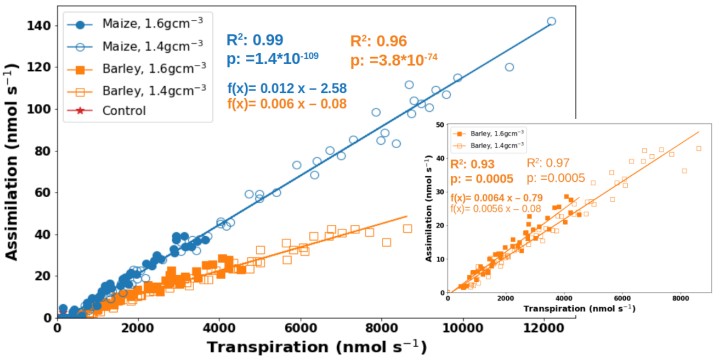

Figure 3.7: Relationship between daily mean aboveground assimilation and transpiration rate. The marker colours represent the different species; (blue: maize, orange: barley). Filled markers represent the high bulk density group (1.60 g cm^{-3}) while the empty markers represent the low bulk density group (1.40 g cm^{-3}). The linear regression p value for each independent variable tests the null hypothesis that the variable has no correlation with the dependent variable.

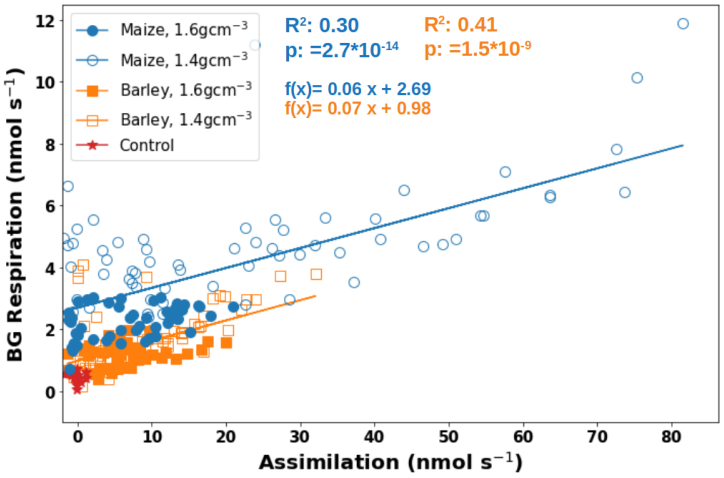

Figure 3.8: Relationship between mean daily assimilation rate and mean daily below-ground (BG) respiration rate. The marker colours represent the different species (blue: maize, orange: barley). Filled markers represent the high bulk density group (1.60 g cm^{-3}) while the empty markers represent the low bulk density group (1.40 g cm^{-3}). The linear regression p value for each independent variable tests the null hypothesis that the variable has no correlation with the dependent variable. The inserted figure is barley data with separate regressions.

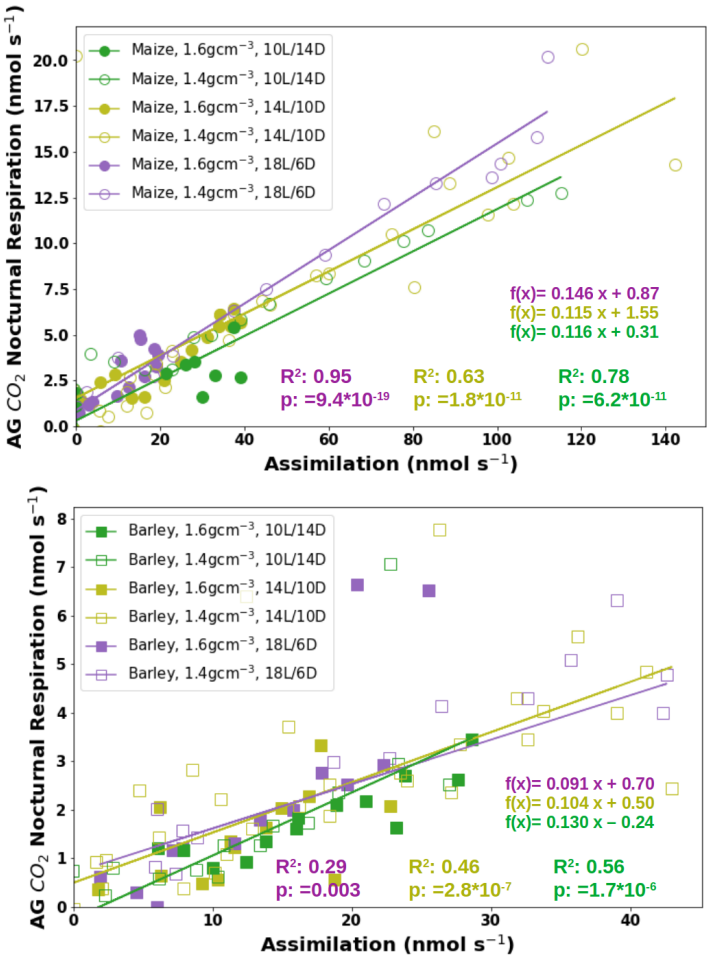

Figure 3.9: Relationship between daily mean aboveground net assimilation and nocturnal respiration rate for **(top)** maize and **(bottom)** barley plants. The marker colours represent the different day lengths; (green: 10/14, olive: 14/10, purple: 18/6 light/dark regime). Filled markers represent the high bulk density group (1.60 g cm^{-3}) while the empty markers represent the low bulk density group (1.40 g cm^{-3}). The linear regression p value for each independent variable tests the null hypothesis that the variable has no correlation with the dependent variable.

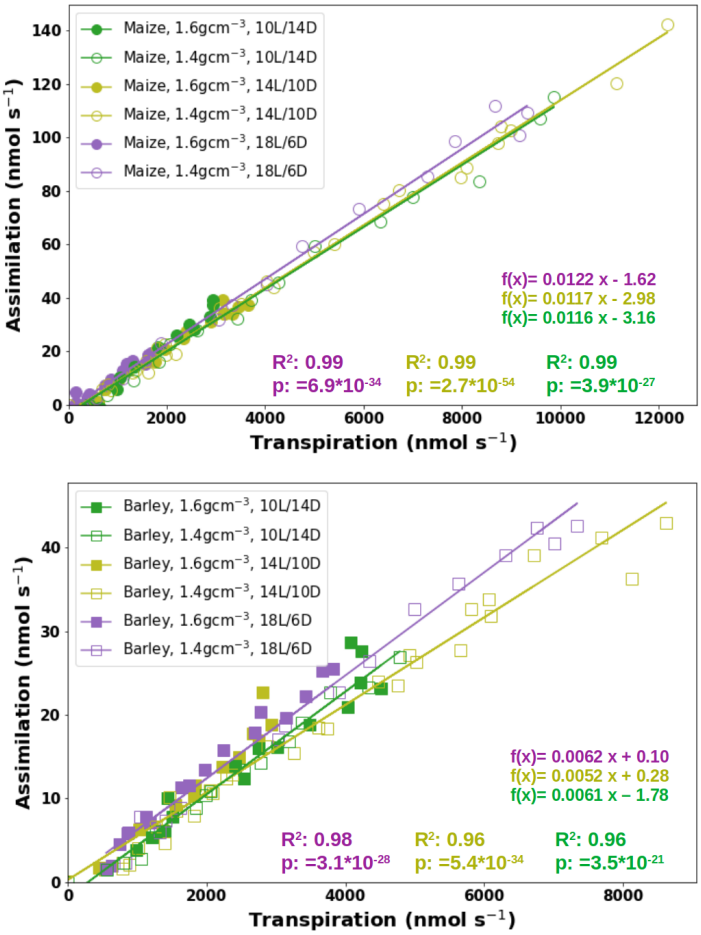

Figure 3.10: Relationship between daily mean aboveground assimilation and transpiration rate for **(top)** maize and **(bottom)** barley plants. The marker colours represent the different day lengths; (green: 10/14, olive: 14/10, purple: 18/6 light/dark regime). Filled markers represent the high bulk density group (1.60 g cm^{-3}) while the empty markers represent the low bulk density group (1.40 g cm^{-3}). The linear regression p value for each independent variable tests the null hypothesis that the variable has no correlation with the dependent variable.

3.8 Appendix

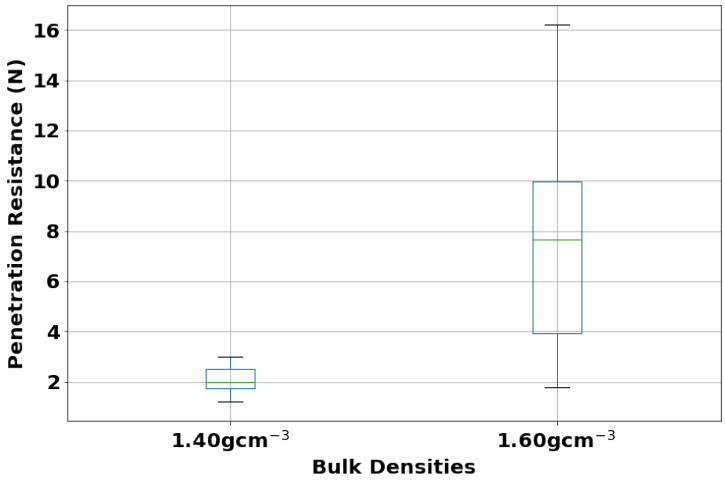

Figure 3.11: Penetration resistance of the two bulk densities used in the experiment. GC 1-4 (maize plants) and GC 12-15 (barley plants) have a bulk density of 1.40 g cm^{-3} and a mean penetration resistance of 2.0 N (0.11 MPa) while GC 5-7 (maize plants) and GC 8-10 (barley plants) have a bulk density of 1.60 g cm^{-3} and a mean penetration resistance of 7.4 N (0.38 MPa). The penetration cone base radius was 2.5 mm. Penetration resistance for each bulk density was measured at 250, 500 and 750 mm soil height and mean values obtained. Each bulk density had two replicates.

Table 3.5: % C allocation of assimilated C to shoots, roots and soil as determined following ^{14}C labelling in the literature

Plant	**Plant age (days)**	**Shoots**	**Roots**	**Soil**	**References**
Wheat	23	36	10.8	52.9	Sun et al., 2018
Barley	25	62.3	15.3	22.4	Zagal et al., 1994
Maize	21	80 - 83	6 - 11	6 - 14	Tubeileh et al., 2003
Maize	27	53.5	46.5	3.8	Meng et al., 2013

Chapter 4

General discussion and outlook

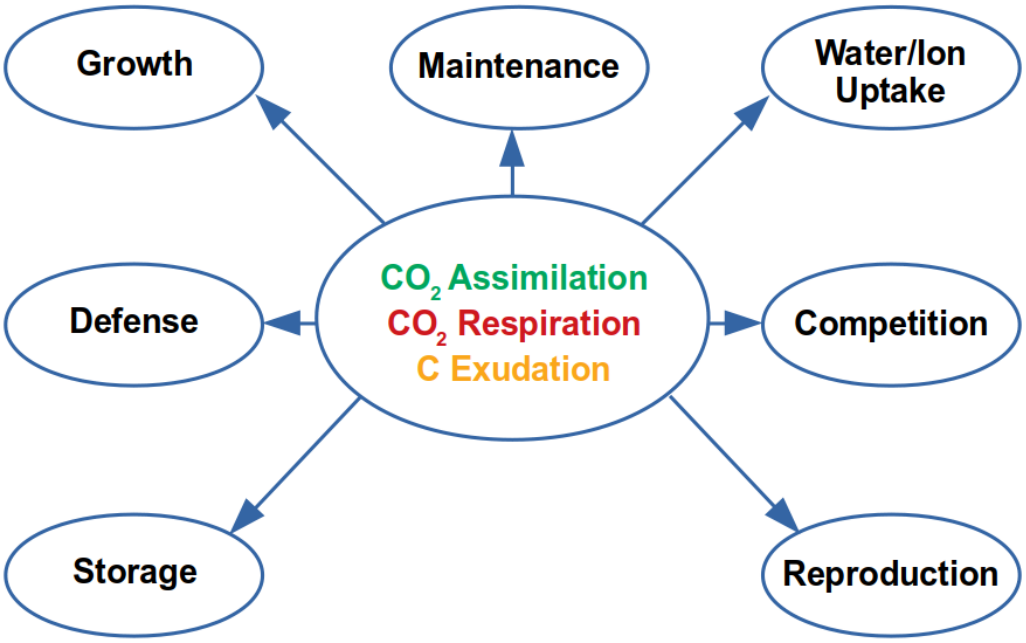

Figure 4: Some plant physiological processes requiring C allocation and trade-offs.

C allocation, the partitioning of primary products synthesized during

photosynthesis into distinct functional pools (Figure 4) has been a subject of extensive investigation, spanning several decades particularly in the context of understanding resource partitioning trade-offs among different functional sinks (Hartmann et al., 2020). More than five decades have passed since Mooney (1972) asserted that acquiring a quantitative understanding of how diverse plants acquire and distribute resources would enable the prediction of their success in specific physical environments, accounting for interactions with competitors and predators. Still, the understanding of the regulatory aspects of C allocation remains deficient, primarily due to challenges in measuring crucial components like respiration and root exudation (Hartmann et al., 2020). Similarly, current ecosystem models are also limited when it comes to predicting long term environmental changes due to their reliance on parameter calibrations extracted from historical observations and the assumption that environmental conditions remain stationary over time (Teuling et al., 2010; Chiew and Vaze, 2015; Robinson et al., 2019; Harper et al., 2021).

In the contemporary scientific landscape, advancements in technology and methodologies have presented new opportunities to study C allocation strategies across different plants under different environmental conditions. Leveraging these developments, this PhD thesis aimed to experimentally explore the costs and benefits of plant roots, alongside the shoots under different environmental conditions. The goal was to quantify these costs and establish more consistent physical underpinnings for existing models, aiming to make more reliable predictions and enhance the accuracy of mid to long-term plant responses to environmental changes.

To do this, a growth chamber allowing precise control of environmental conditions and enabling more accurate measurements of above and below-ground gas exchange in plants was developed, tested and reported in the first chapter of this thesis. Equipped with infrared gas analyzers, this setup allowed simultaneous monitoring of above-ground (CO_2 assimilation, nocturnal respiration, H_2O transpiration) and below-ground fluxes (H_2O evaporation,

CO_2 respiration) of up to 15 chambers. The performance of the system was validated using chemical agents to induce known CO_2 release or uptake. Tests with reference chemicals demonstrated rapid and accurate responses in measured below-ground fluxes to changes in CO_2 evolution, with minimal deviations. Above-ground CO_2 absorption showed an error of 1% while experiments with real plants highlighted a 14-17% discrepancy between cumulative fluxes and plant biomass increase, indicating that plants seemed to take up more C than apparent in their biomass. Furthermore, comparisons of cumulative evapo-transpiration rates and weight loss during watering events indicated a close alignment between these independent water loss estimates (within 11%).

Efforts to account for the additional 14-17% C not found within the plant biomass, exposed a limitation in the experimental approach to C analysis and underscored the necessity for refining methods in future studies involving total C measurements. It became evident that analyzing sub-samples of the large sample (potting mixture and large volumes of soil wash in this context) and extrapolating the results could amplify any potential experimental or systematic errors. However, this study was able to demonstrate that this 14-17% C measured by the gas exchange apparatus but not found in the plant biomass fell within the range of values that are attributed to root exudation in the literature (Sasse et al., 2018).

In the soil respiration experiments, base "soil" respiration in the potting mixture ranged from $1 - 3$ nmol s^{-1} in the absence of any plants. These values could be due to measurement error, CO_2 release from soil carbonates as well as microbial respiration. This discovery highlights the importance of accurately measuring the initial C content in experiments where minimal or no C is required in the setup. Compared to other studies however, the "soil" respiration in the potting mixture was lower than those on bare grassland soil (Dyukarev and Kurakov, 2023) and rootless reconstructed soils (Lei and Han, 2020) and represents a great substrate for root respiration experiments.

In the regression analysis involving the below-ground respiration measurements especially in the second chapter of this thesis, y-intercept values up 6 nmol s^{-1} were identified. The presence of these large intercepts influenced the values of ratios measured in this study, causing them to be significantly different from the slope values. For instance, the root respiration to root length ratio (15 nmol m^{-1} s^{-1}) for the high bulk density group B plants and (7 nmol m^{-1} s^{-1}) for low bulk density group A were at least one order of magnitude higher than the reported slopes (Figure 2.6, top). The presence of this substantial intercept could have stemmed from different activities within the set-up not related to the plant root activities. Therefore the intercept could be made up of CO_2 release from initial background respiration, continued microbial breakdown of organic compounds released by the plants roots and seed respiration. Furthermore, the dispersion of data points relative to the regression line could have also contributed to this intercept. Due to these large intercepts, in each presented regression analysis in the results section, both the slope and the y/x ratio were computed where possible. The comparison between the experimental groups primarily relied on the slope, offering a quantitative measure of the cost/benefit relationship of the variables under consideration. The y/x ratio, offered a more qualitative description. In instances where the regression analyses did not yield statistical significance, group comparisons were then based on their y/x ratios, providing qualitative insights.

In Chapter 2, the growth chamber and custom soil described in Chapter 1 was used to quantitatively evaluate the cost/benefit ratios of C allocation in maize plants grown on 2 levels of soil compaction/penetration resistance over a 3-week period. The investigation analyzed above-ground and below-ground C allocation patterns and their cost-benefit ratios viz the relationship between costs of C assimilation (N investment, transpiratory water loss) and below-ground costs of water and N uptake (respiration, root biomass, exudates). This study included regular imaging of the roots to obtain dynamic

root length measurements. The significant results from the second and third chapter of this thesis are summarized in Table 4 .

While no differences were found in above-ground C allocation between bulk density treatments, the analysis of below-ground C investment highlighted reduced root biomass investment and increased respiration in the high bulk density group. This observation aligns with established scientific literature that emphasizes the heightened metabolic costs linked to root system expansion under constrained soil conditions (Atwell, 1990; Bengough et al., 2011; Colombi et al., 2017). Root respiration, both per root length and growth rate, exhibited a significant increase under high bulk density conditions. High bulk density group B plants exhibited a steeper slope compared to the low bulk density group A plants; 0.4 and 0.9 nmol m^{-1} s^{-1} for group A and B respectively (Table 4). In fact, when translated to energy values, the calculated energy cost of root penetration 0.17 J mm^{-1} for group A and 0.29 J mm^{-1} for group B measured in this study was similar to those measured in a previous study under similar penetration resistances (Colombi et al., 2017). This earlier investigation assessed the heat dissipation of developing wheat roots under varying soil penetration resistance (Colombi et al., 2017) and energy expenditure of root penetration was determined to range from 0.2 to 0.8 J mm^{-1} in the referenced study. Despite an over 100% relative increase in root respiration rate for high bulk density plants, both groups attained similar levels of water and N uptake. The findings challenge the expected decrease in root water uptake per unit root length due to reduced hydraulic conductivity linked to soil compaction (Correa et al., 2019), emphasizing the importance of concurrent evaluation of C costs and benefits.

Chapter 3 expanded on the experiments conducted in Chapter 2, focusing on a comparison between species-specific traits and soil bulk density in shaping the cost-benefit relationships of resource acquisition strategies. Employing the growth chamber and potting mixture described in Chapter 1, the study investigated maize and barley plants grown in soils with different

bulk densities (1.40 and 1.60 g cm^{-3}). To vary plant growth and increase the spread, three different day lengths were used across the two bulk density treatments. The chambers were grouped into three light/dark regimes (10/14 (short day), 14/10 (medium day) and 18/6 hours (long day)). The light intensity was 600 μmols m^{-2} s^{-1} photosynthetic photon flux density (PPFD)). The low bulk density treatment was the same as in Chapter 2. The study started from the seedling stage as in Chapter 2 and but lasted about a week less (15 days). The moisture content was kept constant until the end of the experiment. The experimental plants were grouped by species and bulk density, including high and low bulk for both maize and barley, as well as separate groups for each species across bulk densities. Above and below-ground C allocations was similar across bulk density groups. Similar to the results in Chapter 2 and contrary to a similar study (Tubeileh et al., 2003), root exudation was not significantly higher in the high bulk density group. Although the C allocation proportions measured in Chapter 2 and 3 were in the same order of magnitude as previous studies (Zagal, 1994; Tubeileh et al., 2003; Meng et al., 2013; Sun et al., 2018) (Appendix Table 3.5), the absence of statistically significant differences in the patterns of above-ground C allocation between the bulk density treatments in both chapters could imply that soil bulk density does not exert an influence on above-ground C allocation. It is necessary to highlight that the shorter duration of the experimental period in Chapter 3 led to smaller plants (Table 2.2) compared to Chapter 2 (Table 3.2) and possibly contributed to the lack of statistically significant differences in the below-ground allocation proportions in the bulk density grouping in contrast to Chapter 2.

Species-specific traits indicated distinct C allocation patterns: maize allocated more to shoot biomass above-ground, while barley invested significantly more in root biomass below-ground. Maize exhibited a superior water use efficiency (WUE) compared to barley, (0.01 vs 0.006 mol mol^{-1}) but incurred a twofold higher root respiration cost per water uptake compared to barley

(0.007 vs 0.004 mol mol^{-1}). However, maize demonstrated higher N uptake per root length compared to barley (Table 4), indicating that the heightened respiration cost in maize was related to N acquistion by maize roots. The comparison of the respiratory cost of N uptake between the two species revealed similar slopes, emphasizing that, despite species-specific variations in uptake strategies, the environment imposes consistent costs for resource acquisition. The analogous cost/benefit ratio of N acquisition in maize and barley underscores the fundamental costs associated with resource uptake, suggesting their independence from species-specific traits.

The examination of the impact of the bulk densities separately for each species highlighted amplified C costs in terms of respiration per root length for the high bulk density treatments similar to Chapter 2 (Table 4). However, this group also had higher benefits in terms of water uptake, providing evidence that higher bulk density could be associated with both increased cost and benefit simultaneously. Increased water uptake in the high bulk density treatment indicates the possibility that the roots in the compacted soil had more root hairs and/or better contact to the soil matrix. Root hairs in maize plants for instance has been linked to improved resource accessibility in soils with elevated penetration resistance (Bengough et al., 2016). This enhancement occurs through the improvement of soil penetrability and the anchoring of maize roots to the soil, as indicated by previous research (Bengough et al., 2016). However, root hairs may also be connected to elevated respiration rates, as evidenced by a prior study demonstrating their role in increasing root C allocation (Holz et al., 2018). Connecting this finding with those of Chapter 2 where higher soil penetration resistance did not diminish benefits in terms of water and N acquisition, the findings in this study corresponds with the well-documented adaptive responses of root systems to optimize resource acquisition under constrained conditions (Tubeileh et al., 2003; Grzesiak et al., 2014) and highlights the complexity of cost-benefit relationships under adverse below-ground conditions.

It is noteworthy that the water use efficiency (WUE) of maize plants in both Chapters 2 and 3 remained consistent across various bulk densities. Similarly, while longer day length conditions increased the WUE of barley plants, maize plants remained unaffected. Extended day lengths were however linked to heightened respiration relative to photosynthetic capacity for both species. The higher nocturnal respiration for shorter nights could just be a matter of metabolizing more assimilates in a shorter time. While this discovery aligns with a prior investigation (Xu et al., 2004), it diverges from another study ((Lehmeier et al., 2010). Thus, further investigations into the physiological, biochemical, and molecular aspects of plant responses to diverse day lengths, across different plant species, have the potential to provide valuable insights into the underlying mechanisms influencing the observed patterns.

The innovative experimental setup introduced in this thesis paves the way for future research in this field, offering new avenues for improved understanding of plant physiology and adaptation mechanisms. Moving forward, the insights gained from this study will likely serve as a springboard for further explorations into the dynamics of plant resource allocation across diverse species and environmental conditions. Furthermore, this study can contribute to the refinement of optimality models by providing empirical data on the trade-offs between C allocation and resource acquisition strategies in plants. For instance, data derived from root respiration per root length and growth rate under low (0.4 nmol m^{-1} s^{-1}) and high (0.9 nmol m^{-1} s^{-1}) bulk density treatments, along with the calculated energy cost of root penetration (0.17 J mm^{-1} for low and 0.29 J mm^{-1} for high bulk density treatments) in this study closely align to those measured in a previous study under similar penetration resistances (Colombi et al., 2017). Considering that these measurements were performed with different species and completely different experimental set-up, it instills a high level of confidence in the data's suitability for parameterizing models, particularly as it accounts for the energetic

expenses associated with the mechanical exploration of the soil volume by plant roots.

While the findings of this study provide valuable insights into C allocation patterns and their cost/benefit dynamics over a three-week experimental duration, several questions remain unanswered. In the conducted experiments, the quantified root respiration encompasses a composite of C costs associated with soil penetration, maintenance, water, and nutrient uptake. The fundamental query for future studies arises: What is the pure cost of root penetration? Furthermore, this study evaluated the cost/benefit dynamics within a controlled setting with minimal soil C content and limited microbial interactions. However, the natural environment introduces numerous rhizosphere interactions. Considering this, future studies need to be focused on the cost/benefit ratios associated with these interactions like symbiosis with N-fixing bacteria and mycorrhizal associations in the field.

Scaling these findings to larger plants and establishing unit-less numbers to characterize scaling laws require additional considerations. The relatively short duration of the experiment might limit the ability to directly extrapolate the observed patterns to longer time frames or larger plants and ecosystems. The dynamics of C allocation are influenced by developmental stages (Sun et al., 2018; Meng et al., 2013) that extend beyond the scope of a three-week study. Future research endeavors could involve longer-term experiments to allow measurements across different developmental stages and larger sample sizes for more reliable quantitative data. Additionally, considering the complexities of ecosystems, integrating a multi-scale approach that incorporates various plant species and different environmental conditions may provide a more comprehensive understanding of the scaling relationships of these cost/benefit ratios across a wide range of environmental systems.

Based on the methodologies employed in Experiment 1 and 2 of this thesis, it is evident that the approach used in Experiment 1, involving dynamic root imaging coupled with daily respiration measurements, provides

a more comprehensive understanding of the respiratory cost of root uptake. The continuous monitoring of root growth rates offers valuable insights into the temporal dynamics of the process and the cost of root penetration. For future studies, it is recommended to incorporate dynamic root imaging alongside continuous measurements of respiration throughout the experiment to capture real-time changes in root growth and respiratory activity. This integrated approach ensures a more detailed quantification of the respiratory cost of root uptake, allowing for a thorough exploration of the temporal dynamics and potential variations over the course of the study.

Building upon the successful integration of N uptake measurements alongside water uptake in Experiment 1, it is recommended that future studies adopt a similar dual or even multiple measurement approach. The understanding of the full cost and benefits of C allocation involves the measurements of different aspects of C allocation across different plant physiological processes such as defense, storage and reproduction (Figure 4). This integrated methodology allows for the exploration of potential interactions and trade-offs between these processes, contributing to a comprehensive analysis of plant physiological responses to environmental conditions.

Table 4: All significant results in Chapter 2 and 3, excluding the additional findings on day length effect on WUE and nocturnal respiration.

C allocation proportion above-ground		**Maize**	**Barley**		**p-value**
Chapter 3	Shoot Biomass	60%	46%	Table 3.3, Figure 3.1	0.001
	Root Translocation	20%	38%	Table 3.3, Figure 3.1	0.004
C allocation proportion below-ground		**Maize (0.11 MPa)**	**Maize (0.16 MPa)**		
Chapter 2	Root Biomass	25%	19%	Table 2.4, Figure 2.4	0.03
Chapter 3		**Maize**	**Barley**		
	Root Biomass	30%	40%	Table 3.4, Figure 3.2	0.005
	Root Respiration	43%	33%	Table 3.4, Figure 3.2	0.003
		Barley 1.40 g cm^{-3}	**Barley 1.60 g cm^{-3}**		
		45%	33%		0.03
Below-ground Cost and Benefits		**Maize (0.11 MPa)**	**Maize (0.16 MPa)**		**p-value**
Chapter 2	Root respiration per Root Length (slope)	0.4 nmol m^{-1} s^{-1}	0.9 nmol m^{-1} s^{-1}	Figure 2.6	4.3 * 10^{-5}
	Root respiration per Root Growth Rate (slope)	374 nmol mm^{-1}	657 nmol mm^{-1}	Figure 2.6	0.007
	Respiration per Transpiration (slope)	0.0010 mol mol^{-1}	0.0015 mol mol^{-1}	Figure 2.7	8.9 * 10^{-5}
	Respiration per N uptake (ratio)	3.9 mol mol^{-1}	6.37 mol mol^{-1}	Figure 2.7	0.04

Table 4 (cont'd): All significant results in Chapter 2 and 3, excluding the additional findings on day length effect on WUE and nocturnal respiration.

Below-ground Cost and Benefits		**Maize (0.11 MPa)**	**Maize (0.16 MPa)**		**p-value**
Chapter 2	Root respiration per Root Length (slope)	0.4 nmol m^{-1} s^{-1}	0.9 nmol m^{-1} s^{-1}	Figure 2.6	4.3 * 10^{-5}
	Root respiration per Root Growth Rate (slope)	374 nmol mm^{-1}	657 nmol mm^{-1}	Figure 2.6	0.007
	Respiration per Transpiration (slope)	0.0010 mol mol^{-1}	0.0015 mol mol^{-1}	Figure 2.7	8.9 * 10^{-5}
	Respiration per N uptake (ratio)	3.9 mol mol^{-1}	6.37 mol mol^{-1}	Figure 2.7	0.04
Below-ground Cost and Benefits		**Maize 1.40 g cm^{-3}**	**Maize 1.60 g cm^{-3}**		
Chapter 3	Transpiration per root length (ratio)	0.60 nmol mm^{-1} s^{-1}	2.02 nmol mm^{-1} s^{-1}	Figure 3.3	0.03
	Root respiration per Root Length (ratio)	0.4 nmol m^{-1} s^{-1}	2 nmol m^{-1} s^{-1}	Figure 3.4	0.03
		Barley 1.40 g cm^{-3}	**Barley 1.60 g cm^{-3}**		
	Root respiration per Root Length (ratio)	0.2 nmol m^{-1} s^{-1}	0.5 nmol m^{-1} s^{-1}	Figure 3.4	0.03
	N uptake per Root Length (ratio)	6.3 * 10^{-8} mol mm^{-1}	1.8 * 10^{-7} mol mm^{-1}	Figure 3.3	0.03
		Maize	**Barley**		
	Root respiration per Root Length (slope)	0.3 nmol m^{-1} s^{-1}	0.1 nmol m^{-1} s^{-1}	Figure 3.4	0.01
	N uptake per Root Length (slope)	1.0 * 10^{-7} mol mm^{-1}	3.3 * 10^{-8} mol mm^{-1}	Figure 3.3	0.00005
Above-ground Cost and Benefits		**Maize (0.11 MPa)**	**Maize (0.16 MPa)**		
Chapter 2	Above-ground Assimilation per Below-ground Respiration (slope)	0.07 mol mol^{-1}	0.11 mol mol^{-1}	Figure 2.9	
Chapter 3		**Maize**	**Barley**		
	Assimilation per Transpiration (slope)	0.01 mol mol^{-1}	0.005 mol mol^{-1}	Figure 3.7	0.0001
		Barley 1.40 g cm^{-3}	**Barley 1.60 g cm^{-3}**		
	Assimilation per Transpiration (ratio)	0.006 mol mol^{-1}	0.008 mol mol^{-1}	Figure 3.7	0.007

Bibliography

Aliyu, K. T., Huising, J., Kamara, A. Y., Jibrin, J. M., Mohammed, I. B., Nziguheba, G., Adam, A. M., and Vanlauwe, B. (2021). Understanding nutrient imbalances in maize (Zea mays L.) using the diagnosis and recommendation integrated system (DRIS) approach in the Maize belt of Nigeria. Sci Rep, 11(1):16018. Number: 1 Publisher: Nature Publishing Group.

Alter, P., Bircheneder, S., Zhou, L.-Z., Schlüter, U., Gahrtz, M., Sonnewald, U., and Dresselhaus, T. (2016). Flowering Time-Regulated Genes in Maize Include the Transcription Factor ZmMADS11[OPEN]. Plant Physiol, 172(1):389–404.

Atwell, B., Fillery, I. R. P., McInnes, K. J., and Smucker, A. J. M. (2002). The fate of carbon and fertiliser nitrogen when dryland wheat is grown in monoliths of duplex soil. Plant and Soil, 241(2):259–269.

Atwell, B. J. (1990). The effect of soil compaction on wheat during early tillering. New Phytologist, 115(1):43–49.

Avola, G., Cavallaro, V., Patanè, C., and Riggi, E. (2008). Gas exchange and photosynthetic water use efficiency in response to light, CO2 concentration

and temperature in Vicia faba. Journal of Plant Physiology, 165(8):796–804.

Barthel, M., Hammerle, A., Sturm, P., Baur, T., Gentsch, L., and Knohl, A. (2011). The diel imprint of leaf metabolism on the δ13C signal of soil respiration under control and drought conditions. New Phytologist, 192(4):925–938. _eprint: https://onlinelibrary.wiley.com/doi/pdf/10.1111/j.1469-8137.2011.03848.x.

Bazzaz, F. A., Chiariello, N. R., Coley, P. D., and Pitelka, L. F. (1987). Allocating Resources to Reproduction and Defense. BioScience, 37(1):58–67. Publisher: [American Institute of Biological Sciences, Oxford University Press].

Bebre, I., Marques, I., and Annighöfer, P. (2022). Biomass Allocation and Leaf Morphology of Saplings Grown under Various Conditions of Light Availability and Competition Types. Plants, 11(3):305.

Bengough, A. G., Bransby, M. F., Hans, J., McKenna, S. J., Roberts, T. J., and Valentine, T. A. (2006). Root responses to soil physical conditions; growth dynamics from field to cell. Journal of Experimental Botany, 57(2):437–447.

Bengough, A. G., Loades, K., and McKenzie, B. M. (2016). Root hairs aid soil penetration by anchoring the root surface to pore walls. Journal of Experimental Botany, 67(4):1071–1078.

Bengough, A. G., McKenzie, B. M., Hallett, P. D., and Valentine, T. A. (2011). Root elongation, water stress, and mechanical impedance: a review of limiting stresses and beneficial root tip traits. J Exp Bot, 62(1):59–68.

Berg, S., Kutra, D., Kroeger, T., Straehle, C. N., Kausler, B. X., Haubold, C., Schiegg, M., Ales, J., Beier, T., Rudy, M., Eren, K., Cervantes, J. I., Xu, B., Beuttenmueller, F., Wolny, A., Zhang, C., Koethe, U., Hamprecht,

F. A., and Kreshuk, A. (2019). ilastik: interactive machine learning for (bio)image analysis. Nat Methods, 16(12):1226–1232. Number: 12 Publisher: Nature Publishing Group.

Birami, B., Nägele, T., Gattmann, M., Preisler, Y., Gast, A., Arneth, A., and Ruehr, N. K. (2020). Hot drought reduces the effects of elevated CO2 on tree water-use efficiency and carbon metabolism. New Phytologist, 226(6):1607–1621. _eprint: https://onlinelibrary.wiley.com/doi/pdf/10.1111/nph.16471.

Blažka, P. and Fischer, Z. (2014). Moisture, Water Holding, Drying and Wetting in Forest Soils. OJSS, 04(05):174–184.

Bloom, A. J., Sukrapanna, S. S., and Warner, R. L. (1992). Root Respiration Associated with Ammonium and Nitrate Absorption and Assimilation by Barley. Plant Physiol, 99(4):1294–1301.

Bouma, T. J., Nielsen, K. L., Eissenstat, D. M., and Lynch, J. P. (1997). Estimating respiration of roots in soil: Interactions with soil CO2, soil temperature and soil water content. Plant and Soil, 195(2):221–232.

Brouwer, R. (1983). Functional equilibrium: sense or nonsense? NJAS, 31(4):335–348.

Brüggemann, N., Gessler, A., Kayler, Z., Keel, S. G., Badeck, F., Barthel, M., Boeckx, P., Buchmann, N., Brugnoli, E., Esperschütz, J., Gavrichkova, O., Ghashghaie, J., Gomez-Casanovas, N., Keitel, C., Knohl, A., Kuptz, D., Palacio, S., Salmon, Y., Uchida, Y., and Bahn, M. (2011). Carbon allocation and carbon isotope fluxes in the plant-soil-atmosphere continuum: a review. Biogeosciences, 8(11):3457–3489. Publisher: Copernicus GmbH.

Bryla, D. R., Bouma, T. J., Hartmond, U., and Eissenstat, D. M. (2001). Influence of temperature and soil drying on respiration of individual roots

in citrus: integrating greenhouse observations into a predictive model for the field. Plant Cell and Environment, 24(8):781–790.

Burkart, S., Manderscheid, R., and Weigel, H.-J. (2007). Design and performance of a portable gas exchange chamber system for CO2- and H2O-flux measurements in crop canopies. Environmental and Experimental Botany, 61(1):25–34.

Burton, A. J., Pregitzer, K. S., Zogg, G. P., and Zak, D. R. (1998). Drought reduces root respiration in sugar maple forests. Ecological Applications, 8(3):771–778.

Bushamuka, V. N. and Zobel, R. W. (1998). Differential Genotypic and Root Type Penetration of Compacted Soil Layers. Crop Science, 38(3):cropsci1998.0011183X003800030026x. _eprint: https://onlinelibrary.wiley.com/doi/pdf/10.2135/cropsci1998.0011183X003800030026x.

Byrd, G., Sage, R., and Brown, R. (1992). A Comparison of Dark Respiration between C(3) and C(4) Plants. Plant physiology, 100:191–8.

Chiew, F. and Vaze, J. (2015). Hydrologic nonstationarity and extrapolating models to predict the future: overview of session and proceeding. Proceedings of the International Association of Hydrological Sciences, 371:17–21.

ChunLi, X., Jun, X., Ke, W., DanPing, L., XuanJing, C., YueQiang, Z., XinPing, C., and XiaoJun, S. (2018). The response of maize yield to inherent soil productivity and fertilizer in the southwest China. Scientia Agricultura Sinica, 51(1):129–138. Publisher: Scientia Agricultura Sinica.

Colombi, T., Chakrawal, A., and Herrmann, A. M. (2022). Carbon supply–consumption balance in plant roots: effects of carbon use efficiency and root anatomical plasticity. New Phytologist, 233(4):1542–1547. _eprint: https://onlinelibrary.wiley.com/doi/pdf/10.1111/nph.17598.

Colombi, T., Kirchgessner, N., Walter, A., and Keller, T. (2017). Cortical cell diameter is key to energy costs of root growth in wheat. Plant Physiol, 174(4):2289–2301.

Conover, W. J. and Iman, R. L. (1981). Rank Transformations as a Bridge Between Parametric and Nonparametric Statistics. The American Statistician, 35(3):124–129. Publisher: [American Statistical Association, Taylor & Francis, Ltd.].

Correa, J., Postma, J. A., Watt, M., and Wojciechowski, T. (2019). Soil compaction and the architectural plasticity of root systems. Journal of Experimental Botany, 70(21):6019–6034.

Dakora, F. D. and Phillips, D. A. (2002). Root exudates as mediators of mineral acquisition in low-nutrient environments. In Adu-Gyamfi, J. J., editor, Food Security in Nutrient-Stressed Environments: Exploiting Plants' Genetic Capabilities, pages 201–213. Springer Netherlands, Dordrecht.

Donahue, R. A., Poulson, M. E., and Edwards, G. E. (1997). A method for measuring whole plant photosynthesis in Arabidopsis thaliana. Photosynthesis Research, 52(3):263–269.

Drew, M. C. (1975). Comparison of the Effects of a Localised Supply of Phosphate, Nitrate, Ammonium and Potassium on the Growth of the Seminal Root System, and the Shoot, in Barley. New Phytologist, 75(3):479–490.

Dusenge, M. E., Duarte, A. G., and Way, D. A. (2019). Plant carbon metabolism and climate change: elevated CO2 and temperature impacts on photosynthesis, photorespiration and respiration. New Phytologist, 221(1):32–49. _eprint: https://onlinelibrary.wiley.com/doi/pdf/10.1111/nph.15283.

Dusschoten, D. v., Metzner, R., Kochs, J., Postma, J. A., Pflugfelder, D., Bühler, J., Schurr, U., and Jahnke, S. (2016). Quantitative 3D Analysis

of Plant Roots Growing in Soil Using Magnetic Resonance Imaging. Plant Physiology, 170(3):1176–1188.

Dyukarev, E. A. and Kurakov, S. A. (2023). Response of Bare Soil Respiration to Air and Soil Temperature Variations According to Different Models: A Case Study of an Urban Grassland. Land, 12(5):939. Number: 5 Publisher: Multidisciplinary Digital Publishing Institute.

Eissenstat, D. M. (1992). Costs and benefits of constructing roots of small diameter. Journal of Plant Nutrition, 15(6-7):763–782.

Eshel, A. and Beeckman, T., editors (2013). Plant Roots: The Hidden Half, Fourth Edition. CRC Press, Boca Raton, FL, 4 edition edition.

Evans, J. R. (1989). Photosynthesis and nitrogen relationships in leaves of C3 plants. Oecologia, 78(1):9–19.

Field, C. and Mooney, H. A. (1986). photosynthesis–nitrogen relationship in wild plants. In On the economy of plant form and function : proceedings of the Sixth Maria Moors Cabot Symposium, Evolutionary Constraints on Primary Productivity, Adaptive Patterns of Energy Capture in Plants, Harvard Forest, August 1983.

Gent, M. (1998). Crop evolution, adaptation and yield: L.T. Evans. Cambridge University Press, UK, 1996. ISBN 0-521-29588-0, 500 pp., paperback, UK, 22.95, US$ 42.95, Hardback version published 1993, ISBN 0-521-22571-X, UK, 65.00, US$ 100.00. Field Crops Research, 55:283–284.

Givnish, T. J. (1986). Optimal stomatal conductance, allocation of energy between leaves and roots, and the marginal cost of transpiration. In Givnish, T. J., editor, On the economy of plant form and function, pages 171–213. Cambridge University Press, Cambridge.

Givnish, T. J. (1988). Adaptation to Sun and Shade - a Whole-Plant Perspective. Australian Journal of Plant Physiology, 15(1-2):63–92.

Grassi, G. and Bagnaresi, U. (2001). Foliar morphological and physiological plasticity in Picea abies and Abies alba saplings along a natural light gradient. Tree Physiology, 21(12-13):959–967.

Green, S. R., Kirkham, M., and Clothier, B. E. (2006). Root uptake and transpiration: From measurements and models to sustainable irrigation. Agricultural Water Management, 86(1-2):165–176.

Grzesiak, M. T., Ostrowska, A., Hura, K., Rut, G., Janowiak, F., Rzepka, A., Hura, T., and Grzesiak, S. (2014). Interspecific differences in root architecture among maize and triticale genotypes grown under drought, waterlogging and soil compaction. Acta Physiol Plant, 36(12):3249–3261.

Guswa, A. J. (2010). Effect of plant uptake strategy on the water-optimal root depth. Water Resources Research, 46(9).

Hansen, L. D., Macfarlane, C., McKinnon, N., Smith, B. N., and Criddle, R. S. (2004). Use of calorespirometric ratios, heat per CO2 and heat per O2, to quantify metabolic paths and energetics of growing cells. Thermochimica Acta, 422(1):55–61.

Hanson, P., Edwards, N., Garten, C., and Andrews, J. (2000). Separating root and soil microbial contributions to soil respiration: A review of methods and observations. Biogeochemistry, 48(1):115–146.

Harper, A. B., Williams, K. E., McGuire, P. C., Duran Rojas, M. C., Hemming, D., Verhoef, A., Huntingford, C., Rowland, L., Marthews, T., Breder Eller, C., Mathison, C., Nobrega, R. L. B., Gedney, N., Vidale, P. L., Otu-Larbi, F., Pandey, D., Garrigues, S., Wright, A., Slevin, D., De Kauwe, M. G., Blyth, E., Ardö, J., Black, A., Bonal, D., Buchmann, N., Burban, B., Fuchs, K., de Grandcourt, A., Mammarella, I., Merbold, L., Montagnani, L., Nouvellon, Y., Restrepo-Coupe, N., and Wohlfahrt, G. (2021). Improvement of modeling plant responses to low

soil moisture in JULESvn4.9 and evaluation against flux tower measurements. Geoscientific Model Development, 14(6):3269–3294. Publisher: Copernicus GmbH.

Hartmann, H., Bahn, M., Carbone, M., and Richardson, A. D. (2020). Plant carbon allocation in a changing world – challenges and progress: introduction to a Virtual Issue on carbon allocation. New Phytologist, 227(4):981–988. _eprint: https://onlinelibrary.wiley.com/doi/pdf/10.1111/nph.16757.

Herrmann, A. M. and Colombi, T. (2019). Energy use efficiency of root growth – a theoretical bioenergetics framework. Plant Signaling & Behavior, page 1685147.

Hikosaka, K., Hanba, Y. T., Hirose, T., and Terashima, I. (1998). Photosynthetic nitrogen-use efficiency in leaves of woody and herbaceous species. Functional Ecology, 12(6):896–905. _eprint: https://onlinelibrary.wiley.com/doi/pdf/10.1046/j.1365-2435.1998.00272.x.

Hikosaka, K., Ishikawa, K., Borjigidai, A., Muller, O., and Onoda, Y. (2006). Temperature acclimation of photosynthesis: mechanisms involved in the changes in temperature dependence of photosynthetic rate. Journal of Experimental Botany, 57(2):291–302.

Ho, M. D., Rosas, J. C., Brown, K. M., and Lynch, J. P. (2005). Root architectural tradeoffs for water and phosphorus acquisition. Functional Plant Biol., 32(8):737.

Hobson, L. A., Hartley, F. A., and Ketcham, D. E. (1979). Effects of Variations in Daylength and Temperature on Net Rates of Photosynthesis, Dark Respiration, and Excretion by Isochrysis galbana Parke 1. Plant Physiol, 63(5):947–951.

Hodgkinson, L., Dodd, I. C., Binley, A., Ashton, R. W., White, R. P., Watts, C. W., and Whalley, W. R. (2017). Root growth in field-grown winter wheat: Some effects of soil conditions, season and genotype. European Journal of Agronomy, 91:74–83.

Hoffmann, C. and Jungk, A. (1995). Growth and phosphorus supply of sugar beet as affected by soil compaction and water tension. Plant and Soil, 176(1):15–25. Publisher: Springer.

Holz, M., Zarebanadkouki, M., Kuzyakov, Y., Pausch, J., and Carminati, A. (2018). Root hairs increase rhizosphere extension and carbon input to soil. Ann Bot, 121(1):61–69.

Iersel, M. W. v. and Bugbee, B. (2000). A Multiple Chamber, Semicontinuous, Crop Carbon Dioxide Exchange System: Design, Calibration, and Data Interpretation. Journal of the American Society for Horticultural Science, 125(1):86–92. Publisher: American Society for Horticultural Science Section: Journal of the American Society for Horticultural Science.

Irving, L. (2015). Carbon Assimilation, Biomass Partitioning and Productivity in Grasses. Agriculture, 5(4):1116–1134.

Jahnke, S., Menzel, M. I., Van Dusschoten, D., Roeb, G. W., Bühler, J., Minwuyelet, S., Blümler, P., Temperton, V. M., Hombach, T., Streun, M., Beer, S., Khodaverdi, M., Ziemons, K., Coenen, H. H., and Schurr, U. (2009). Combined MRI–PET dissects dynamic changes in plant structures and functions. The Plant Journal, 59(4):634–644. _eprint: https://onlinelibrary.wiley.com/doi/pdf/10.1111/j.1365-313X.2009.03888.x.

James, G., Witten, D., Hastie, T., and Tibshirani, R. (2013). An Introduction to Statistical Learning: with Applications in R. Springer Science & Business Media. Google-Books-ID: qcI_AAAAQBAJ.

Kennedy, R. A. and Johnson, D. (1981). Changes in photosynthetic characteristics during leaf development in apple. Photosynth Res, 2(3):213–223.

Kläring, H.-P., Hauschild, I., and Heißner, A. (2014). Fruit removal increases root-zone respiration in cucumber. Annals of Botany, 114(8):1735–1745.

Kläring, H.-P. and Körner, O. (2020). Design of a Real-Time Gas-Exchange Measurement System for Crop Stands in Environmental Scenarios. Agronomy, 10(5):737. Number: 5 Publisher: Multidisciplinary Digital Publishing Institute.

Koebernick, N., Huber, K., Kerkhofs, E., Vanderborght, J., Javaux, M., Vereecken, H., and Vetterlein, D. (2015). Unraveling the hydrodynamics of split root water uptake experiments using CT scanned root architectures and three dimensional flow simulations. Frontiers in Plant Science, 6.

Kölling, K., George, G. M., Künzli, R., Flütsch, P., and Zeeman, S. C. (2015). A whole-plant chamber system for parallel gas exchange measurements of Arabidopsis and other herbaceous species. Plant Methods, 11(1):48.

Kopczewski, T., Kuźniak, E., Kornaś, A., Rut, G., Nosek, M., Ciereszko, I., and Szczepaniak, L. (2020). Local and Systemic Changes in Photosynthetic Parameters and Antioxidant Activity in Cucumber Challenged with Pseudomonas syringae pv lachrymans. International Journal of Molecular Sciences, 21(17):6378. Number: 17 Publisher: Multidisciplinary Digital Publishing Institute.

Kruskal, W. H. and Wallis, W. A. (1952). Use of Ranks in One-Criterion Variance Analysis. Journal of the American Statistical Association, 47(260):583–621. Publisher: [American Statistical Association, Taylor & Francis, Ltd.].

Kuzyakov, Y. and Larionova, A. A. (2005). Root and rhizomicrobial respiration: A review of approaches to estimate respiration by autotrophic

and heterotrophic organisms in soil. Journal of Plant Nutrition and Soil Science, 168(4):503–520.

Lambers, H. (1987). Growth, respiration, exudation and symbiotic association: The fate of carbon translocated to the roots. In Root Development and Function, pages 125–145. Journal Abbreviation: Root Development and Function.

Lambers, H., Szaniawski, R., and De Visser, R. (1983). Respiration for growth, maintenance and ion uptake. An evaluation of concepts, methods, values and their significance. Physiologia Plantarum - PHYSIOL PLANT, 58:556–563.

Lawlor, D. W. (1995). Photosynthesis, productivity and environment. Journal of Experimental Botany, 46:1449–1461. Publisher: Oxford University Press.

Lawlor, D. W. (2002). Carbon and nitrogen assimilation in relation to yield: mechanisms are the key to understanding production systems. Journal of Experimental Botany, 53(370):773–787.

Lehmeier, C. A., Lattanzi, F. A., Gamnitzer, U., Schäufele, R., and Schnyder, H. (2010). Day-length effects on carbon stores for respiration of perennial ryegrass. New Phytologist, 188(3):719–725. _eprint: https://onlinelibrary.wiley.com/doi/pdf/10.1111/j.1469-8137.2010.03457.x.

Lei, N. and Han, J. (2020). Effect of precipitation on respiration of different reconstructed soils. Sci Rep, 10:7328.

Lipiec, J. and Stepniewski, W. (1995). Effects of soil compaction and tillage systems on uptake and losses of nutrients. Soil and Tillage Research, 35(1):37–52.

Long, S. P. and Bernacchi, C. J. (2003). Gas exchange measurements, what can they tell us about the underlying limitations to photosynthesis? Procedures and sources of error. Journal of Experimental Botany, 54(392):2393–2401.

Lynch, J. (1995). Root Architecture and Plant Productivity. Plant Physiology, 109(1):7–13.

Lynch, J. P., Ho, M. D., and phosphorus, L. (2005). Rhizoeconomics: Carbon costs of phosphorus acquisition. Plant and Soil, 269(1-2):45–56.

Lyzenga, W. J., Liu, Z., Olukayode, T., Zhao, Y., Kochian, L. V., and Ham, B.-K. (2023). Getting to the roots of N, P, and K uptake. Journal of Experimental Botany, 74(6):1784–1805.

Mann, H. B. and Whitney, D. R. (1947). On a Test of Whether one of Two Random Variables is Stochastically Larger than the Other. The Annals of Mathematical Statistics, 18(1):50–60. Publisher: Institute of Mathematical Statistics.

Martínez, F., Lazo, Y. O., Fernández-Galiano, J. M., and Merino, J. (2002). Root respiration and associated costs in deciduous and evergreen species of Quercus. Plant, Cell & Environment, 25(10):1271–1278. _eprint: https://onlinelibrary.wiley.com/doi/pdf/10.1046/j.1365-3040.2002.00903.x.

Mascheretti, I., Turner, K., Brivio, R. S., Hand, A., Colasanti, J., and Rossi, V. (2015). Florigen-Encoding Genes of Day-Neutral and Photoperiod-Sensitive Maize Are Regulated by Different Chromatin Modifications at the Floral Transition. Plant Physiology, 168(4):1351–1363.

Masle, J. (1992). Genetic Variation in the Effects of Root Impedance on Growth and Transpiration Rates of Wheat and Barley. Functional Plant Biol., 19(2):109–125. Publisher: CSIRO PUBLISHING.

Masle, J. and Passioura, J. (1987). The Effect of Soil Strength on the Growth of Young Wheat Plants. Functional Plant Biol., 14(6):643.

Matesanz, S., Gianoli, E., and Valladares, F. (2010). Global change and the evolution of phenotypic plasticity in plants. Annals of the New York Academy of Sciences, 1206(1):35–55. _eprint: https://onlinelibrary.wiley.com/doi/pdf/10.1111/j.1749-6632.2010.05704.x.

McKee, G. W. (1964). A Coefficient for Computing Leaf Area in Hybrid Corn1. Agronomy Journal, 56(2):240–241. _eprint: https://onlinelibrary.wiley.com/doi/pdf/10.2134/agronj1964.00021962005600020038x.

Meng, F., Dungait, J. A. J., Zhang, X., He, M., Guo, Y., and Wu, W. (2013). Investigation of photosynthate-C allocation 27 days after 13C-pulse labeling of Zea mays L. at different growth stages. Plant Soil, 373(1):755–764.

Minchin, F. R., Neves, M. C. P., Summerfield, R. J., and Richardson, A. C. (1977). A Chamber Designed for Continuous, Long-term Monitoring of Legume Root Respiration. J Exp Bot, 28(2):507–514.

Mokhele, B., Zhan, X., Yang, G., and Zhang, X. (2012). Review: Nitrogen assimilation in crop plants and its affecting factors. Can. J. Plant Sci., 92(3):399–405. Publisher: NRC Research Press.

Monson, R. K., Trowbridge, A. M., Lindroth, R. L., and Lerdau, M. T. (2022). Coordinated resource allocation to plant growth–defense tradeoffs. New Phytologist, 233(3):1051–1066. _eprint: https://onlinelibrary.wiley.com/doi/pdf/10.1111/nph.17773.

Mooney, H. A. (1972). The Carbon Balance of Plants. Annual Review of Ecology and Systematics, 3:315–346. Publisher: Annual Reviews.

Moroke, T. S., Schwartz, R. C., Brown, K. W., and Juo, A. S. R. (2005). Soil Water Depletion and Root Distribution of Three Dryland Crops. Soil Science Society of America Journal, 69(1):197–205. _eprint: https://onlinelibrary.wiley.com/doi/pdf/10.2136/sssaj2005.0197.

Nielsen, K. L., Lynch, J. P., Jablokow, A. G., and Curtis, P. S. (1994). Carbon cost of root systems: an architectural approach. Plant and Soil, 165(1):161–169.

Nishida, H., Ishihara, D., Ishii, M., Kaneko, T., Kawahigashi, H., Akashi, Y., Saisho, D., Tanaka, K., Handa, H., Takeda, K., and Kato, K. (2013). Phytochrome C Is A Key Factor Controlling Long-Day Flowering in Barley1[W]. Plant Physiol, 163(2):804–814.

Palta, J. A. and Nobel, P. S. (1989). Influences of Water Status, Temperature, and Root Age on Daily Patterns of Root Respiration for Two Cactus Species. Annals of Botany, 63(6):651–662.

Poorter, H., Niklas, K. J., Reich, P. B., Oleksyn, J., Poot, P., and Mommer, L. (2012). Biomass allocation to leaves, stems and roots: meta-analyses of interspecific variation and environmental control. New Phytologist, 193(1):30–50. _eprint: https://onlinelibrary.wiley.com/doi/pdf/10.1111/j.1469-8137.2011.03952.x.

Popova, L., van Dusschoten, D., Nagel, K. A., Fiorani, F., and Mazzolai, B. (2016). Plant root tortuosity: an indicator of root path formation in soil with different composition and density. Ann Bot, 118(4):685–698.

Poulet, L., Gildersleeve, M., Koss, L., Massa, G. D., and Wheeler, R. M. (2020). Development of a photosynthesis measurement chamber under different airspeeds for applications in future space crop-production facilities. In International Conference on Environmental Systems, volume 77. 2020

International Conference on Environmental Systems. Accepted: 2020-08-04T17:41:13Z.

Rawson, H. M., Begg, J. E., and Woodward, R. G. (1977). The effect of atmospheric humidity on photosynthesis, transpiration and water use efficiency of leaves of several plant species. Planta, 134(1):5–10.

Redmond, M. D., Davis, T. S., Ferrenberg, S., and Wion, A. P. (2019). Resource allocation trade-offs in a mast-seeding conifer: piñon pine prioritizes reproduction over defence. AoB PLANTS, 11(6):plz070.

Reich, P. B., Tjoelker, M. G., Pregitzer, K. S., Wright, I. J., Oleksyn, J., and Machado, J.-L. (2008). Scaling of respiration to nitrogen in leaves, stems and roots of higher land plants. Ecology Letters, 11(8):793–801.

Reich, P. B., Walters, M. B., and Ellsworth, D. S. (1997). From tropics to tundra: Global convergence in plant functioning. Proceedings of the National Academy of Sciences, 94(25):13730–13734. Publisher: Proceedings of the National Academy of Sciences.

Reich, P. B., Wright, I. J., Cavender-Bares, J., Craine, J. M., Oleksyn, J., Westoby, M., and Walters, M. B. (2003). The Evolution of Plant Functional Variation: Traits, Spectra, and Strategies. International Journal of Plant Sciences, 164(S3):S143–S164.

Ridge, I., editor (2002). Plants. Oxford University Press, Oxford ; New York.

Robinson, D. A., Hopmans, J. W., Filipovic, V., van der Ploeg, M., Lebron, I., Jones, S. B., Reinsch, S., Jarvis, N., and Tuller, M. (2019). Global environmental changes impact soil hydraulic functions through biophysical feedbacks. Global Change Biology, 25(6):1895–1904. _eprint: https://onlinelibrary.wiley.com/doi/pdf/10.1111/gcb.14626.

Ruiz, S., Or, D., and Schymanski, S. J. (2015). Soil Penetration by Earthworms and Plant Roots—Mechanical Energetics of Bioturbation of Compacted Soils. PLOS ONE, 10(6):e0128914.

Ruiz, S., Schymanski, S. J., and Or, D. (2017). Mechanics and Energetics of Soil Penetration by Earthworms and Plant Roots: Higher Rates Cost More. Vadose Zone Journal, 16(8):0.

Ruiz, S., Straub, I., Schymanski, S. J., and Or, D. (2016). Experimental Evaluation of Earthworm and Plant Root Soil Penetration–Cavity Expansion Models Using Cone Penetrometer Analogs. Vadose Zone Journal, 15(3):vzj2015.09.0126.

Rutkowska, A., Pikula, D., and Stepien, W. (2014). Nitrogen use efficiency of maize and spring barley under potassium fertilization in long-term field experiment. Plant Soil and Environment, 60:550–554.

Sage, R. F., Sage, T. L., and Kocacinar, F. (2012). Photorespiration and the evolution of C4 photosynthesis. Annu Rev Plant Biol, 63:19–47.

Saglio, P. H., Raymond, P., and Pradet, A. (1983). Oxygen Transport and Root Respiration of Maize Seedlings. Plant Physiol, 72(4):1035–1039.

Salvatori, N., Alberti, G., Muller, O., and Peressotti, A. (2021). A low-cost automated growth chamber system for continuous measurements of gas exchange at canopy scale in dynamic conditions. Plant Methods, 17.

Sasse, J., Martinoia, E., and Northen, T. (2018). Feed Your Friends: Do Plant Exudates Shape the Root Microbiome? Trends in Plant Science, 23(1):25–41.

Schlüter, U., Muschak, M., Berger, D., and Altmann, T. (2003). Photosynthetic performance of an Arabidopsis mutant with elevated stomatal density (sdd1-1) under different light regimes. J Exp Bot, 54(383):867–874.

Schymanski, S. J. and Osuebi-Iyke, E. (2023). LI-6800.

Schymanski, S. J., Roderick, M. L., Sivapalan, M., Hutley, L. B., and Beringer, J. (2007). A test of the optimality approach to modelling canopy properties and CO2 uptake by natural vegetation. Plant, Cell & Environment, 30(12):1586–1598.

Schymanski, S. J., Sivapalan, M., Roderick, M. L., Beringer, J., and Hutley, L. B. (2008). An optimality-based model of the coupled soil moisture and root dynamics. vegetation dynamics, page 20.

Schymanski, S. J., Sivapalan, M., Roderick, M. L., Hutley, L. B., and Beringer, J. (2009). An optimality-based model of the dynamic feedbacks between natural vegetation and the water balance. Water Resources Research, 45(1). _eprint: https://agupubs.onlinelibrary.wiley.com/doi/pdf/10.1029/2008WR006841.

Shane, M. W. and Lambers, H. (2005). Cluster Roots: A Curiosity in Context. Plant Soil, 274(1):101–125.

Shapiro, S. S. and Wilk, M. B. (1965). An analysis of variance test for normality (complete samples). Biometrika, 52(3-4):591–611.

Singh, N. T., Patel, M. S., Singh, R., and Vig, A. C. (1980). Effect of Soil Compaction on Yield and Water Use Efficiency of Rice in a Highly Permeable Soil [1]. Agronomy Journal, 72(3):499–502.

Smittle, D. A. and Williamson, R. E. (1977). Effect of Soil Compaction on Nitrogen and Water Use Efficiency, Root Growth, Yield, and Fruit Shape of Pickling Cucumbers1. J. Amer. Soc. Hort. Sci., 102(6):822–825.

Sun, Z., Chen, Q., Han, X., Bol, R., Qu, B., and Meng, F. (2018). Allocation of photosynthesized carbon in an intensively farmed winter wheat–soil system as revealed by 14CO2 pulse labelling. Sci Rep, 8(1):3160. Number: 1 Publisher: Nature Publishing Group.

Swinnen, J., Van Veen, J. A., and Merckx, R. (1995a). Carbon fluxes in the rhizosphere of winter wheat and spring barley with conventional vs integrated farming. Soil Biology and Biochemistry, 27(6):811–820.

Swinnen, J., Van Veen, J. A., and Merckx, R. (1995b). Root decay and turnover of rhizodeposits in field-grown winter wheat and spring barley estimated by 14C pulse-labelling. Soil Biology and Biochemistry, 27(2):211–217.

Teuling, A. J., Seneviratne, S. I., Stöckli, R., Reichstein, M., Moors, E., Ciais, P., Luyssaert, S., van den Hurk, B., Ammann, C., Bernhofer, C., Dellwik, E., Gianelle, D., Gielen, B., Grünwald, T., Klumpp, K., Montagnani, L., Moureaux, C., Sottocornola, M., and Wohlfahrt, G. (2010). Contrasting response of European forest and grassland energy exchange to heatwaves. Nature Geosci, 3(10):722–727. Number: 10 Publisher: Nature Publishing Group.

Tubeileh, A., Groleau-Renaud, V., Plantureux, S., and Guckert, A. (2003). Effect of soil compaction on photosynthesis and carbon partitioning within a maize–soil system. Soil and Tillage Research, 71(2):151–161.

Vogan, P. J. and Sage, R. F. (2011). Water-use efficiency and nitrogen-use efficiency of C3-C4 intermediate species of Flaveria Juss. (Asteraceae). Plant, Cell & Environment, 34(9):1415–1430. _eprint: https://onlinelibrary.wiley.com/doi/pdf/10.1111/j.1365-3040.2011.02340.x.

Wang, J., Gao, J., Wu, Y., Xu, B., Shi, F., Zhou, H., Bisht, N., and Wu, N. (2021a). Effects of Heterogeneous Environment After Deforestation on Plant Phenotypic Plasticity of Three Shrubs Based on Leaf Traits and Biomass Allocation. Frontiers in Ecology and Evolution, 9.

Wang, M., He, D., Shen, F., Huang, J., Zhang, R., Liu, W., Zhu, M., Zhou, L., Wang, L., and Zhou, Q. (2019). Effects of soil compaction on plant

growth, nutrient absorption, and root respiration in soybean seedlings. Environ Sci Pollut Res, 26(22):22835–22845.

Wang, M., Mori, S., Kurosawa, Y., Ferrio, J. P., Yamaji, K., and Koyama, K. (2021b). Consistent scaling of whole-shoot respiration between Moso bamboo (Phyllostachys pubescens) and trees. J Plant Res, 134(5):989–997.

Westoby, M., Falster, D. S., Moles, A. T., Vesk, P. A., and Wright, I. J. (2002). Plant Ecological Strategies: Some Leading Dimensions of Variation Between Species. Annual Review of Ecology and Systematics, 33(1):125–159. _eprint: https://doi.org/10.1146/annurev.ecolsys.33.010802.150452.

White, D. G. and Childers, N. F. (1944). A METHOD FOR MEASURING ROOT RESPIRATION. Plant Physiology, 19(4):699. Publisher: Oxford University Press.

Wong, S. C., Kriedemann, P. E., and Farquhar, G. D. (1992). CO2 x Nitrogen Interaction on Seedling Growth of Four Species of Eucalypt. Aust. J. Bot., 40(5):457–472. Publisher: CSIRO PUBLISHING.

Wullschleger, S. D., Epstein, H. E., Box, E. O., Euskirchen, E. S., Goswami, S., Iversen, C. M., Kattge, J., Norby, R. J., van Bodegom, P. M., and Xu, X. (2014). Plant functional types in Earth system models: past experiences and future directions for application of dynamic vegetation models in high-latitude ecosystems. Annals of Botany, 114(1):1–16.

Xie, Y., Islam, S., Legesse, H. T., and Kristensen, H. L. (2021). Deep root uptake of leachable nitrogen in two soil types is reduced by high availability of soil nitrogen in fodder radish grown as catch crop. Plant Soil, 465(1):213–227.

Xu, Q., Huang, B., and Wang, Z. (2004). Effects of Extended Daylength on Shoot Growth and Carbohydrate Metabolism for Creeping Bentgrass Exposed to Heat Stress. jashs, 129(2):193–197.

Yu, C., Yao, W., and Bai, X. (2014). Robust Linear Regression: A Review and Comparison. arXiv:1404.6274 [stat].

Zagal, E. (1994). Influence of light intensity on the distribution of carbon and consequent effects on mineralization of soil nitrogen in a barley (Hordeum vulgare L.)-soil system. Plant Soil, 160(1):21–31.

Zhang, X., Xu, M., Sun, N., Xiong, W., Huang, S., and Wu, L. (2016). Modelling and predicting crop yield, soil carbon and nitrogen stocks under climate change scenarios with fertiliser management in the North China Plain. Geoderma, 265:176–186.